DEPARTMENT OF THE AIR FORCE

AIR UNIVERSITY

AIR FORCE INSTITUTE OF TECHNOLOGY

Wright-Patterson Air Force Base, Ohio

AFIT/GAE/ENY/91M-4

TRANSIENT HEAT TRANSFER MEASUREMENTS ON A FILM COOLED FLAT PLATE IN A SHOCK TUBE

THESIS

Presented to the Faculty of the School of Engineering
of the Air Force Institute of Technology
Air University
in Partial Fulfillment of the
Requirements for the Degree of
Master of Science in Aeronautical Engineering

Rakhman Gul, B.E.
Flight Lieutenant, Pakistan Air Force

March 1991

REPORT DOCUMENTATION PAGE

Form Approved
OMB No 0704-0188

1. AGENCY USE ONLY (Leave blank)	2. REPORT DATE	3. REPORT TYPE AND DATES COVERED
	MARCH 15 1991	MASTER'S THESIS

4. TITLE AND SUBTITLE
TRANSIENT HEAT TRANSFER MEASUREMENTS ON A FILM COOLED FLAT PLATE IN A SHOCK TUBE.

5. FUNDING NUMBERS

6. AUTHOR(S)
RAKHMAN GUL, CAPT, PAKISTAN AIR FORCE.

7. PERFORMING ORGANIZATION NAME(S) AND ADDRESS(ES)
Air Force Institute of Technology,
WPAFB,OH 45433-6583

8. PERFORMING ORGANIZATION REPORT NUMBER

9. SPONSORING/MONITORING AGENCY NAME(S) AND ADDRESS(ES)
Dr R. B. Rivir
WL/POTC

10. SPONSORING/MONITORING AGENCY REPORT NUMBER

11. SUPPLEMENTARY NOTES

12a. DISTRIBUTION/AVAILABILITY STATEMENT
Approved for public release; distribution unlimited.

12b. DISTRIBUTION CODE

13. ABSTRACT *(Maximum 200 words)*
During this study a simple model of a flat plate was chosen to determine heat flux from a high speed flow behind a shock wave into the film cooled flat plate. An electrical analog was used to convert the output of the heat flux gages into heat flux. Free stream turbulence within the flow behind the shock wave and that generated by a turbulence generator was determined and its effects on the heat transfer data were then studied for comparison with previous experimental work. The thin-film heat flux gages were caliberated and their caliberation constants were then used to determine the true heat flux into the flat plate. Film cooling flows were studied under three different primary flow conditions. Cool air was injected into the boundary layer on the flat plate, and analyzed for its effects on the heat transfer to the flat plate.

14. SUBJECT TERMS
Heattransfer, free-stream turbulence, Film-cooling

15. NUMBER OF PAGES
155

16. PRICE CODE

17. SECURITY CLASSIFICATION OF REPORT	18. SECURITY CLASSIFICATION OF THIS PAGE	19. SECURITY CLASSIFICATION OF ABSTRACT	20. LIMITATION OF ABSTRACT
Unclassified	Unclassified	Unclassified	Unlimited

GENERAL INSTRUCTIONS FOR COMPLETING SF 298

The Report Documentation Page (RDP) is used in announcing and cataloging reports. It is important that this information be consistent with the rest of the report, particularly the cover and title page. Instructions for filling in each block of the form follow. It is important to ***stay within the lines*** to meet ***optical scanning requirements***.

Block 1. Agency Use Only *(Leave blank)*.

Block 2. Report Date. Full publication date including day, month, and year, if available (e.g. 1 Jan 88). Must cite at least the year.

Block 3. Type of Report and Dates Covered. State whether report is interim, final, etc. If applicable, enter inclusive report dates (e.g. 10 Jun 87 - 30 Jun 88).

Block 4. Title and Subtitle. A title is taken from the part of the report that provides the most meaningful and complete information. When a report is prepared in more than one volume, repeat the primary title, add volume number, and include subtitle for the specific volume. On classified documents enter the title classification in parentheses.

Block 5. Funding Numbers. To include contract and grant numbers; may include program element number(s), project number(s), task number(s), and work unit number(s). Use the following labels:

C	- Contract	**PR**	- Project
G	- Grant	**TA**	- Task
PE	- Program Element	**WU**	- Work Unit Accession No.

Block 6. Author(s). Name(s) of person(s) responsible for writing the report, performing the research, or credited with the content of the report. If editor or compiler, this should follow the name(s).

Block 7. Performing Organization Name(s) and Address(es). Self-explanatory.

Block 8. Performing Organization Report Number. Enter the unique alphanumeric report number(s) assigned by the organization performing the report.

Block 9. Sponsoring/Monitoring Agency Name(s) and Address(es). Self-explanatory.

Block 10. Sponsoring/Monitoring Agency Report Number. *(If known)*

Block 11. Supplementary Notes. Enter information not included elsewhere such as: Prepared in cooperation with...; Trans. of...; To be published in.... When a report is revised, include a statement whether the new report supersedes or supplements the older report.

Block 12a. Distribution/Availability Statement. Denotes public availability or limitations. Cite any availability to the public. Enter additional limitations or special markings in all capitals (e.g. NOFORN, REL, ITAR).

- **DOD** - See DoDD 5230.24, "Distribution Statements on Technical Documents."
- **DOE** - See authorities.
- **NASA** - See Handbook NHB 2200.2.
- **NTIS** - Leave blank.

Block 12b. Distribution Code.

- **DOD** - Leave blank.
- **DOE** - Enter DOE distribution categories from the Standard Distribution for Unclassified Scientific and Technical Reports.
- **NASA** - Leave blank.
- **NTIS** - Leave blank.

Block 13. Abstract. Include a brief ***(Maximum 200 words)*** factual summary of the most significant information contained in the report.

Block 14. Subject Terms. Keywords or phrases identifying major subjects in the report.

Block 15. Number of Pages. Enter the total number of pages.

Block 16. Price Code. Enter appropriate price code ***(NTIS only)***.

Blocks 17. - 19. Security Classifications. Self-explanatory. Enter U.S. Security Classification in accordance with U.S. Security Regulations (i.e., UNCLASSIFIED). If form contains classified information, stamp classification on the top and bottom of the page.

Block 20. Limitation of Abstract. This block must be completed to assign a limitation to the abstract. Enter either UL (unlimited) or SAR (same as report). An entry in this block is necessary if the abstract is to be limited. If blank, the abstract is assumed to be unlimited.

★U.S.GPO: 1990-0-273-271

AFIT/GAE/ENY/91M-4

TRANSIENT HEAT TRANSFER MEASUREMENTS ON A FILM COOLED FLAT PLATE IN A SHOCK TUBE

THESIS

RAKHMAN GUL
FLT.LT, PAKISTAN AIR FORCE

AFIT/GAE/ENY/91M-4

PREFACE

This study is a continuation of the work done by previous researchers, at A.F.I.T, to investigate the heat transfer to a flat plate. Much of the focus, however, was deliberated to the calibration of the heat flux gages and the effect of film cooling on the rate of heat transfer to a flat plate in a shock tube.

Keeping in view the vicissitudes involved in an experimental project of this nature it was necessary to seek help from various sources and people. A timely abet from all those asked for, indeed, helped me in finishing this project.

My greatest gratitude certainly would go to my advisor Dr. William C. Elrod, who at all times was available to help me at some very crucial moments. His careful supervision not for once allowed me to go astray.

It had mostly been the efforts of Lt. Col Paul I. king and Mr Jay Anderson whose experimental expertise got me through the cumbersome job of calibration. I owe acknowledgment to them for their expertise and patient listening.

To the Laboratory staff: Mr Nicholas Yardich, Mr Andy Pitts, Mr Dan Rioux, Mr Mark Derriso; I am extremely grateful for the consistent help and consultation on the instrumentation and hardware throughout my research study.

Last, but not the least, I extend my thankfulness to my wife Saeeda and my lovely daughter Qurat-ul-Ain for their equanimity.

Rakhman Gul

TABLE OF CONTENTS

LIST OF FIGURES

LIST OF TABLES

LIST OF SYMBOLS

Symbol	Description	Units
B	Blowing ratio	
c	Sonic velocity	m/sec
	Capacicitance per unit volume	$\mu F/m^2$
C_p	Constant pressure specific heat	J/Kg°K
h	Convective heat transfer coefficient	$W/m^2°K$
Hg	Mercury	
i	Current	amp
i	Laplace transform of current	
k	Thermal conductivity	W/m °K
m	meters	
M	Mach *number*	
Nu	Nusselt number	
P	Pressure	in of Hg
Pr	Prandtl number	
q	Heat flux	kW/m^2
r	Recovery factor	
	Resistance per unit length	ohm/m
R	Resistance	ohms
	Gas constant	J/gm°K
Re	Reynolds number	
St	Stanton number	
s	Laplace variable	

t	Time	s
T	Temperature	°K
Tu	Turbulence intensity	
U	Velocity	m/s
u	Velocity fluctuations about the mean velocity	m/s
u	Mean velocity	m/s
V	Voltage	volts
V	Laplace transform of voltage	
x	Downstream distance	m

Greek letters

α	Dimensionless variable	
ρ	Density	kg/m^2
Δ	Difference	
μ	Dynamic viscosity	Pa s
π	Arithmetic constant	
γ	Ratio of specific heats	
ν	Kinamatic viscosity	m^2/s
τ	Laplace transform of time	

Subscripts

aw	Adiabatic wall
c	Coolant
gly	Glycerine
mean	Arithmatic average
o	Initial condition
	total

out	Output
ref	Reference
rms	Root mean square
s	Shock
subs	Heat flux gage substrate
t	Time dependent
t_{max}	Maximum at throat
x	Local
w	Wall
1	ambient
2	Region behind the shock wave
4	High pressure region (Driver Section)

Superscript

*	Reference conditions
α	Dimensionless variable
γ	Ratio of specific heats
λ	Dimensionless variable

ABSTRACT

Owing to the complexities involved in studying heat transfer to complex geometries, initial research is carried out on simple models. The results of such initial studies can be used to understand some complex flow patterns.

During this study a simple model of a flat plate was chosen to determine heat flux from high speed flow behind a shock wave into the plate. An electrical analog circuit was used to convert the output of the heat flux gages into heat flux.

The free stream turbulence withen the flow behind a shock wave and that generated by a turbulence generator was determined and its effects on the heat transfer data were then studied for comparison with previous experimental work. The main focus, however, was laid upon the calibration of heat flux gages and the effects of film cooling on heat flux.

Thin film heat flux gages were calibrated for their material properties. The calibration constants were then used to determined the true heat flux into the flat plate.

Film cooling flows were studied under three different primary flow conditions. Cool air was injected into the boundary layer on the flat plate and analyzed for its effects on heat transfer.

Owing to the transient nature of the flow behind the shock wave some critical properties like the adiabatic wall temperature of the flat plate, and the heat transfer coefficient could not be determined during the film-cooling studies. As a result this part

of the research was restricted to the analysis of the experimentally obtained data.

TRANSIENT HEAT TRANSFER MEASUREMENTS ON A FILM COOLED FLAT PLATE IN A SHOCK TUBE

I. INTRODUCTION

Current aviation applications demand extensive research in the field of gas dynamics. With the increasing interest of gas turbine designers to improve upon the turbine blade technology; researchers are getting more and more involved in exploring and understanding the basic heat transfer processes taking place in this extremely complex zone of highly turbulent flow region. However, in order to minimize the complexities involved in the heat transfer measurements of turbine cascade flow geometry, researchers have simplified their initial stages of research by confining themselves to a comparatively facile problem of the flat plate. The results of such a study can lead to a better understanding of flow over complex geometries like the turbine blade.

An impulsive rise in gas temperature can be achieved by generating a normal shock in a transient facility like the shock tube. The measurement of heat transfer is easier in a shock tube than a continuous facility like a hot tunnel. Models in hot tunnels require internal cooling to establish a temperature gradient from which heat transfer can be deduced. It must also be capable of withstanding recovery temperatures continuously, and if the model has a large thermal capacity the tunnel itself must be operated for

an extended period of time so as to achieve uniform conditions within the model. In contrast, a model in a transient facility, like the shock tube, never attains an equilibrium that enables the heat flux to be determined (Shultz and Jones, 1973:3).

Owing to the short duration of tests in the shock tube, fast response measurement devices are required to collect the requisite information. Such a collection of data can be achieved by using fast response thin film heat flux gages which allow transient affects to be properly sampled and recorded.

An increase in the rate of heat transfer can be achieved by generating turbulence within the flow. However, to protect a surface exposed to high temperature environments, an effective way of reducing heat flux to the operating surface is required. one such way is by using film-cooling techniques which not only reduce the heat flux but also increase the component life.

BACKGROUND

The history of the shock tube goes back to the 19ØØ's. However, its widespread use has been facilitated by the technological boom during World War II. The slow growth of the shock tube use during its early years is mostly attributed to the lack of fast response instrumentation. With the advancements of piezoelectric gages, high speed photography, and an increased research into supersonic flow phenomena in the post World War II era, the shock tube has become an important research tool, especially in the fields of chemical kinetics, dissociation and

ionization, aerodynamics, and heat transfer (Bradly, 1962; Hartunian, et al, 1959; Gaydon, 1963).

Lam and Crocco (1959) studied the characteristics of the shock induced unsteady laminar boundary layer on a semi infinite flat plate. They experimentally found the existence of two distinct domains: one near the shock where the flow is quasi-steady and the other an unsteady region where the flow characteristics approach a steady state asymptotically.

Mirels (1961) presented numerical solutions for the laminar boundary layer behind a strong shock advancing into stationary air. Boundary layer transition and the steady rate of heat transfer to a shock induced turbulent boundary layer was studied by Spence (196Ø) and Hartunian, Russo and Marrone (196Ø). They obtained correlations, based on empirical data, for the rate of heat transfer.

Davies and Bernstein (1969) investigated the shock induced boundary layer on a semi-infinite flat plate. They found that for the laminar boundary layer, with zero pressure gradient, the flow is steady at a distance x from the leading edge of the flat plate after some time t and is given by :

$$t = \frac{X}{0.3U} \qquad (1)$$

where U is the velocity of the flow , outside the boundary layer, behind the shock wave. For a turbulent boundary layer they discovered that half the boundary layer length is steady.

With the advancements in the development of fast response

instrumentation, the use of shock tubes has further been enhanced. Dillon and Stoddard (1977) studied the heat flux to turbine components in a shock tube. Dillon an Nagamatsu (1984) studied the rate of heat transferred to the walls of a shock tube from the flow behind a shock wave. Novak (1987) investigated heat transfer to a flat plate by using thin film heat flux gages. Jurgelwicz (1989) developed a numerical technique to obtain heat flux from the data obtained by heat flux gages, mounted on a flat plate, exposed to flow behind a shock wave. He also extended his study to determine the effects of film cooling on the rate of heat transferred to a flat plate from flow behind a shock. Rockwell (1989) developed an analog circuit to directly record the heat flux measured by the thin film heat flux gages in terms of voltages. This direct conversion of voltages into heat flux tends to reduce the errors introduced by other methods like numerical techniques etc.

The high temperatures encountered in modern gas turbines necessitated studies of ways of protecting exposed surfaces from a hot stream of gases. One such way is to inject cooler gas under the boundary layer, thus forming a protective film along the surface. Goldstein (1971), in his book "ADVANCES IN HEAT TRANSFER", has consolidated the work of many researchers pertaining to film-cooling. It provides correlations from experimental film-cooling studies and the consequent effects of film-cooling on the rate of heat transfer.

Inspite of the commonalities involved between film cooling in steady and transient facilities no direct comparison between the

two can be made. An essential element to understand here is that the flow conditions in a transient facility do not reach a steady state at any time and are thus different than the flow conditions encountered in a steady state facility .

Schlichting (1987) states that the local Nusselt number can be increased by generating free-stream turbulence. Blair (1981) found that the Reynolds analogy factor increased by slightly more than one percent for every one percent increase in free-stream turbulence intensity. Simonich and Bradshaw (1978) determined that grid generated free-stream turbulence increased the rate of heat transfer by about five percent for every one percent increase in the longitudinal turbulence level.

OBJECTIVES AND SCOPE

This study was a continuation of the research carried out by Jurgelwicz (1989) and Rockwell (1989). the general purpose of the study was to use a shock tube to investigate the rate of heat transfer to a flat plate under the transient conditions behind the incident shock wave. The broad objectives of this study were:

1. To calibrate the heat flux gages for temperature coefficient and the material properties forming the rooted product of density, specific heat and thermal conductivity.

2. To determine the rate of heat transfer to a flat plate, with round leading edge, from flow behind a shock wave in a shock tube.

3. To study the effects of free-stream turbulence on the rate

of heat transfer to a flat plate.

4. To study the effects of film-cooling on the rate of heat transfer to a flat plate.

The scope of the research ranged from generating shock Mach numbers from 1.1 to about 1.5 thereby resulting in flow behind the incident shock wave with temperatures and pressures as high as about 92 degrees centigrade and 6Ø in of Hg respectively. During the film-cooling analysis the blowing ratio of the film-cooling flow was varied from Ø.2 to about 5.5 depending on the flow conditions of the primary flow.

An understanding of the phenomena taking place during the heat transfer to a flat plate and the effects of free-stream turbulence and film-cooling on the rate of heat transfer would help in extending the acumen to the complexities involved in gas turbine heat transfer.

II. THEORY

THE SHOCK TUBE

As defined by Chapmann And Walker (1971) a shock tube is a device that allows the experimental studies of many of the phenomena associated with the occurrence of shock waves. A conceptually simple shock tube is shown in Figure 1. It essentially consists of two sections divided by a diaphragm. The high pressure section of the tube is called the driver section whereas the low pressure section is called the driven section. By pressurizing the driver section and rupturing the diaphragm, a shock wave, the strength of which is determined by the pressure ratio between the two sections, is generated. This results in a discontinuity in the properties of the medium across the shock wave. This can best be understood with the help of Figures 2(a) to (d).

At time t=Ø the high pressure gas in the driver section is separated from the low pressure gas by a diaphragm. When the diaphragm is ruptured a shock wave travels into the driven section while an expansion wave travels into the driver section. The initial condition in the driver section is designated as region 4 and the driven section as region 1. Before the two waves reach either ends of the shock tube, at some time $t=t_1$ the region notated as region 3 in Figure 2(a) has been traversed by the expansion wave moving into the driver section whereas the region notated as region 2 in Figure 2(a) has been traversed by the shock wave. Though the velocities and pressures of region 2 and 3 are equal, since the gas

state in region 3 is obtained by an isentropic process the specific entropies and the temperatures of the two regions are not equal thus implying that a "contact discontinuity" exist between the two regions. This contact discontinuity moves in the same direction as the shock wave with a velocity and pressure $V_2=V_3$ and $P_2=P_3$ respectively and always separates the shocked region 2 from the "expanded region 3". The section of the flow with uniform pressure and velocity, i.e region 2, is utilized as the test section unless a condition with high temperature and high pressure at zero velocity is desired which is obtained in region 5 of Figure 2(d).

Figure 2(b) shows the pressure distribution in the shock tube at $t=t_1$. The pressure ratio P_4/P_1 and the temperature in region 1 determines the speed of the shock wave (Chapmann and Walker, 1971).

$$\frac{P_4}{P_1}=\left[\frac{\gamma-1}{\gamma+1}\right]\left[\frac{2\gamma}{\gamma-1}M_s^2-1\right]\left[1-\frac{\frac{\gamma-1}{\gamma+1}M_s^2-1}{M_s}\right]^{\frac{-2\gamma}{\gamma-1}} \qquad (2)$$

Note: It has been assumed that the gas in the driver section is the same as that in the driven section.

The test conditions of interest for this investigation are those established in region 2. The properties of this region can be determined from the known properties of region 1 and the strength of the shock wave. The governing equations, extracted from the text of Shapiro (1987), to determine the fluid properties behind a normal shock wave are:

$$\frac{P_2}{P_1} = 1 + \frac{2\gamma}{\gamma+1}[M_s^2 - 1] \qquad (3)$$

$$\frac{T_2}{T_1} = 1 + \frac{2(\gamma-1)}{(\gamma+1)^2}\gamma M_s^2 - \frac{1}{M_s^2} - (\gamma-1) \qquad (4)$$

$$U_2 = C_1\left(\frac{2}{\gamma+1}\right)\left(1 + \frac{1}{M_s^2}\right)M_s \qquad (5)$$

Figure 2(c) represents the temperature distribution withen the shock tube at time $t=t_1$ whereas Figure 2(d) essentially indicates the limited time available for a test to be carried out before the properties of the shocked region are changed by a reflected shock wave or the arrival of the contact discontinuity. A detailed account of the shock tube phenomena can be obtained from texts dealing with compressible flow dynamics.

THE BOUNDARY LAYER.

In his paper "FLUID MOTION WITH VERY SMALL FRICTION" L. Prandtl (19Ø4) proved that the flow about a solid body can be divided into two regions: a very thin layer in the neighborhood of the body where friction plays an important role and a region outside this layer where friction may be neglected.

This very thin layer, where friction plays an important role, is known as the "boundary layer". The problem of heat flux between a solid body and the fluid flow past it belongs to the class of problems where boundary layer phenomena plays a decisive part (Schlichting, 1987: 1-4).

Consider a round leading edge flat plate suspended in a shock tube. When an incident shock wave passes over the flat plate a thin boundary layer develops over it as a result of the gas velocity established in region 2. If the plate temperature is T_w, the shock velocity is U_s and the temperature and velocity of the free stream flow behind the shock wave is T_2 and U_2 then, as shown in Figure 3, the temperature and free stream velocity, T_2 and U_2 become T_w and zero at the surface of the plate.

Blasius (1908) presented solutions to equations governing the flow in the steady region of the boundary layer, whereas Mirels (1956) obtained empirical solutions to equations governing the transition region. A detailed discussion of this is given by Davies and Bernstein (1969).

HEAT TRANSFER THROUGH THE BOUNDARY LAYER

The prime focus of this research is to understand the process of heat transfer and the influence of free-stream turbulence and film-cooling on heat transfer to a flat plate. The pressure, temperature, and velocity relationships given by Equations (3), (4), (5), used in conjunction with the equations presented herewith provide the theoretical heat transfer basis for comparison with experimental results.

The heat transfer to the flat plate in a high speed subsonic flow is given by (Kays and Crawford, 1980:299):

$$q_x = h_x (T_{aw} - T_w) \qquad (6)$$

For a constant property perfect gas, the adiabatic wall temperature is given by the relationship (Mirels, 1956:23)

$$T_{aw}=T_w+r\frac{U_2^2}{2C_p} \tag{7}$$

The recovery factor "r" for a steady turbulent boundary layer can be approximated as (Mirels, 1956:23)

$$r=Pr^{\frac{1}{3}} \tag{8}$$

The heat transfer coefficient h_x can be determined from the expression for the local Nusselt number for turbulent flow (Kays and Crawford, 1980) as:

$$Nu_x=\frac{h_x x}{k} \tag{9}$$

This would then imply that in order to find the local heat transfer coefficient we need to know the local Nusselt number which can be obtained from the expression (Kakac, et al, 1987: 14-24)

$$Nu_x=0.00287Re_x^{\frac{4}{5}}Pr^{\frac{3}{5}} \tag{10}$$

The local Reynolds number can be obtained from the expression:

$$Re_x=\frac{U_2 x}{\nu} \tag{11}$$

The Prandtl and Stanton numbers for a steady turbulent flow are expressed as:

$$StPr^{0.4}=0.0287Re_x^{-0.2} \tag{12}$$

$$Pr=\frac{C_p\mu}{k} \tag{13}$$

Since the fluid properties are not constant across the boundary layer in high speed flow, they need to be evaluated at some reference temperature T^*. According to Eckert (1976), the low speed constant properties correlations for Nusselt number can be used for air for Mach numbers up to 2Ø with an approximate error not exceeding more than just a few percent.

The expression for reference temperature, as given by Kays and Crawford (198Ø) is:

$$T^*=\frac{T_{aw}+T_w}{2}+0.22(T_{aw}-T_2) \tag{14}$$

Equations (6) to (14) constitute the theoretical results for the steady turbulent boundary layer.

ELECTRICAL ANALOG FOR HEAT TRANSFER

One dimensional heat transfer to a semi infinite medium is expressed as :

$$\frac{\partial q}{\partial x}=-\rho C_p\frac{\partial T}{\partial t} \tag{15}$$

$$q=-k\frac{\partial T}{\partial x} \tag{16}$$

Equations (15) and (16) can be reduced to a diffusion equation by substitution to get:

$$\frac{\partial T}{\partial t}=\frac{k}{\rho C_p}\frac{\partial^2 T}{\partial x^2} \tag{17}$$

The solution to Equations (15), (16) and (17) for a semi-infinite medium is given, in the Laplace domain, by OLdfield (1978) as:

$$q=\sqrt{\rho C_p k}.\sqrt{s}.\tau \qquad (18)$$

One dimensional diffusion of electrical charge through a medium with distributed capacitance per unit volume and resistance per unit length is given by Oldfield (1978) as:

$$\frac{\partial i}{\partial x}=-c\frac{\partial V}{\partial t} \qquad (19)$$

$$i=-\frac{1}{r}\frac{\partial V}{\partial x} \qquad (20)$$

Combining Equations (19) and (20) gives:

$$\frac{\partial V}{\partial t}=\frac{1}{rc}\frac{\partial^2 V}{\partial x^2} \qquad (21)$$

Equations (19), (20), and (21) can be solved in the Laplace domain to get:

$$\overline{I}=\sqrt{\frac{c}{r}}.\sqrt{s}.\overline{V} \qquad (22)$$

Note that Equations (18) and (22) have identical forms. As such analogous thermal and electrical systems can be constructed. Theoretical insight for analogy and construction of the analogous electrical system for heat flux is documented by Rockwell (1989). Only the final form of the heat flux equation, as obtained by Oldfield (1984) is presented here as:

$$q=\sqrt{\rho C_p k}\cdot\frac{1}{G}\sqrt{\frac{r}{c}}\cdot\frac{V_{out}}{R_1 V_o \alpha k} \qquad (23)$$

The term $\sqrt{(\rho C_p k)}$ is a calibration constant for the heat flux gage, $V_0\alpha k$ is the temperature coefficient of the heat flux gage and $(1/G)\sqrt{(r/c)}$ is the calibration constant for the heat flux analog circuits. The calibration constants for the heat flux analog circuits used in this study were obtained by the Rockwell and are reproduced as Table I . For details please refer to Rockwell (1989).

Table I: Calibration Data for the Heat Flux Analog Circuit.

CIRCUIT	SLOPE	ST. DEVIATION	CORRELATION
31-1Ø5	Ø.74371	1.928	Ø.99945
31-79Ø	Ø.78699	1.957	Ø.99942
31-82Ø	Ø.73212	1.67Ø	Ø.99958
31-85Ø	Ø.73858	2.ØØØ	Ø.99941
31-87Ø	Ø.79757	1.248	Ø.99955
32-1ØØ	Ø.73695	2.Ø18	Ø.99939
32-2ØØ	Ø.7Ø37Ø	2.149	Ø.99927

HEAT TRANSFER WITH FREE-STREAM TURBULENCE

Free-stream turbulence is defined as the ratio of velocity fluctuations about the mean velocity to the mean flow velocity:

$$Tu = \frac{(\overline{u^2})^{\frac{1}{2}}}{u} \qquad (24)$$

Free-stream turbulence serves to increase the rate of heat transfer. This increase in the rate of heat transfer results from the fact that the free-stream eddies get entrained in the boundary layer thereby transitioning the flow from laminar to turbulent. The free-stream eddies also have a profound effect in increasing the heat transfer in the case where the boundary layer is already turbulent.

Simonich and Bradshaw (1978) found that the ratio of Stanton numbers of flows with and without turbulence can be established for low turbulence levels (Simonich and Bradshaw, 1978 :671)

$$\frac{St}{St_o} = 1 + 5Tu \qquad (25)$$

HEAT TRANSFER WITH FILM-COOLING

As stated earlier, film cooling is an effective way of forming a protective film on a surface by injecting a cooler fluid under the boundary layer which is established by the flow of a hot stream of air over the surface.

The injected fluid can enter the boundary layer in a number of different ways. However, to keep the analysis relatively simple a flat plate with injection holes at 90^0 to the main hot stream of air has been used during this study.

With the assumption that film cooling produces turbulent

boundary layer (Kakac, et al, 1987:2-28), the heat transfer rate is expressed as:

$$q_x = h_x(T_{aw} - T_w) \qquad (26)$$

It should be kept in mind that the adiabatic wall temperature for flow with film cooling is different than the adiabatic wall temperature for flow without film cooling.

Though a number of studies on film cooling has been done in steady state facilities like wind tunnels, etc; no such literature is available for studies carried in transient facilities like shock tube. The most intriguing problem in a transient facility like the shock tube is that the flow does not get sufficient time to attain steady state conditions (steady wall temperature). This results in a situation where the adiabatic wall temperature cannot be achieved and thus measured.

The experimental data for this part of the study can thus only be presented in terms of physically measurable quantities like the heat flux, blowing rate, and the Reynolds number without any theoretical or experimental comparison.

III EXPERIMENTAL APPARATUS

SHOCK TUBE

The shock tube used for this study was the AFIT low pressure shock tube. This shock tube has four main sections: the driver section, the driven (expansion) section, the 1Ø.16 cm x 2Ø.32 cm test section and the dump tank section. Figure 4 shows a schematic of the shock tube. The high and low pressure sections: that is, the driver and the driven sections are separated by a Mylar diaphragm (available in thicknesses varying from 25.4 μm to 177.8 μm) their use being dependent on the required strength of the shock wave. For most of this study 127.Ø μm thick diaphragms were used. Ordinary compressed dry air of up to 1ØØ psig was used to pressurize the driver section of the shock tube. The pressure of the driver section "P_4" was measured by a calibrated pressure gage in inches of mercury. The pressure of the driven section "P_1" was assumed to be the same as ambient pressure. The diaphragm was ruptured by a mechanically controlled plunger.

INSTRUMENTED FLAT PLATE

An instrumented flat plate was used as the test model for the heat transfer study and was installed in the center of the test section. The plate was 64.ØØ8 cm long, 1Ø.16 cm wide, 1.915 cm thick and had a round leading edge. It was instrumented with seven heat flux gages and a single row of forty one film-cooling holes. Each film cooling hole was 1 mm in diameter and separated 1.9812 mm

center to center. Figure 5 illustrates the instrumentation of the flat plate.

FILM COOLING SYSTEM

The film-cooling holes were located 5.Ø8 cm downstream of the leading edge of the flat plate. These holes were supplied with dry filtered air from the main air supply system. The air pressure was regulated through a regulating system consisting of a dome valve and a pressure regulated air bottle. Bottle air of known pressure was applied to the reference side of the dome valve through an electrically controlled solenoid valve. This, in turn, controlled the pressure of the dry filtered air (approximately the same pressure) to a chamber supplying air to the film-cooling holes. The air pressure for the row of film-cooling holes was measured by a pressure transducer located in the pipe connected to the air chamber. Figure 6 shows a schematic of the film-cooling system.

TURBULENCE GENERATING SYSTEM

A turbulence generator system was used to form an air grid across the shock tube so as to generate free-stream turbulence in the flow over the flat plate. The turbulence generator was installed just in front of the leading edge of the flat plate. Figure 6 illustrates a schematic of the turbulence generating system. Regulated, dry, filtered air was injected perpendicular to the flow at twelve locations: two each on top and bottom walls of the turbulence generator and four each on the side walls. The

supply of high pressure air at these locations formed a strong air grid across the on-coming flow in the shock tube. This yielded an increase in the free-stream turbulence intensity.

FLOW VISUALIZATION

The schlieren flow visualization system was used to obtain images of the boundary layer and shock patterns across the test section. Two mirrors of 3Ø" focal length, along with a spark source, a camera and a knife edge, were used to obtain photographs of the flow across the plate. The spark source, supplied by a high voltage power supply, was triggered by a delayed voltage signal from the front pressure transducer. The voltage signal was delayed by a combination of the Cordin proportional delay generator Model 435 and a Cordin delay generator Model 453. The flow images were captured on Polaroid type 52 (ASA 3ØØØ) film. Figure 7 illustrates the configuration of the schlieren system.

INSTRUMENTATION

1. THIN-FILM HEAT FLUX GAGES

Seven thin-film heat flux gages were mounted along the centerline of the plate, spaced proportionally downstream of the film cooling holes. Figure 8 shows the proportional location of the heat flux gages along the instrumented plate. The thin-film gages are made of a platinum film Ø.5 mm wide and Ø.1 μm thick deposited on a Pyrex 774Ø substrate. The $\sqrt{(\rho C_p k)}$ value of the heat flux gages was obtained by calibration of the gages. The temperature

coefficient "$V_0 \alpha k$" used in equation 3 was also obtained by calibration. The heat flux gages available for this study were gage numbers 2, 4, and 6, counting from the leading to trailing edge of the plate. These gages were powered by an excitation voltage from the PSC 8Ø15-1 dc amplifier.

2. PRESSURE TRANSDUCERS

Two Endevco Model 853ØA-1ØØ pressure transducers were flush mounted on the top wall of the shock tube. The forward pressure transducer was 1.1811 m upstream of the leading edge of the flat plate whereas the rear pressure transducer was located Ø.4699 m upstream of the plate leading edge. A third pressure transducer was located upstream of the film cooling air supply line to ensure accurate measurements of the film cooling air pressure. The excitation voltage to all three pressure transducers was supplied by a Power Mate Corporation power supply. The main purpose of the pressure transducers in the shock tube was to measure the time interval between their responses to the pressure change induced by the passage of a shock wave. This lapse time was then used to calculate the speed of shock wave and thus its Mach number. During schlieren photography the output of the front and rear pressure transducers was supplied to the time delay generators to control the timing for the photography. The front pressure transducer was also used to trigger the DL-12ØØ Datalab recorder, to be described forthwith. Calibration details of these pressure transducers is given in Appendix D.

3. HOT WIRE ANEMOMETER

To measure the turbulence level of the flow behind the normal shock wave, a TSI model intelligent flow analyzer model IFA 100, embedded with a hot wire anemometer, was used to provide and measure the hot wire bridge output voltage. A TSI model 1214-10 hot film sensor was mounted in the test section to collect the required data.

4. THERMOCOUPLE

The calibration procedure to obtain the temperature coefficient of the heat flux gages required a thermocouple to measure the temperature of the water bath. A K type (chromel-alumel) thin foil thermocouple was used in conjunction with a battery powered ice point for temperature measurements. The temperature of the water bath was indicated in ^{0}F on a previously calibrated Omega Digicator.

5. SIGNAL GENERATOR

The procedure used to obtain the $\sqrt{(\rho C_p k)}$ values of the heat flux gages required that a square pulse of known amplitude, period and width be applied to the heat flux gage connected as one leg of a bridge circuit. Application of such a pulse raised the temperature of the gage. This changed the resistance of the platinum foil in the heat flux gage which in turn produced a measurable voltage by the bridge circuitry. To produce a single

square pulse of known amplitude, period and width a Wavetek Model signal generator was used during the calibration phase.

6. PSC MODEL BRIDGE/AMPLIFIER

The response of a heat flux gage to any temperature change can be measured by replacing one leg of a Wheatstone bridge circuit with the heat flux gage. A temperature change in the environments of the heat flux gage unbalance the previously balanced bridge and thus the output of the bridge. The PSC 8115 provided the three legs of the bridge circuitry with precision resistors and a variable resistor in parallel to the leg opposite to the heat flux gage, thereby enabling the user to balance the bridge. The constant bridge excitation voltage was set at 2.5 volts for each bridge circuit in series with a 1ØØØ Ω precision resistor. This limited the supply current to a nominal value of 2.5 mamps to avoid damage to the heat flux gages.

Any temperature change sensed by the heat flux gage changed the resistance of the gage by a proportional amount and thus unbalanced the bridge. The output of the bridge, being extremely low, required high amplification. Thus an amplifier circuit was also required for each bridge module in use. PSC 8Ø15-1 high gain differential amplifiers were used for this purpose. The bridge/amplifier circuits for each heat flux gage were card mounted and installed in a Transamerica instruments rack designed for these modules.

6. HEAT TRANSFER ANALOG CIRCUIT

The heat transfer analog circuit, designed by Rockwell (1989) was used to convert the amplified output of the heat flux gages into potential heat flux. The output of the heat flux analog in combination with the calibration constants resulted in the measured heat flux (Equation 31). A block diagram of the analog circuit is shown in Figure 9. The details of construction and working of the heat flux analog circuit were reported by Rockwell (Rockwell, 1989).

7. WAVE FORM RECORDER

A high-speed digital data recorder, Datalab DL 12ØØ, was used to record the required output from the respective instruments. The DL-12ØØ waveform recorder is a 12 bit device that transforms an analog voltage input to a digital value for eight channels simultaneously. Each channel has its own gain and filter settings. During the course of this study each channel was sampled at its maximum sampling rate, i.e one sample per channel every 2 μs. The recorded data from each test was then downloaded from the DL-12ØØ 12 bit memory to Zenith 16 bit computer and stored for analysis.

8. SIGNAL DELAY GENERATORS

The Cordin proportional and simple delay generators were used to delay the voltage signals, from the front pressure transducer, used to trigger the spark source of the schlieren system. The delay time on both the delay generators can be set such that the combination of the two equals the time required for

the shock wave to be positioned at a point desired by the operator. The combination of two delay generators was relatively easier to handle than using Cordin Model 453 delay generator only.

IV EXPERIMENTAL PROCEDURE

The basic requirement for any experimental set-up is to have a sensing element which can discern the requisite information for further analysis. As mentioned earlier, the sensing elements used during this study to measure heat flux were the thin film heat flux gages. However, to analyze the data obtained by the heat flux gages, knowledge about some of the properties of the heat flux gages was required. These properties were the temperature coefficient, $V_0 \alpha k$, and bulk thermal diffusivity, $\sqrt{\rho C_p k}$. These properties can either be obtained from theoretical data or established by calibration. To acquire credible results it was desirable to choose the latter option of calibrating the heat flux gages.

CALIBRATION OF HEAT FLUX GAGES

1. CALIBRATION FOR TEMPERATURE COEFFICIENT

The calibration circuit used to obtain the temperature coefficient of the heat flux gages is shown in Fig 1Ø. The calibration procedure adopted was as follows:-

The heat flux gages, flush mounted on the flat plate, were loosened such that with the plate inverted they could dangle freely.

The gage to-be-calibrated was then connected as one leg of the wheatstone bridge already built in the PSC 8115 bridge module.

The PSC 8Ø15-1 differential amplifier controls were set at a gain 25Ø and a filter setting of 1Ø kHz. The circuit was then zeroed out by cycling through the internal zeroing routine pre-programmed into the module.

Setting the bridge/amplifier module at an AMP-D mode and connecting the bridge output to a previously zeroed voltmeter, the variable resistor on the PSC 8115 bridge module was used to balance the bridge.

The heat flux gage was then placed in a water proof, thin plastic bag along with a J-type thermocouple. An Omega digicator, which sensed the thermocouple output, referenced it to its internal ice point and displayed the temperature of the water bath in degrees Fahrenheit.

A 1ØØØ ml beaker filled with about 75Ø ml of water was placed on a thermal mixer. A magnetic stirrer was then placed inside the beaker. The plastic bag, containing the heat flux gage and the J-type thermocouple, was then submersed in the water bath such that the water could not enter the bag.

The thermal mixer was turned "on" so as to slowly mix the water to eliminate any hot spots. The heating element was then turned "on" to a slow heating position so as to minimize the difference between the response times of the gage and the thermocouple. A schematic of the instrument interfacing for this calibration is shown in Figure 11.

A change in the digicator display was noted along with the output voltage of the now unbalanced bridge. A total of 11 such

readings of the digicator and the output voltage of the bridge, indicating the response of the heat flux gage to the change of temperature of its environments, were taken for each heat flux gage.

The calibration data was then plotted and the slope of the fitted curve gave the temperature coefficient of the heat flux gage. Table II shows the temperature coefficients to the heat flux gages calibrated for this study. The calibration plots are shown in Appendix C.

Table II: Temperature Coefficients of the Heat Flux Gages.

Gage Number	Gage Serial Number	α (V/^{0}F)
2	516	Ø.Ø241ØØ6
4	5Ø3	Ø.Ø236467
6	12Ø	Ø.Ø178865

2. CALIBRATION FOR BULK THERMAL DIFFUSIVITY $\sqrt{(\rho C_p K)}$

Thin film heat flux gages consist of a very thin platinum film, Ø.5 mm wide and Ø.1 μm thick, deposited on Pyrex 774Ø substrate. The calibration method required to obtain the $\sqrt{(\rho C_p K)}$ values of the Pyrex 774Ø substrate used in the heat flux gages is a development of a pulse technique. Figures 12 and 13 show the bridge circuit and the instrument interfacing used for calibration.

A step current, of known amplitude, is applied to the heat flux gage which acts as one leg of the balanced bridge. The

passage of current allows the platinum film to heat up thereby changing its resistance. This change in resistance unbalance the bridge and the output voltage can be recorded to the DL-12ØØ.

A small droplet of liquid, of known bulk thermal diffusivity, (in this case glycerine) is then deposited on the surface of the heat flux gage. With the bridge balanced, current of the same amplitude as before is again passed through the heat flux gage. This time heat flows both into the substrate of the gage and glycerine. The output voltage of the now unbalanced bridge is recorded to the DL-12ØØ.

The two voltage records have the same time dependence but different amplitudes. For illustration refer to Figure 14. As can be seen from the figure, the output voltage of both the experiments is parabolic in nature. This would imply that a linear relationship can be established between the change in resistance ΔR of the platinum foil of heat flux gages and $\sqrt{t}$.

If $\Delta R_1/\sqrt{t}$ is the slope of the linearly fitted curve obtained from an experiment in air and $\Delta R_2/\sqrt{t}$ is the slope of the linearly fitted curve obtained from an experiment in glycerine then, following the analysis given in Shultz and Jones (1973), the correct value of $\sqrt{\rho C_p k}$ of the Heat Flux gage substrate can be obtained from the relationship:

$$\sqrt{(\rho C_p k)}_{subs} = \frac{\sqrt{(\rho C_p k)}_{gly}}{\frac{\Delta R_1/\sqrt{t}}{\Delta R_2/\sqrt{t}} - 1} \qquad (27)$$

A complete derivation of this expression is given as Appendix

A.

Since constant current of equal amplitudes is passed through the heat flux gages in both experiments, Equation (27) can also be written as:

$$\sqrt{(\rho C_p k)}_{subs} = \frac{\sqrt{(\rho C_p k)}_{gly}}{\frac{\Delta V_1/\sqrt{t}}{\Delta V_2/\sqrt{t}} - 1} \qquad (28)$$

where the bulk thermal diffusivity for glycerine is:

$$\sqrt{\rho C_p k}_{gly} = 925 J.cm^{-2}.^{\circ}K^{-1}.sec^{-\frac{1}{2}} \qquad (29)$$

Table III shows the results obtained during the calibration of the thin-film heat flux gages used to carry out this study.

Table III: Bulk Thermal Diffusivity of Heat Flux Gages.

Gage Number	$\Delta V_1/\sqrt{t}$	$\Delta V_2/\sqrt{t}$	$\sqrt{\rho C_p k}_{subs}$
516	Ø.1Ø1388	Ø.Ø63Ø46	1521
5Ø3	Ø.Ø81732	Ø.Ø52482	166Ø
12Ø	Ø.Ø17Ø39	Ø.Ø1Ø646	154Ø

A detailed calibration procedure for determining the bulk thermal diffusivity of the heat flux gages used during this research is given in Appendix B. The calibration curves are also given in Appendix B.

SHOCK GENERATION

To achieve repeatable free-stream flow conditions a Mylar diaphragm of the same thickness was used and the shock speed was monitored for every run. The same shock speed for two different runs essentially means that the free-stream flow properties behind the shock wave are same for both the runs. This implies then that they would also produce the same heat transfer at some given point on the flat plate. During the film-cooling and turbulence generation runs, to avoid any flow anomalies from occurring in the boundary layer, film-cooling/turbulence generation were initiated at approximately the same time the shock was generated by bursting the Mylar diaphragm between the high and low pressure sections of the shock tube.

DATA COLLECTION

All the data required for analysis was amplified and filtered through the PSC 81Ø15-1 differential amplifier. The amplifier was set at a gain of 1ØØØ and a Low Pass filter of 3 kHz. This amplified and filtered data was then converted into heat flux voltages through the heat flux analog and recorded in the datalab DL-12ØØ recorder. The DL-12ØØ recorder was remotely controlled by an upgraded Z-248 computer. For almost all the test runs the DL-12ØØ was set at the following settings:

TRIGGER LEVEL	PRE DELAY	SAMPLE INTERVAL
4%	5%	2 μsec

A NEWDL software package was used to interface the DL-12ØØ and Z-248 computer whereas a POST program, developed by Rockwell (1989), was used for data reduction and analysis.

V. DATA REDUCTION

SHOCK MACH NUMBER

The shock Mach number was measured for every run. The passage of a shock across the front and rear pressure transducers and the heat flux gages caused a significant increase in the output voltage of each sensor because of changed flow conditions. The time of passage of the shock wave across these sensors can be determined from their output. Knowing the lapse time between the passage of the shock wave across the front and rear pressure transducers and the distance between them, the shock speed was evaluated by using the equation:

$$U_s = \frac{\Delta x}{\Delta t} \tag{30}$$

The temperature T_1 of the driver section of the shock tube is assumed to be the same as ambient temperature. The Mach number of the shock wave was determined by using equation:

$$M_s = \frac{U_s}{\sqrt{\gamma R T_1}} \tag{31}$$

Having calculated the shock Mach number, the temperature, pressure, Mach number,and the density of the flow behind the shock wave and its velocity with respect to the hardware of the shock tube was determined.

TURBULENCE INTENSITY

The purpose of measuring the free-stream turbulence and the

generated turbulence intensities was to verify the measurements made by Rockwell (1989) and study their effect on the heat transfer solution of the flat plate.

The procedure for turbulence measurements was also adopted from Rockwell (1989). Several test runs were made using the same driver pressure of 1ØØ in of Hg but different hot film overheat parameter. The TSI 1214-1Ø hot film probe with a 9Ø° arm and probe support was placed, through the top wall of the shock tube, such that the hot film was perpendicular to the flow and about 3 cm above the forth heat flux gage. The $9Ø^0$ arm support was used to minimize the vibrations caused by the passage of the shock wave. Beside the TSI 1214-1Ø hot film probe other probes like TSI 1214-T1.5 hot wire probe and TSI 1214-2Ø hot film probes were also tried. However, as can be seen from Figure 15, the TSI 1214-T1.5 hot wire probe showed periodic oscillations caused by the vibrations due to the passage of the shock wave whereas the TSI 1214-2Ø hot film probe was too slow to respond during the short duration of the test runs. High frequency vibrations could also be seen in the data obtained from the TSI 1214-1Ø hot film probe but since most of the turbulence data occurs between 5 Hz and 1Ø kHz frequencies above 1Ø kHz were filtered out without damaging the integrity of the data.

The TSI 1214-1Ø hot film probe was connected to the IFA 1ØØ. The output of the IFA 1ØØ was recorded on DL 12ØØ which was triggered by a signal from the front pressure transducer generated by the passage of a shock wave.

The POST program was used to filter out the high frequency spikes from the data and then used to calculate the mean and rms values of the data. The turbulence sub-routine in the POST program calculated and plotted a least quadratic fit between the ratio $(4V_{rms}^2/V_{mean}^2)$ and the hot film over heat parameter. The turbulence intensity of the flow was obtained from the y-intercept of the least quadratic curve fit. For theoretical details refer to Rockwell (1989).

The same procedure was repeated with the turbulence generator "on" and the results were then compared with those obtained by Rockwell (1989).

HEAT TRANSFER

Figure 16 shows the circuitry and interfacing of the instrumentation used to determine the heat flux into the flat plate.

The flow behind the shock is at an elevated temperature compared to the flat plate and the flow in front of the shock wave. This flow of hot air over the plate results in heat transfer to the flat plate. The heat flux gages sense the change of the flat plate temperature caused by the change in its environment and respond almost instantaneously. The change in resistance of the platinum foil of the heat flux gages unbalance their respective bridge circuitry in the PSC 8115 modules. This results in a voltage output by the PSC 8115 modules which is amplified and filtered by the differential amplifiers in the PSC 81Ø5-1 modules. The

amplified and filtered output of the PSC 8Ø15-1 modules is fed into the heat flux analog which converts the raw voltages into heat flux voltages. These voltages are recorded by the DL-12ØØ for storage by the Z-248 computer. Multiplying the heat flux voltages with the calibration constants of their respective heat flux gages give the actual heat transfer into the flat plate at each specific location.

FILM-COOLING

The process of data collection and reduction for film-cooling runs was essentially the same as that for the heat transfer runs. The main feature of the film-cooling runs was to determine the blowing ratio, B, and its consequent effects on the rate of heat transfer. The pressure of the coolant flow was determined from the pressure transducer located a short distance from the coolant chamber of the flat plate. Refer to Figure 6 for an illustrative schematic of the film cooling system.

Knowing both the pressures of the coolant flow and the flow behind the shock wave the velocity of the coolant flow can be determined from equation:

$$\frac{P_{oc}}{P_2} = \left(1 + \frac{\gamma - 1}{2} M_c^2\right)^{\frac{\gamma}{\gamma - 1}} \qquad (32)$$

Since the velocity and the density of the coolant and the primary flows are now known, the blowing ratio, B, into the primary flow can be determined from the relationship expressed as:

$$B=\frac{\rho_c V_c}{\rho_2 V_2} \tag{33}$$

If the pressure of the coolant flow is continuously increased a stage would come when the Mach number of the coolant flow would reach unity. The velocity of the flow at this point can be determined by the equation (Zucrow and HOffman, 1976):

$$V_{t_{max}}=C_{o2}\left(\frac{2}{\gamma+1}\right)^{\frac{1}{2}} \tag{34}$$

Under such conditions the flow is said to be choked. Any further increase in the pressure of the coolant flow would not increase the velocity of the flow. Instead, the density of the flow would continue to increase and thus increase the blowing rate. The density of the choked coolant flow can be determined from the equation:

$$\rho_c=P_{oc}\frac{\left(\frac{2}{\gamma+1}\right)^{\frac{\gamma}{\gamma-1}}}{2RT_{oc}}(\gamma+1) \tag{35}$$

VI. RESULTS AND DISCUSSION

SHOCK MACH NUMBER

The theoretical Mach number of a shock wave can be calculated by using Equation 2. However, experimental observations show that for identical pressure ratio P_4/P_1 the shock Mach number calculated experimentally, using Equation (31), is not quite the same as that calculated theoretically. Table IV shows the minor variations between the experimental and theoretical shock Mach numbers for the same pressure ratio.

TABLE IV: COMPARISON OF MEASURED AND THEORETICAL SHOCK Mach Number

DATA RUN NUMBER	PRESSURE P_4" Hg	PRESSURE P_1" Hg	EXPERIMENTAL SHOCK MACH NO	THEORETICAL SHOCK MACH NO
RØØ2	6Ø	29.Ø7	1.2Ø9	1.268
RØØ4	8Ø	29.Ø7	1.269	1.323
RØØ6	1ØØ	29.Ø7	1.32Ø	1.369
RØØ8	12Ø	29.Ø7	1.36Ø	1.4Ø9
FC6Ø3	6Ø	29.3Ø	1.197	1.26Ø
FC6Ø5	6Ø	29.3Ø	1.197	1.26Ø
FC8Ø4	8Ø	29.2Ø	1.265	1.3Ø4
FC8Ø6	8Ø	29.2Ø	1.265	1.3Ø4
FC1ØØ7	1ØØ	29.2Ø	1.31Ø	1.358
FC1ØØ9	1ØØ	29.2Ø	1.31Ø	1.358

QUALITATIVE FLOW CHARACTERISTICS

Schlieren photography was used for qualitative flow analysis. Images of the flow were captured on Polaroid Type 52 film. Shock patterns over the flat plate can be seen from the photographs shown in Figures 17 - 2Ø. The boundary layer can be seen to have substantial activity indicating that the boundary layer is turbulent which is in accordance with the heat transfer results discussed in the later portion of this chapter. From close observation of the photographs some flow activity beyond the boundary layer may be observed which can be speculated to be free stream turbulence. Such images are more enhanced in photographs of flow when using the turbulence generator which could be a further confirmation that it does increase free stream turbulence. However, such speculations can be brought to further substance by using high speed photography.

The most interesting part of Schlieren photography was with film-cooling tests. As can be seen from the comparison of Figures 17 - 2Ø, the film cooled boundary layer may grow substantially in thickness compared to the uncooled boundary layer. As will be discussed in the film cooling section of this chapter, an increase in the film cooling flow beyond a certain point causes an increase in the thickness of the boundary layer and has the adverse effect of increasing the heat transfer. High speed photography could also be useful in optimizing the method of introducing the cooling air.

During the film-cooling tests it was observed from the heat transfer data (to be discussed later) that an instantaneous spike

occurred at about 1.5 ms of the shock passage across each heat transfer gage. Since the heat flux gages could not be seen by the camera in the test section, a new test section with the heat flux gages visible through the windows, had to be installed in an effort to capture the view of the flow over the heat flux gages at that particular time.

FLOW PROPERTIES BEHIND THE SHOCK WAVE

The passage of shock wave across a medium produces abrupt changes in the properties of the flow across the medium . The pressure, temperature and density of the flow behind the shock wave increases whereas the velocity decreases. The accuracy of the measurements of these properties determine the validity of the heat transfer solution.

The normal shock tube relationships given by Equations (3) to (5) determine the theoretical pressure, temperature and velocity of the flow behind the shock wave.

The pressure behind the shock wave was measured experimentally by the front and rear pressure transducers located at some distance upstream of the flat plate. The temperature and velocity measurements, under the present set up, were difficult to make because of the very short duration of the test runs. As such the theoretical values of temperature and velocity, based on the measured shock speed, were used for analysis of all experimental data.

Flow properties like viscosity and thermal conductivity were

evaluated at reference temperature calculated by using Equation (15). The adiabatic wall temperatures were evaluated using the theoretical temperatures and Mach numbers behind the shock wave, based on measured shock speed. The data presented as Appendix E represent the flow properties evaluated from the above mentioned equations.

It may be noted that a large error between the actual and measured properties would pronouncedly influence the heat transfer solution. A discussion to such effect follows later in this chapter.

Real complications of evaluating the data occurred with the film cooling studies. Since the adiabatic wall temperature of a film cooled surface is different than the adiabatic wall temperature of a surface with no film-cooling, Equation 16 could not be used for a film-cooled case. The transient nature of the tests did not allow the surface to reach an adiabatic condition and thus neither could Equation (16) be used for theoretical calculation of the adiabatic wall temperature (which would have been a misrepresentation) nor was there any other way of getting around the problem. The lack of knowledge of such an important property of the flow prevented the evaluation of properties like film-cooling effectiveness, heat transfer coefficient, Nusselt number and Stanton number. The absence of such an erudition strictly limited the investigation of the data obtained during this part of the study. A discussion to this effect follows in the section of heat transfer with film-cooling.

TURBULENCE INTENSITY

To acquire a true heat transfer solution to the flat plate problem, knowledge of the free-stream turbulence level and the effect of increasing free-stream turbulence on heat transfer was required. This part of the study was a repetition of the work carried out by Rockwell (1989). For comparison purposes, the same methodology, as adopted by Rockwell (1989) from Oldfield (1984), was employed to determine the free-stream turbulence level of the flow in the shock tube.

Table V presents the data obtained during the turbulence runs and was used to determine the turbulence intensity of the flow.

TABLE V: Turbulence Data obtained from Turbulence Runs

Background Turbulence			Turbulence Generation		
Run No	$R_d(\Omega)$	$4V_{rms}^2/V_{mean}^2$	Run No	$R_d(\Omega)$	$4V_{rms}^2/V_{mean}^2$
H2Ø1	7.5	Ø.ØØØ454	T1Ø1	6.5Ø	Ø.ØØØ7Ø2
H2Ø2	7.6	Ø.ØØØ455	T1Ø2	6.75	Ø.ØØØ5Ø8
H2Ø3	7.7	Ø.ØØØ545	T1Ø3	7.ØØ	Ø.ØØØ593
H2Ø4	7.8	Ø.ØØØ431	T1Ø4	7.25	Ø.ØØØ468
H2Ø5	7.9	Ø.ØØØ4Ø3	T1Ø5	7.5Ø	Ø.ØØØ524
H2Ø6	8.Ø	Ø.ØØØ48Ø	T1Ø6	7.75	Ø.ØØØ448
H2Ø7	8.1	Ø.ØØØ592	T1Ø7	8.ØØ	Ø.ØØØ586
H2Ø8	8.2	Ø.ØØØ572	T1Ø8	8.25	Ø.ØØ125Ø
H2Ø9	8.3	Ø.ØØØ582	T1Ø9	8.5Ø	Ø.ØØ179Ø

Plots of the ratio ($4V_{rms}^2/V_{mean}^2$) against the overheat parameter are shown in Figures 21 and 22. Figure 21 shows a quadratic curve fit of the background turbulence data whereas Figure 22 shows a quadratic curve fit of the data obtained when the turbulence generator was used. Table VI shows the turbulence intensities obtained from the quadratic curve fits of Figures 21 and 22.

Table VI: Measured Turbulence Intensities

Background Turbulence	Turbulence Injection
9.4%	11.6%

The background turbulence level of the flow behind the shock wave was found to be a relatively high 9.4%. The turbulence generator did not help much in increasing the turbulence level of the flow. The increased turbulence intensity, due to turbulence generation, was found to be 11.6%. These values of turbulence intensities correspond extremely well with the results of Rockwell (1989) and the forthcoming heat transfer data.

It would be worthwhile to note that though the turbulence intensity values of this study and the ones obtained by Rockwell (1989) correlate extremely well, the verity of the matter that the hot film exhibit vibrations after the passage of a shock wave thwart the confidence in the data. The use of a probe specially designed to dampen dynamic loadings caused by the passage of a shock wave can substantially increase our confidence in the data.

Such probes can be provided by TSI corporation on special orders.

HEAT TRANSFER WITHOUT FILM-COOLING

The passage of a shock wave across a flat plate in the shock tube initiates a high temperature flow, following the shock wave. The resulting heat flow into the plate causes its temperature to increase. This change in the plate temperature is sensed by the heat flux gages. The response of the heat flux gages in terms of temperature change is illustrated by Figures 23 to 25. It can be observed from these figures that a step change in the environment produces a parabolic response by the heat flux gages. Though the difference between the temperatures of the flow and the plate is quite high, the rise in the plate temperature is very nominal because of the very short duration of the test runs.

The output of the heat flux gages, after filtering and amplification, were converted into analog voltages by the analog circuits and finally into actual heat flux by using Equation (23). Figures 26 to 28 represent the plots exhibiting the heat flux into the flat plate as a function of time. Note that all these figures show three distinct regions. The region immediately following the passage of the shock wave in this impulsively started flow initially have no boundary layer and therefore the rate of heat transfer to the flat plate is high. Rapidly following the shock wave is the formation of an unsteady boundary layer which starts reducing the heat flux to the plate. This unsteady boundary layer, however, transitions fairly quickly into a steady boundary layer

which may still be laminar. This whole region is denoted as laminar region in Figure 26. The small bump in the data within this region, which is consistent for all the heat flux gages, may well be the transitioning of the unsteady boundary layer into steady laminar boundary layer. Following the laminar region is the region of low heat transfer to the flat plate which is denoted by transition region in Figure 26. The boundary layer within this region transitions from laminar to turbulent. The third region, denoted by turbulent region, is a region of fairly constant heat transfer. The boundary layer in this region is fully turbulent.

Figures 23 - 25 are also indicative of the advantage of using the heat flux analog circuit in which case, unlike other analytical techniques, instantaneous values of heat flux can be calculated without getting negative values of heat flux.

To determine properties like Nusselt number, and Stanton number of the flow, an average heat flux value for the turbulent region was determined from the heat flux versus time plots. The Nusselt number and Stanton number for each run were then determined by using the following equations:

$$h_x = \frac{q_{avg}}{(T_{aw} - T_w)} \tag{36}$$

$$Nu_x = \frac{h_x x}{k} \tag{37}$$

$$St_x = \frac{h_x}{\rho C_p U_2} \tag{38}$$

From the results of the free-stream turbulence it was established that the turbulence intensity of the flow with and without turbulence generation was 11.6% and 9.4% respectively. The presence of turbulence in the free-stream flow is expected to affect the rate of heat transfer. Such an effect can be seen in Figures 29 and 3Ø.

Figure 29 shows Stanton number as a function of Reynolds number. The solid and the dotted lines represent the theoretical Stanton number as a function of Reynolds number with zero and 9.4% free stream turbulence respectively. The solid line was obtained from Equation 46 whereas the dotted line was obtained from Equation 33. The experimentally calculated Stanton numbers, represented as data points on the Figure 29, correspond fairly well to the 9.4% free-stream turbulence curve.

Figure 3Ø is a representation of similar data obtained from flow with 11.6% free-stream turbulence. The heat transfer data, in terms of Stanton number, seem to have a fair agreement with the theoretical data.

Such a compatibility between experimental and theoretical results validates the authenticity of the experimental data. A comparison of this data with Rockwell (1989) reveals the importance of calibration of the heat flux gages for $\sqrt{(\rho C_p k)}$. The profound scatter in Rockwell's data is fairly attributable to the fact that he used a book value of 1388.84 $J/s^{\emptyset.5}\text{-}m^2\text{-}^\circ K$ for all the heat transfer gages whereas in actual the $\sqrt{(\rho C_p k)}$ value of heat flux gages is quite different than the book value (refer to calibration

curves in Appendix B). The use of correct values of the calibration constants reduces this scatter to a great extent and can be seen from the comparison of Figure 29 with the data of Rockwell (1989) shown in Figure 31.

HEAT TRANSFER WITH FILM-COOLING

To determine the effects of film-cooling on the heat transfer solution, cool air was injected into the turbulent boundary layer formed on the surface of the flat plate due to the passage of hot air following the shock wave. Several test runs, at three different driver pressures of 6Ø, 8Ø and 1ØØ in of Hg, were made. Assuming very slight variations in the properties of the primary flow from run to run for each pressure, coolant air was blown into the boundary layer at pressures such that any desired blowing ratio could be maintained. The pressure of the coolant air was maintained through the film cooling system described previously. The blowing ratio was determined from Equation 33, whereas the properties of both the coolant and the primary flows were determined from a series of equations stated in Chapters II and IV.

Examining the output of the heat flux gages in terms of the rise in temperature of the flat plate. Figure 32 shows the outputs of Gage No 2 for four different test runs with three different blowing ratios but the same driver pressure. With an increase in the blowing rate, the rate of change of temperature decreases. However, the output curve with the highest blowing ratio shows that the temperature of the plate has started increasing though the rate

of change of temperature has decreased. This is demonstrative of the fact that there comes a point during the process of film-cooling beyond which any further increase in the blowing ratio starts showing adverse effects. It may be mentioned here that the slight shift in the initial values of the data can be attributed to the slight changes in the ambient conditions taking place during the span of time in which the data was taken.

Analyzing next the effects of film-cooling on heat transfer into the flat plate; Figures 33 to 42 show a few examples of the heat flux as a function of time for the film-cooling runs. A systematic observation of these graphical representations show that the heat flux decreases with increasing blowing ratio. However, as stated before, a stage does arise where any further increase in the blowing ratio does not decrease the heat flux any more. Instead, the heat flux tends to start increasing. This reverse increment of the heat flux could not be explored deeply due to hardware limitations.

One important change that can be observed by comparison of the heat flux output of test runs without film-cooling to that of the output of test runs with film-cooling is an impulsive fluctuation in the heat flux at about 2.Ø msec after the shock passage over an individual heat flux gage in the later case. The reason for such a phenomenon, however, is not clear at present.

Ignoring the above mentioned phenomenon, the heat flux outputs of the gages reveal another important and understandable fact about the film-cooling effectiveness in terms of heat transfer. A

comparison of Figures 43 and 44, both for different gage locations, show that the film-cooling effectiveness (not by definition but by its ability to reduce heat transfer) of the injected coolant air decreases along the length of the flat plate. An illustration to this effect can be seen, though grimly, from the limited data presented in Figure 45. The data limitation arises from the fact that only three of the seven heat flux gages mounted along the length of the plate were available for data collection.

The observations pertaining to the effects of film-cooling on the rate of heat transfer to the flat plate cannot be concluded with a forceful argument without its comparison to theoretical or other experimental research.

Heat transfer, in common, is mostly represented in terms of heat transfer coefficient and Stanton/Nusselt numbers. To determine the Stanton/Nusselt numbers the heat transfer coefficient is a required element. For high speed flows, the heat transfer coefficient can be determined from the equation:

$$h_x = \frac{q_x}{T_{aw} - T_w} \tag{39}$$

which means that knowledge of heat flux q_x, adiabatic wall temperature T_{aw} and the wall temperature T_w is imperative.

What is important to note in this study is that the testing facility -the shock tube- is transient in nature implying that the short duration of test time does not allow the test piece, in this case the flat plate, to reach an adiabatic state and thus the adiabatic wall temperature cannot be determined.

Film-cooling is most commonly analyzed in terms of film-cooling effectiveness which for high speed flows is defined by the equation:

$$\eta = \frac{T_{aw} - T_2}{T_t - T_2} \qquad (40)$$

As mentioned earlier, lack of such critical information blindfolded this analysis from expansion into some extremely important aspects of analysis thereby compelling it to remain within the limits of utilizing the only available data of heat flux from the heat flux gages.

As such Figures 46 shows a plot of heat flux ratio "q/q_0" as a function of blowing ratio "B". The three curves represent the effects of increasing blowing ratio at different driver pressures, in this case 6Ø, 8Ø and 1ØØ" Hg. The three important aspects of film-cooling, for the range of conditions investigated, revealed by this figure are:

1. An increase in the primary flow conditions: i.e, pressure, temperature and Mach number of the primary flow,, the effectiveness of film-cooling in reducing the heat transfer to the flat plate decreases.

2. A maximum decrease in the rate of heat transfer (represented by the minima of the curves) occurs at a point where the injected coolant flow gets choked. Beyond this point, any further increase in the blowing ratio starts showing adverse effects in terms of increasing the heat flux to the flat plate.

3. The point of minimum heat transfer shifts upwards (higher

rate of heat transfer) and towards a lower blowing ratio by increasing the primary flow conditions.

4. The rate of decrease of heat flux to the flat plate is identical for all the three primary flow conditions up to a blowing ratio of unity. Beyond this point the data starts segregating on the basis of individual primary flow conditions.

Table VI shows a consolidated form of the above discussion in terms of numerical values:

TABLE:VI Film Cooling Results

P_4 = 6Ø" Hg			P_4 = 8Ø" Hg			P_4 = 1ØØ" Hg		
R.NO	B	q/q_0	R.NO	B	q/q_0	R.NO	B	q/q_0
FC6Ø2	Ø.3Ø	1.ØØ	FC8Ø1	Ø.34	1.ØØ	FC1ØØ1	Ø.37	1.ØØ
FC6Ø4	1.22	Ø.88	FC8Ø3	1.39	Ø.88	FC1ØØ2	1.Ø2	Ø.93
FC6Ø6	2.51	Ø.7Ø	FC8Ø5	2.97	Ø.68	FC1ØØ3	1.99	Ø.85
FC6Ø8	3.93	Ø.58	FC8Ø7	3.23	Ø.6Ø	FC1ØØ5	2.81	Ø.78
FC61Ø	5.Ø1	Ø.52	FC8Ø8	3.45	Ø.56	FC1ØØ6	3.Ø8	Ø.68
FC612	6.63	Ø.61	FC81Ø	3.9Ø	Ø.58	FC1ØØ7	3.46	Ø.7Ø
FC614	7.93	Ø.64	FC811	4.57	Ø.6Ø	FC1ØØ8	3.83	Ø.73
FC616	9.22	Ø.66	FC812	5.Ø2	Ø.64	FC1Ø1Ø	4.58	Ø.82

Note:- The shaded portion of the Table VI indicate that the flow is choked.

It may, however, be noted here that the qualitative analysis of the effects of film-cooling on heat transfer from the schlieren photography reveal a somewhat different viewpoint. A systematic view of the schlieren photographs shown in Figures 18 - 2Ø show that by increasing the blowing ratio of the film-cooling flow to about Ø.8 the boundary layer on the flat plate increases with no observable indication of an increase in turbulence or the separation of the boundary layer. Any further increase in the blowing ratio beyond Ø.8 separates the boundary layer from the surface of the plate. Though the boundary layer quickly attaches back to the surface, the turbulence withen the boundary layer increases significantly. This should indicate a decrease in the effectiveness of the film-cooling flow. However the quantitative analysis of the data obtained in terms of heat transfer from the heat flux gages, discussed in the preceding paragraphs, contradict this qualitative analysis. A better understanding of such contradictions could be possible by using high speed photography for qualitative analysis.

In view of the data available it can only be speculated that film cooling is most effective in high speed flows at the early choked conditions of the film cooling flow through discrete holes. However, a complete picture of the scenario can only be determined after obtaining the knowledge of properties like the adiabatic wall temperature of the plate and the heat transfer coefficient of the flow with film cooling or by determining empirical relationships which would allow estimation of these properties.

VII CONCLUSIONS

1. Calibration of the properties of sensing elements that have a direct effect on the outcome of a solution is extremely necessary and important. The effect of correct calibration constants could seriously be felt to have a positive influence on the heat transfer solution.

2. The new method of calibrating the heat flux gages works extremely well and its results are backed up strongly by the heat transfer solution.

3. The heat transfer solution of the flat plate, with consideration for free-stream turbulence and calibration constants, compares well with the theoretical solution.

4. Even though the film-cooling effectiveness could not be determined from the present experimental set-up; it can be established from the data that the heat transfer to a surface can be reduced by as much as 50% with film-cooling.

5. An increase in the primary flow conditions results in a decrease in the effectiveness of the film-cooling flow in reducing the heat flux to the flat plate.

6. The point of minimum heat transfer due to film-cooling shift towards a high heat transfer rate and lower blowing ratio by increasing the primary flow conditions.

VIII RECOMMENDATIONS

The observations made during the course of this study lead to the following recommendations:

1. Further studies on measuring the turbulence level of the flow in the shock tube may be carried out using special purpose hot film/wire probes with a capacity to dampen the effects of vibrations. This would relieve the suspicion of relying on turbulence data which might be having vibration effects within it.

2. Since the boundary layer region has the main effect on the heat transfer solution of the flat plate it would be worthwhile to measure the turbulence level of the boundary layer itself.

3. In view of the last conclusion stated in Chapter VII it is deemed necessary that high speed photography be used for the qualitative analysis of the film-cooling flow.

4 Compare the effects of film-cooling on heat transfer by using both the 9Ø° and inclined film-cooling injection holes.

5. Find a way to either determine the adiabatic wall temperature of the flat plate in a transient facility like the shock tube, or a correlation that would lead to establishing properties like the Stanton number and Nusselt number of the flow with film cooling affects.

BIBLIOGRAPHY

Ammari, H.d., et al. "The effect of Density ratio on the Heat Transfer Coefficient from a Film Cooled Flat Plate", ASME Gas Turbine and Aero Engine Congress and Exposition, Toronto, Canada, June 4-8, 1989.

Blair, M.F. "Influence of Free Stream Turbulence on Turbulent Boundary Layer Heat Transfer and Mean Profile Development, Part II - Analysis and Results.", Journal of Heat Transfer, November, 1983.

Blasius, H. "Grenzschichten in Flussigkeiten mit kleiner Reibung.", Z. Math Physics, 56, 1908. English Translation in NACA TM 1256, 1956.

Bogdan, Leonard B. "High Temperature, Thin Film Resistance Thermometers For Heat Transfer Measurements", Cornell Aeronautical Laboratory Inc, June, 1967.

Bradshaw, P. "An Introduction to Turbulence and Its Measurement", Pergammon Press, 1971.

Chapmann, Alan J. and W.F. Walker. "Introductory Gas Dynamics", Holt, Rinehart and Wilson Inc, New York, 1971.

Crawford, M.E, et al, "Film Cooling Effectiveness Downstream of a Single Row of Holes with Variable Density Ratio", Gas Turbine and Aeroengines Congress and Exposition, June 11-14, 1990.

Davis, W.R. and L. Bernstein, "Heat Transfer and Transition to Turbulence in a Shock Induced Boundary Layer on a Semi Infinite Flat Plate", Journal of Fluid Mechanics, Volume 36: Part 1, 1969.

Dillon, R.e. and H.T. Nagamatsu. "Heat Transfer and Transition Mechanism on a Shock Tube Wall", AIAA Journal, 22: no 11, November, 1984.

Dunn, M.G. and R.J. Goldstein. "Measurements in Heat Transfer to Gas Turbine Components", Technical Report AFAPL-TR-77-66 Calspan Corporation, New York, October, 1977.

Eckert, E.P.G and R.J. Goldstein. "Measurements in Heat Transfer", Second Edition, McGraw Hill Book Company, NY, 1976.

Gaydon, A.G. and I.R. Hurle. "Shock Tube in High Temperature Chemical Physics", Reinhold Publishing Corporation, NY, 1963.

Glass, I.I. "Shock Tubes, Part I: Theory and Performance of Simple Shock Tubes", UTIA Review No 12, Toronto,Canada: Institute of

Aerophysics, University of Toronto, 1958.

Goldstein, R.J., et al. "Advances in Heat Transfer", Academic Press NY, 1971.

Goldstein, R.J., et al. "Film Cooling Following Injection Through Inclined Circular Holes", NASA Report No CR-72612, November, 1969.

Han, J.C. and A.B. Mehendale. "Influence of High Mainstream Turbulence on Leading Edge Film Cooling Heat Transfer", Gas Turbine and Aeroengines Congress and Exposition, June 11-14, 199Ø.

Hartunian,R.A., et al "Boundary Layer Transition and Heat Transfer in Shock Tubes",Journal of Aerospace Sciences,27:587, 196Ø

Hinze, J.O. "Turbulence: An Introduction to Its Mechanism", McGraw-Hill Book Company, 198Ø.

Jurgelewicz, Scott a. "Investigation of Heat Transfer with Film Cooling to a flat plate in a Shock Tube", Masters Thesis, School of Engineering, Air Force Institute of Technology (AU), Wright Patterson Air Force Base, OH, December, 1989.

Kays, W.M. and M.E. Crawford. "Convection Heat and Mass Transfer", McGraw-Hill Book Company, NY, 198Ø.

Kakac, S. et al. "Hand Book of Single Phase Convective Heat Transfer", John Willy and Sons, NY, 1987.

Ko,Y.S. and D.Y. Liu. "Experimental Investigation on The Effectiveness, Heat Transfer Coefficient and Turbulence of Film Cooling", AIAA, August, 198Ø.

Lam, H. and L.Crocco. "Shock Induced Unsteady Laminar Compressible Boundary Layer on a Semi Infinite Flat Plate, "Princeton University Report No 428, 1958.

MacMullin, R., et al. "Free Stream Turbulence From a Circular Wall Jet on a Flat Plate Heat Transfer and Boundary Layer", ASME, January, 1989.

McQueen, Stephen M. "Velocity and Transient Measurements in a Shock Tube Using a Hot Wire Anemometer", Masters Thesis, School of Engineering, Force Institute of Technology (AU), Wright Patterson Air Force Base OH, December, 1984.

Mirels, J. "Boundary Layer Behind Shock of Thin Expansion Wave Moving into a Stationary Fluid", NACA TN 3712, 1956.

Novak, Joseph T. "Investigation f Heat Transfer To a Flat Plate in

a Shock Tube", Masters Thesis, School of Engineering, Air Force Institute of Technology (AU), Wright Patterson Air Force Base, OH, December, 1987.

Oldfield, M.L.G., et al. "On Line Computer for Transient Turbine Cascade Instrumentation", IEEE Transactions on Aerospace and Electronic Systems Vol AES-14, No 5, September, 1978.

Prandtl,L. "Uber Flussigkeitsbewegung Bei Sher Kleiner Reibung Proc", Third International Math Congress, Heidelberg: 484-491, 19Ø4

Rockwell, Richard K. "Transient Heat Transfer Measurements on a Flat PLate in Turbulent Flow Using an Electrical Analog", Masters Thesis, School of Engineering, Air Force Institute of Technology (AU), Wright Patterson Air Force Base, OH, December, 1989.

Schlichting, Hermann. "Boundary Layer Theory (Seventh Edition)", McGraw-Hill Book Company, 1989.

Schmitz, L.S. "Nonlinear Analog Network to Convert Surface Temperature to Heat Transfer", Cornell Aeronautical Laboratory, Inc, Buffalo, NY, June, 1963.

Schultz, D.L. and T.V. Jones. "Heat transfer Measurements in Short Duration Hypersonic Facilities", AGARDograph No. 165, February, 1973.

Shapiro, Ascher H. "The Dynamics and Thermodynamics of Compressible Fluid Flow, Vol. 2, The Ronald press company, NY, 1987.

Simonich, J.C. and P. Bradshaw. "Effect of Free Stream Turbulence on Heat Transfer Through Turbulent Boundary Layer", Journal of Heat Transfer, November, 1978.

Skinner, George t. "Analog Network To Convert Surface Temperature to Heat Flux", Report no CAL-1ØØ, Cornell Aeronautical Laboratory,Inc, Buffalo, NY, February, 196Ø.

Smith, Bret J. "Investigation of Heat Transfer to a Sharp Leading Edged Flat Plate Using a Shock Tube", Masters Thesis, School of Engineering, Air Force Institute of Technology, Wright Patterson Air Force Base OH, December, 1986.

Spence, D.A. "Velocity and Enthalpy Distribution in Compressible Turbulent Boundary Layer on a Flat Plate", Journal of Fluid Mechanics,18:117, 196Ø.

Zucrow, Maurice J. and J.D. Hoffman. "Gas Dynamics, Vol. I", John Willy and Sons, NY, 1976.

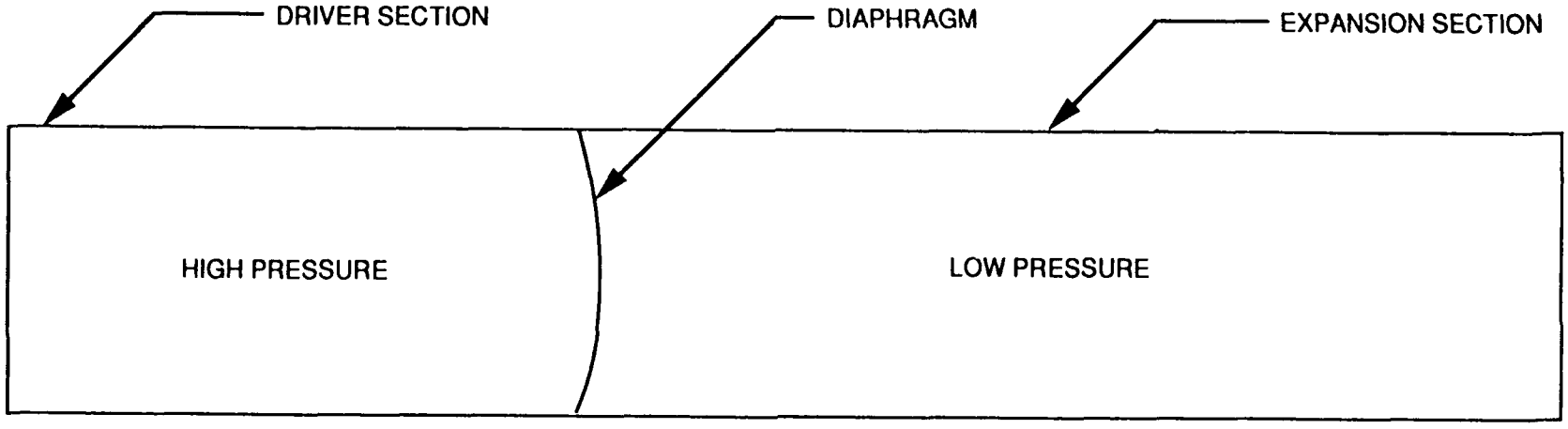

Fig. 1: A Simple Shock Tube

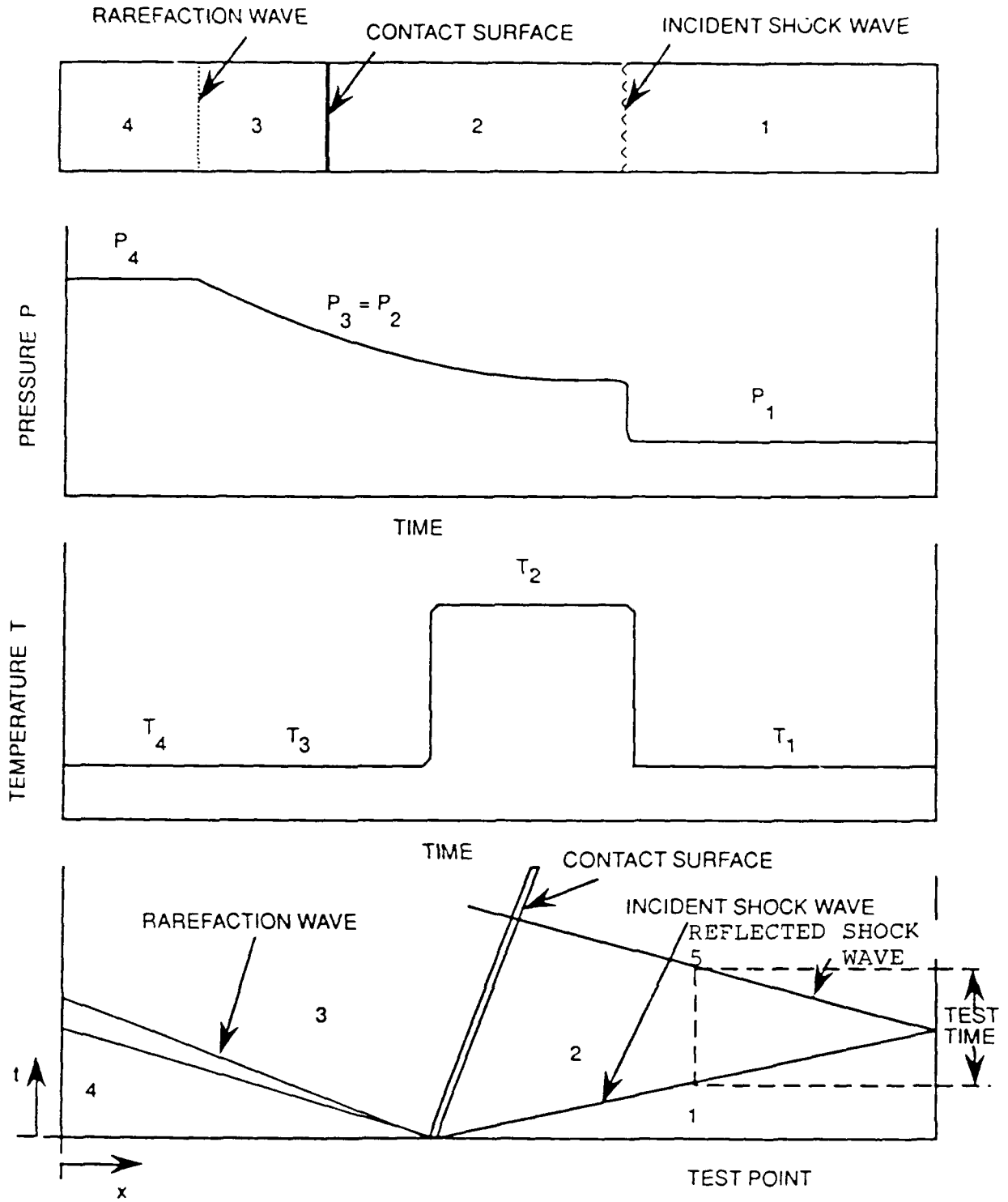

(a) Flow pattern in a shock tube at $t=t_1$
(b) Pressure distribution in a shock tube at $t=t_1$
(c) Temperature distribution in a shock tube at $t=t_1$
(d) Physical plane, showing shock wave, rarefaction wave, and contact discontinuity (Shapiro, 1987: 1007)

Figure 2: Illustration of Flow Properties/Patterns in a Shock Tube

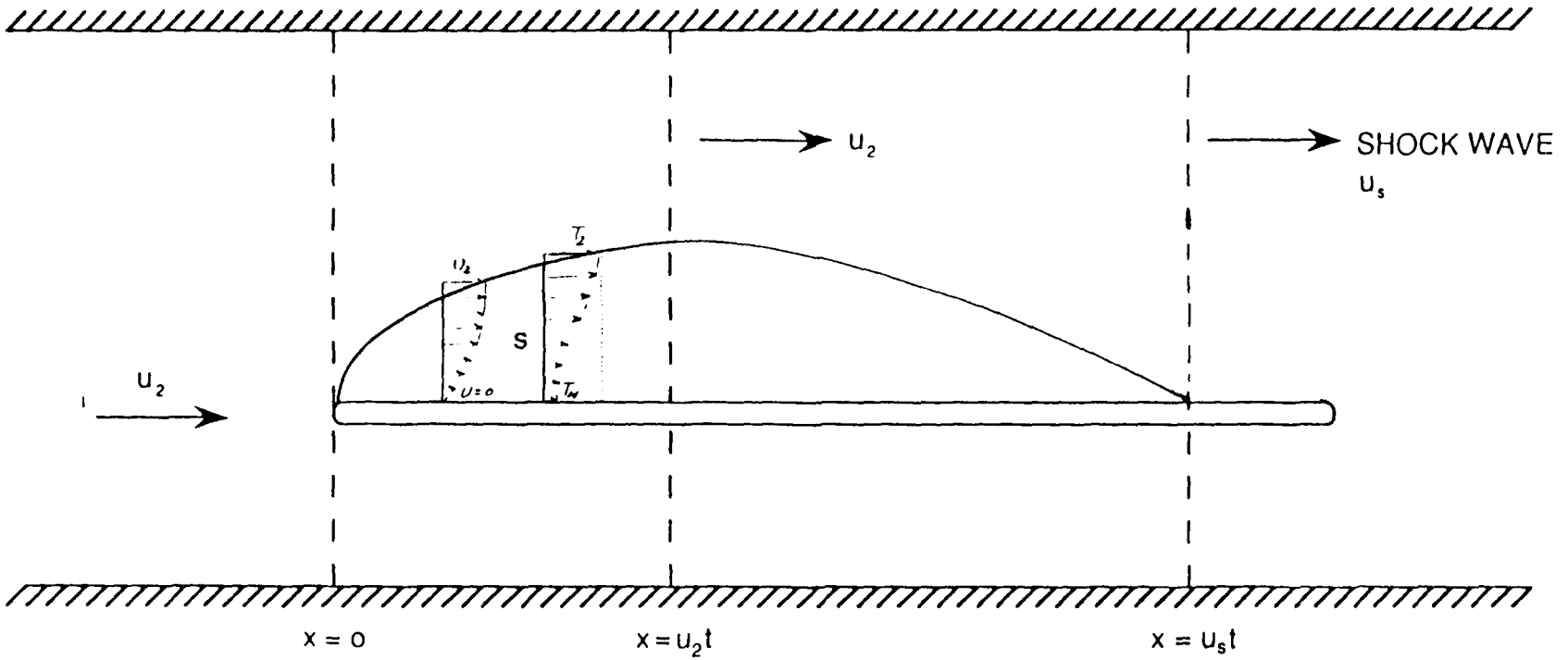

Fig. 3: Boundary Layer Formation Behind a Shock Wave
(Schlichting, 1987)

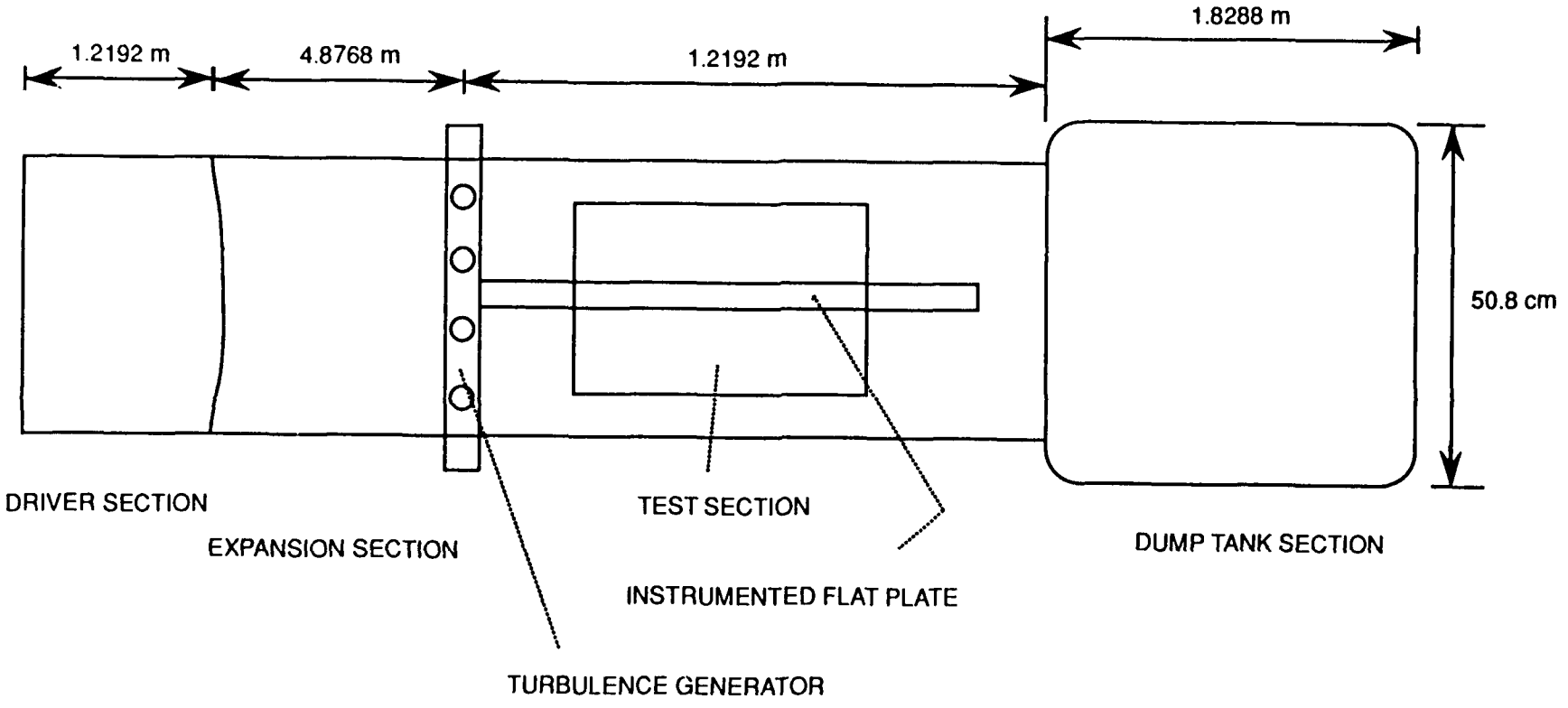

Fig. 4: A.F.I.T. Low Pressure Shock Tube (not to scale)

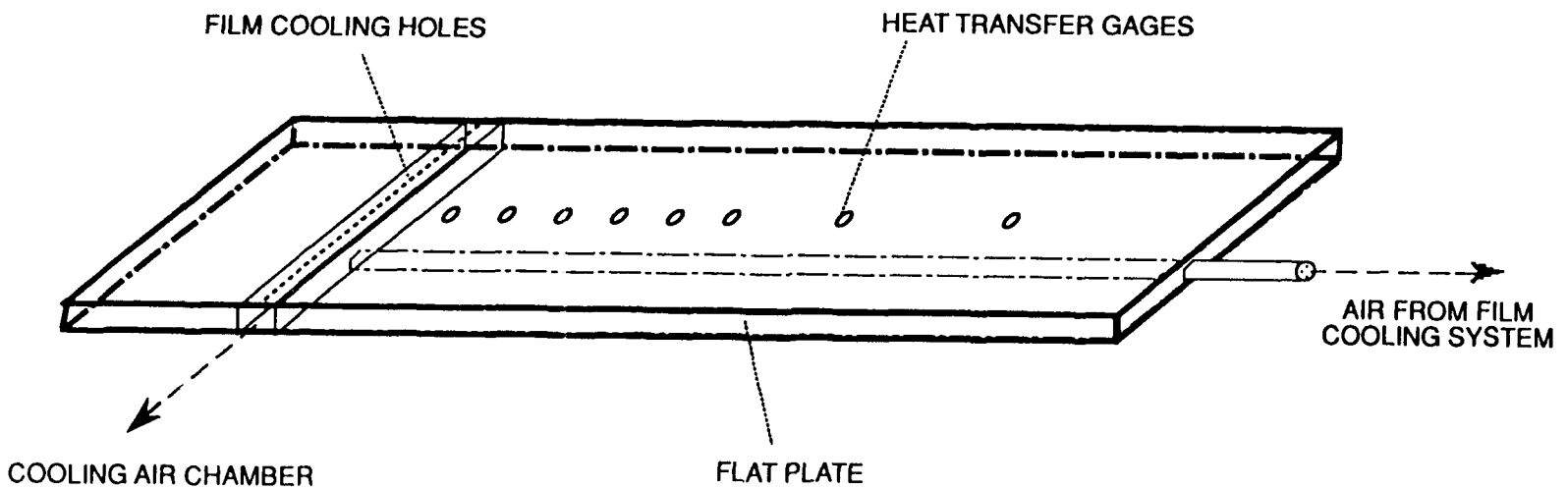

Fig. 5: Instrumented Flat Plate

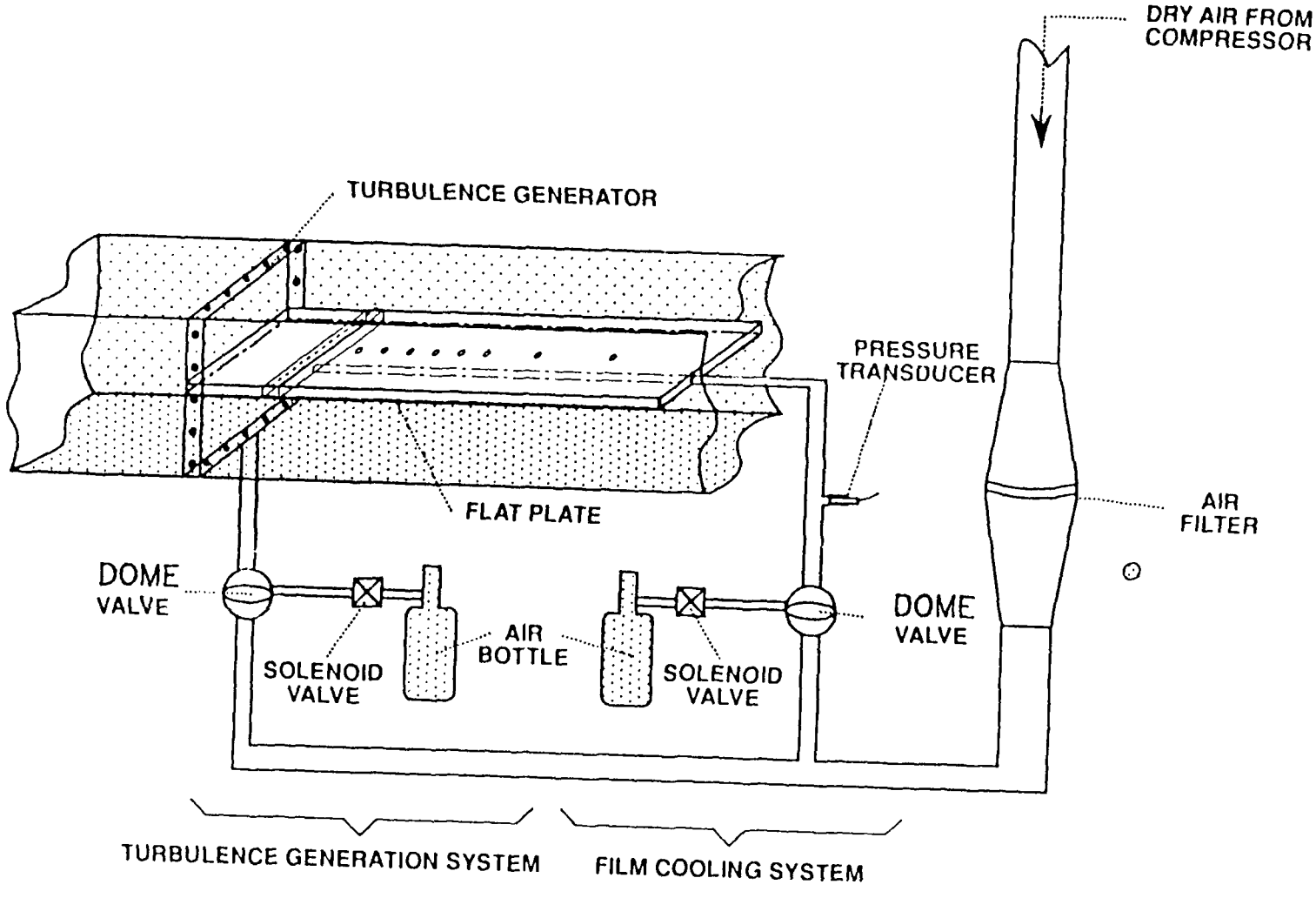

Fig. 6: Film Cooling and Turbulence Generation Systems

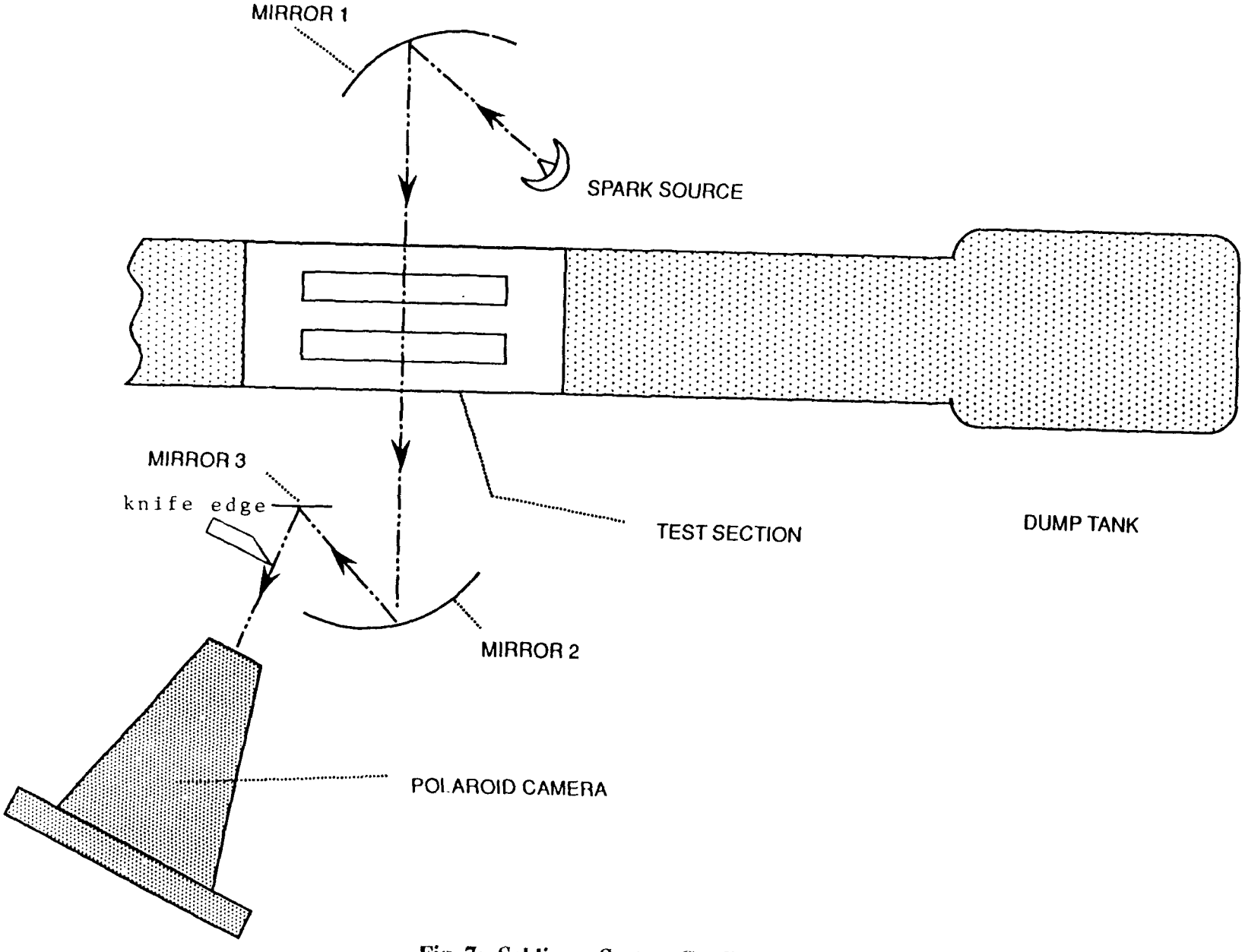

Fig. 7: Schlieren System Configuration

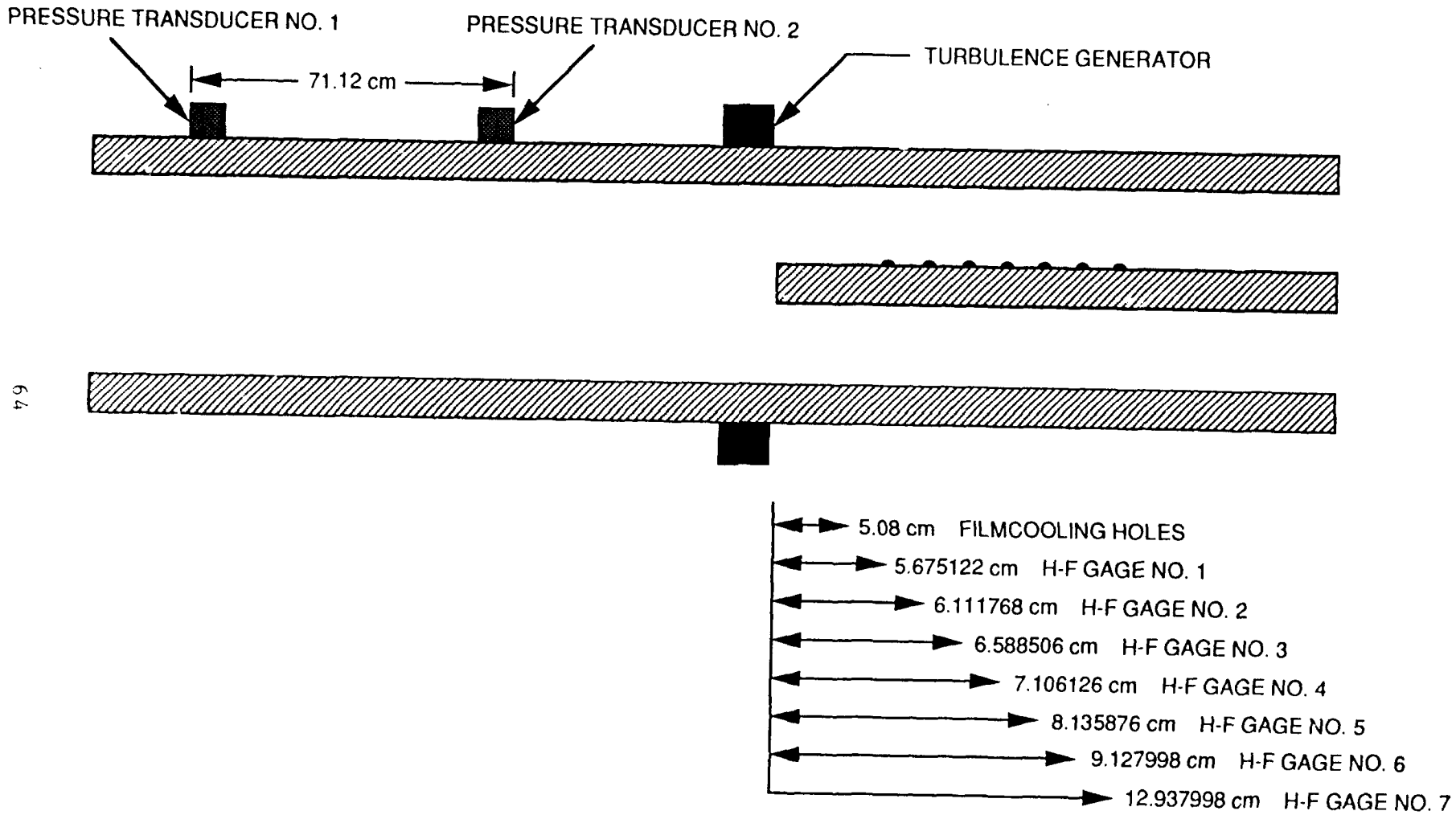

Fig. 8: Pressure Transducers and Heat Flux Gage Locations in the Shock Tube

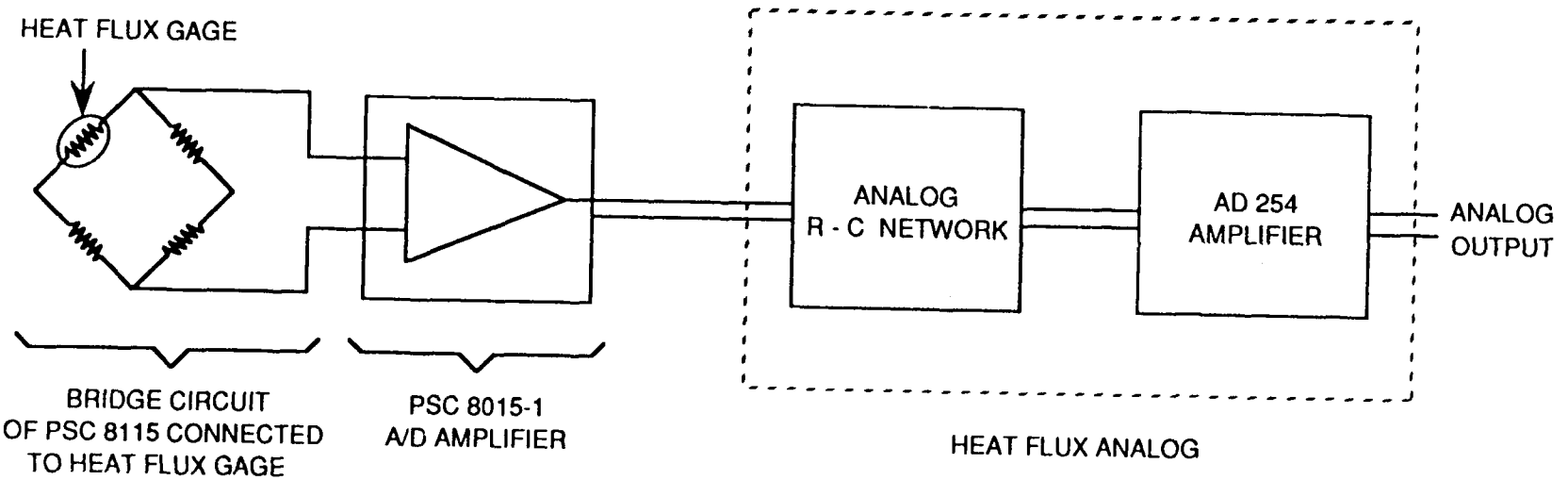

Fig. 9: Schematic of Heat Flux Analog Circuit

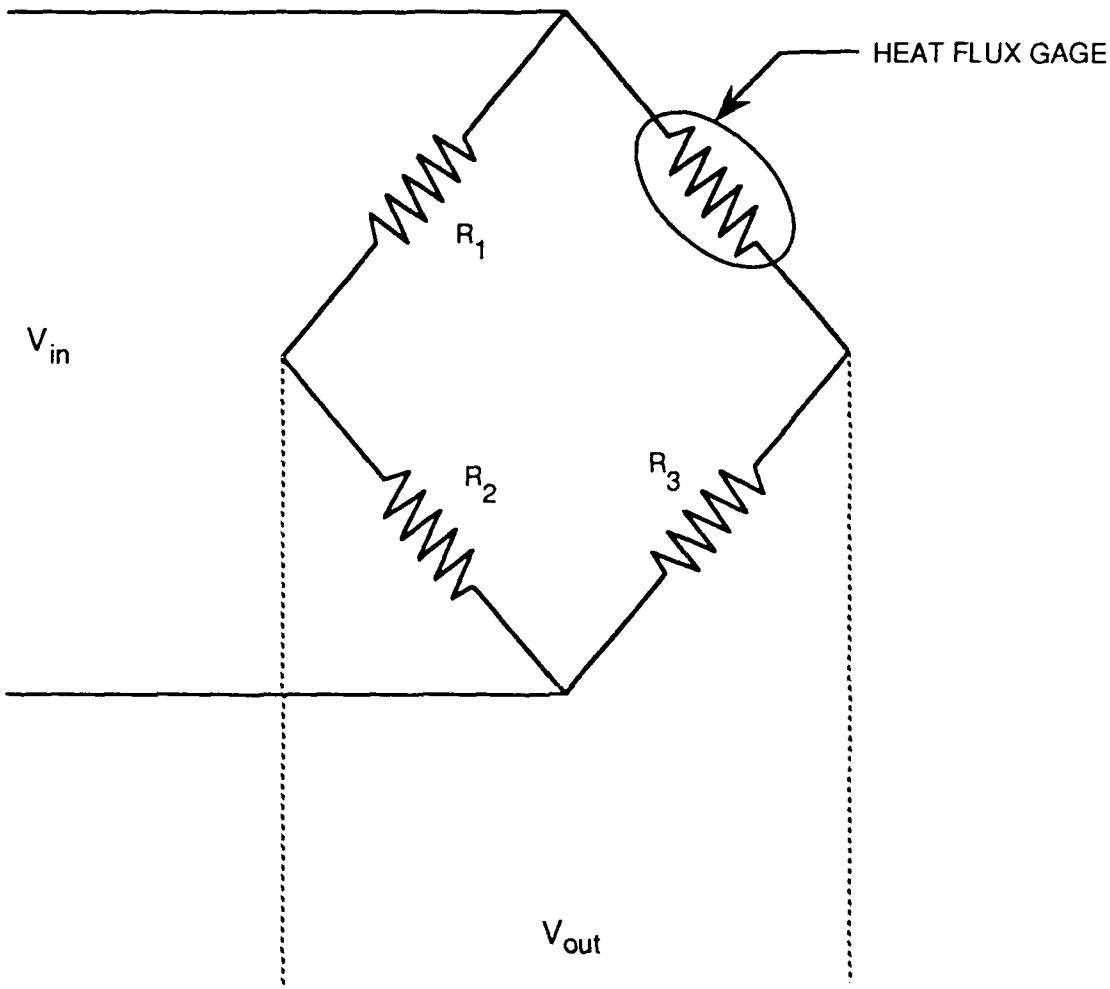

Fig. 10: Bridge Circuit for Calibration and Collection of Data from H-F Gages

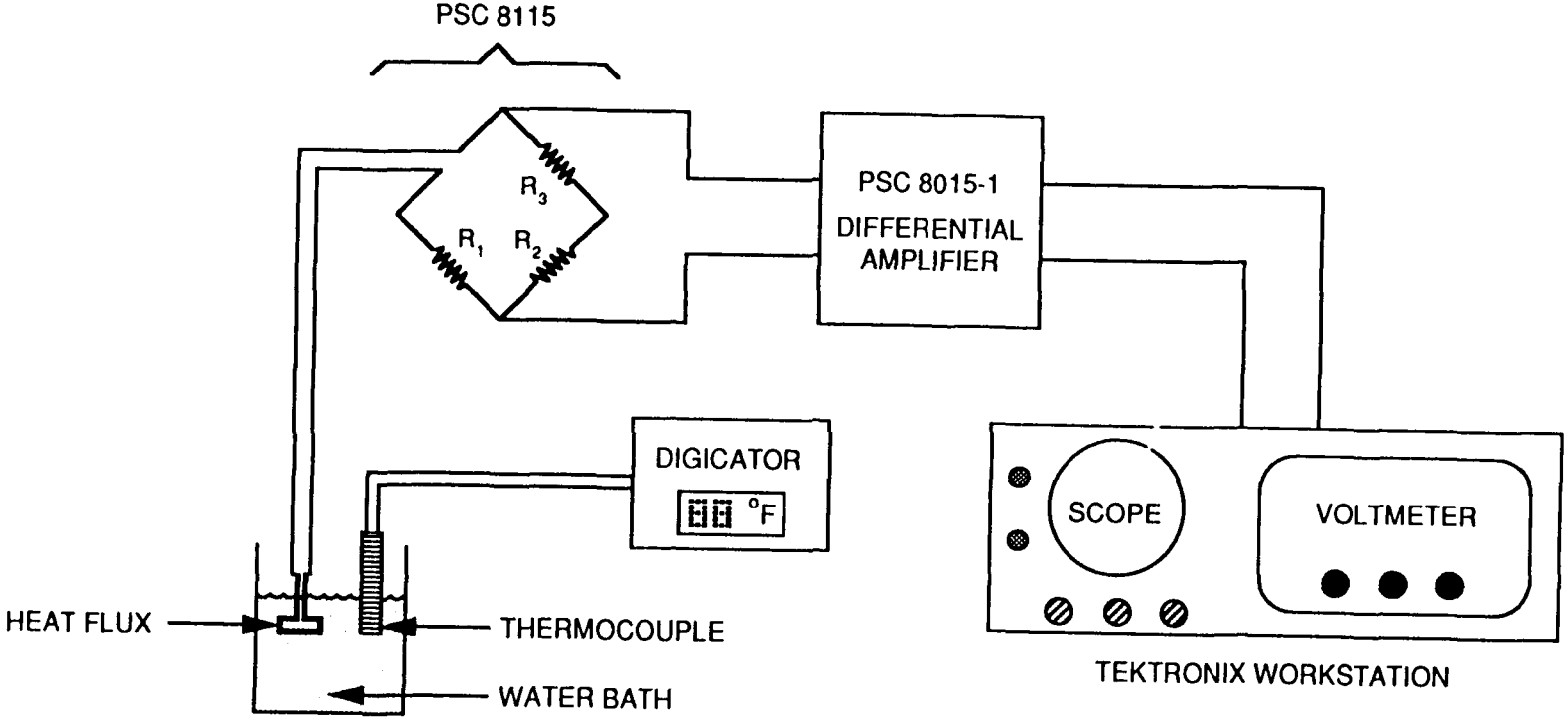

Fig. 11: Schematic of Calibration Circuit to Determine Temperature Coefficient of Heat Flux Gages

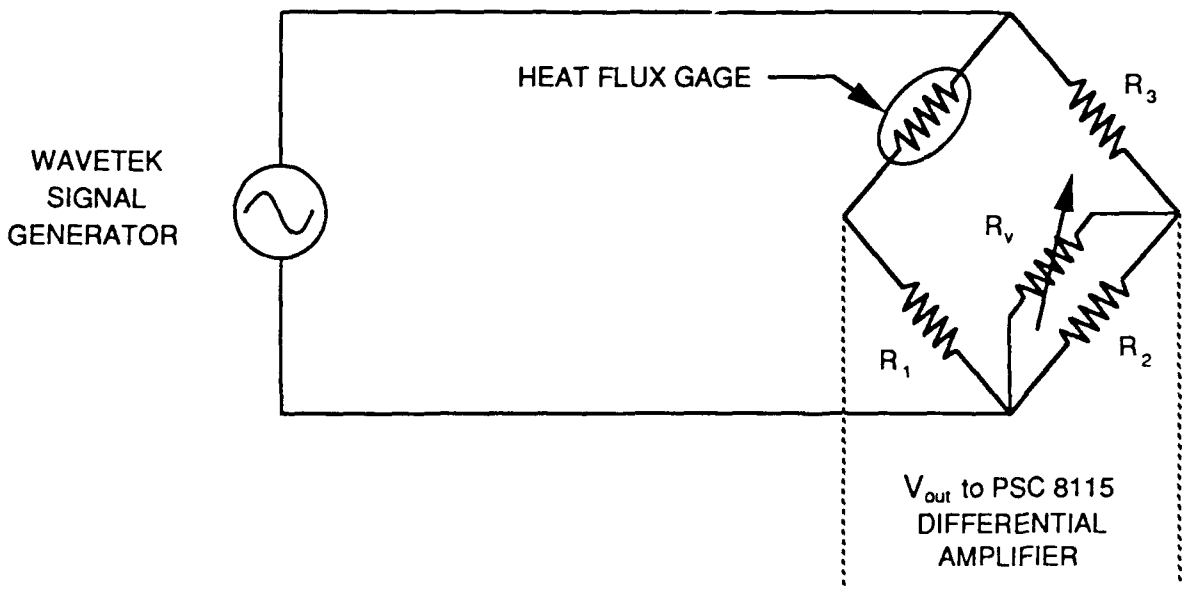

Fig. 12: Calibration Circuit to Determine $\sqrt{\rho C_p k}$ of Heat Flux Gages

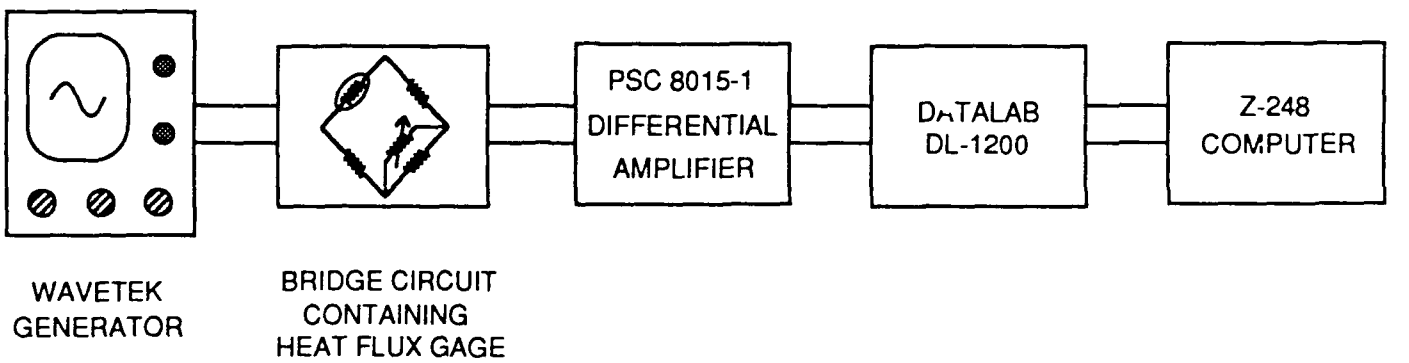

Fig. 13: Schematic of Calibration Circuit to Determine $\sqrt{\rho C_p k}$ of Heat Flux Gages

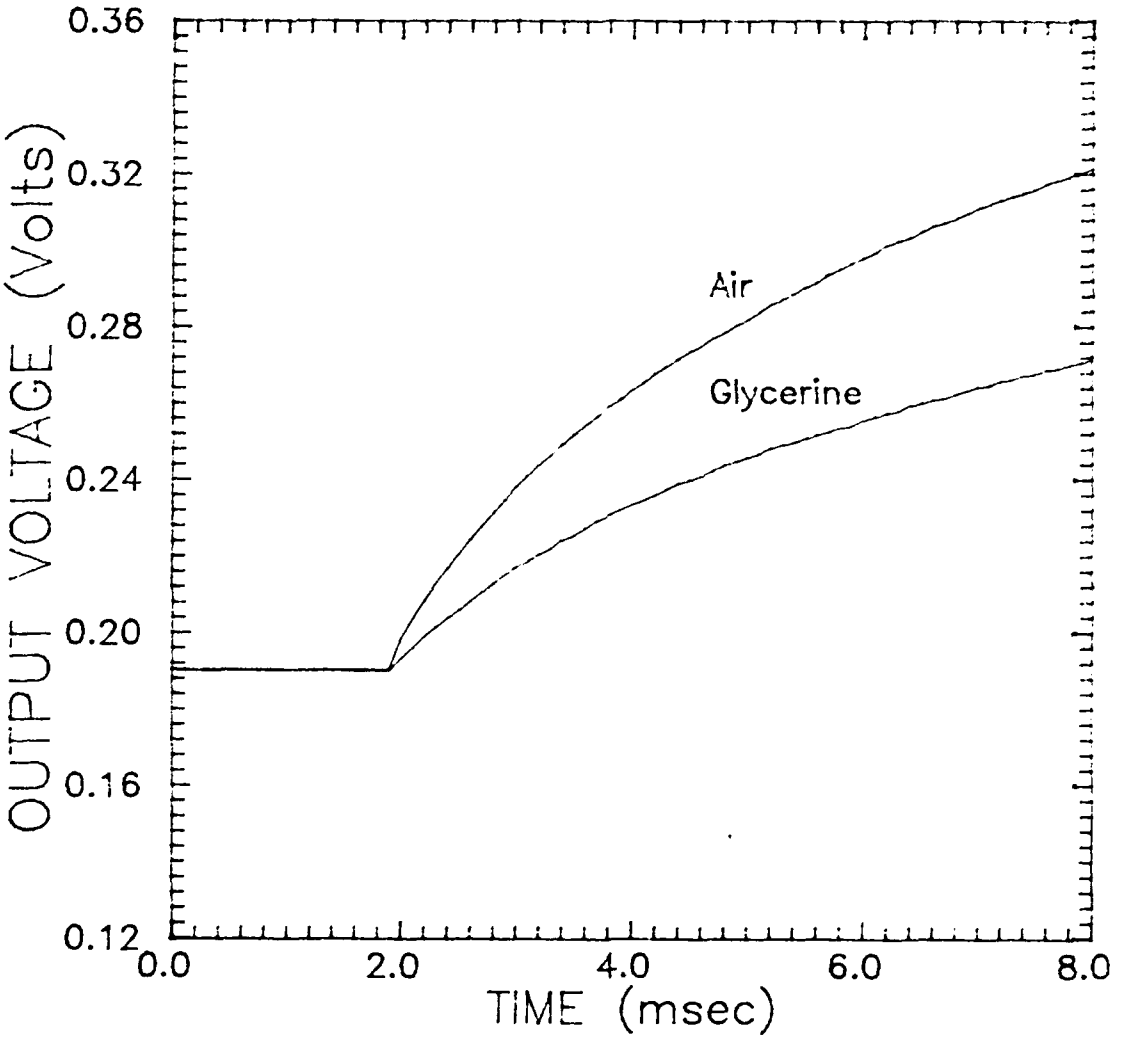

Figure 14: Parabolic Output of Heat Flux Gage No 4

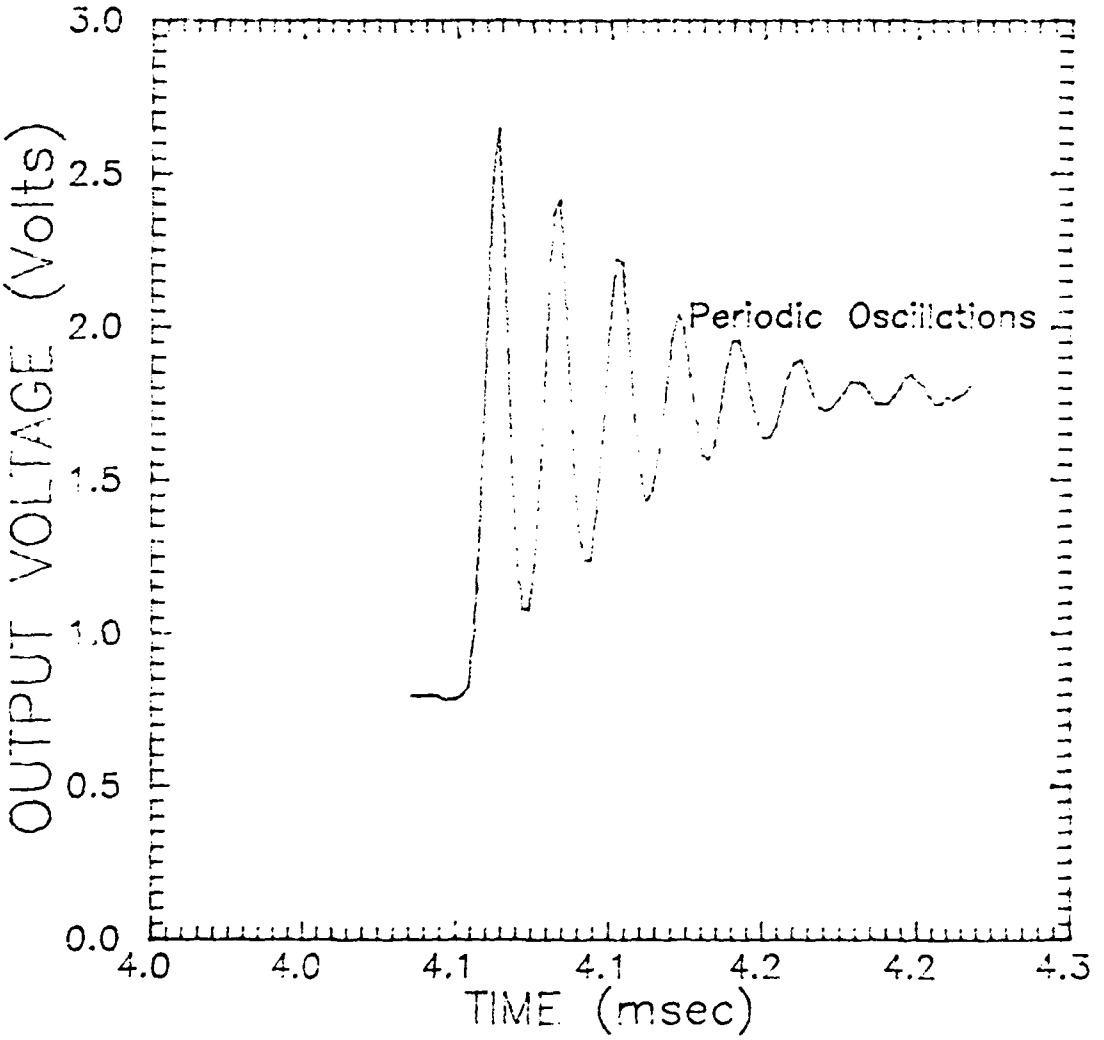

Figure 15: Output of TSI 1214-T1.5 Hotwire

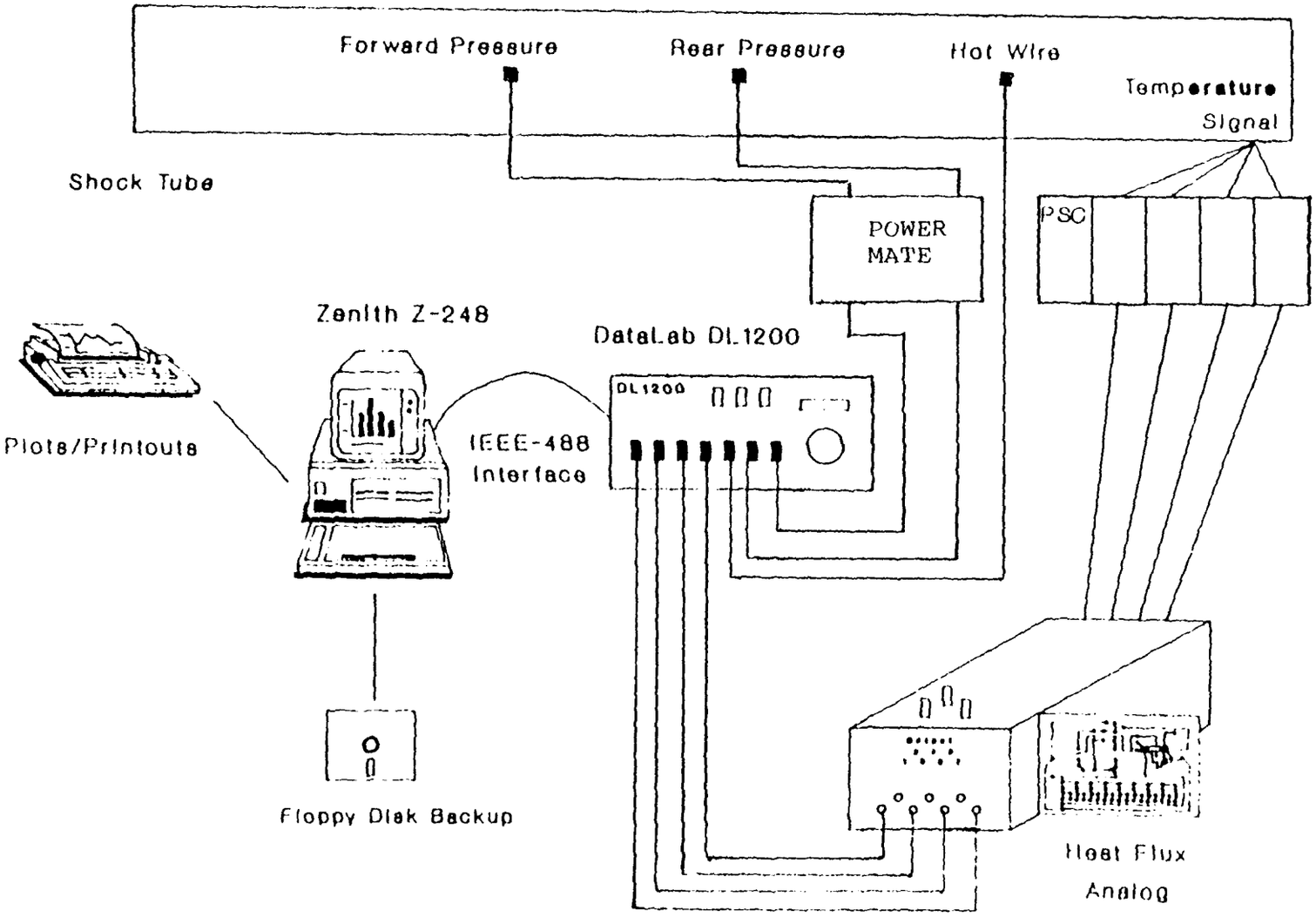

Figure 16: Instrumentation-Hardware Interface
(Rockwell, 1989)

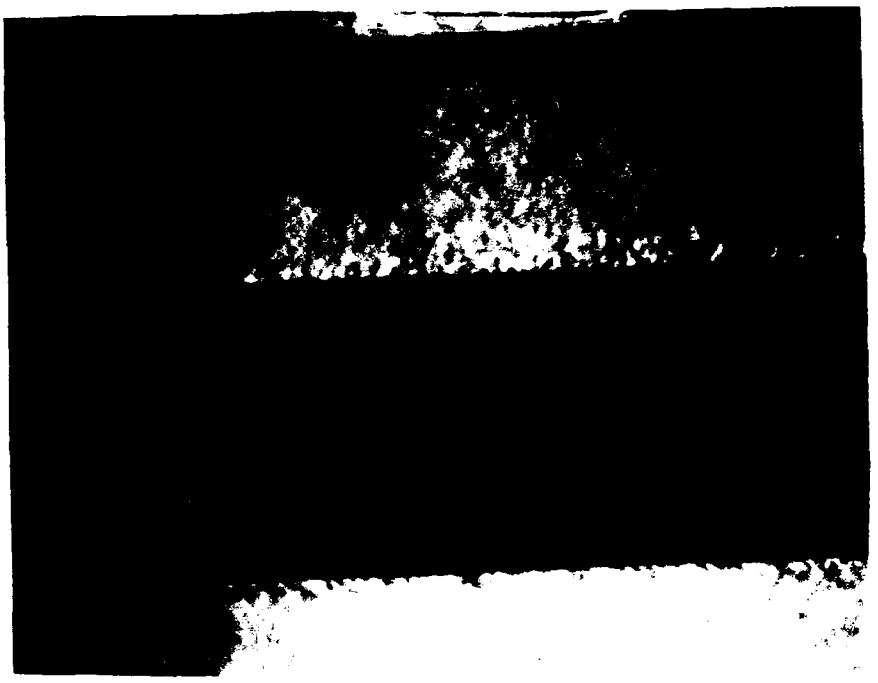

Figure 17: Schlieren Photograph of Flow Behind a Shock Wave
:No Film Cooling or Turbulence Generation

Figure 18: Schlieren Photograph of Flow Behind a Shock Wave
:With Film Cooling B = Ø.2Ø

Figure 19:Schlieren Photograph of Flow Behind a Shock Wave
:With Film Cooling B = Ø.8Ø

Figure 2Ø: Schlieren Photograph of Flow Behind a Shock Wave
:With Film Cooling B = 2.ØØ

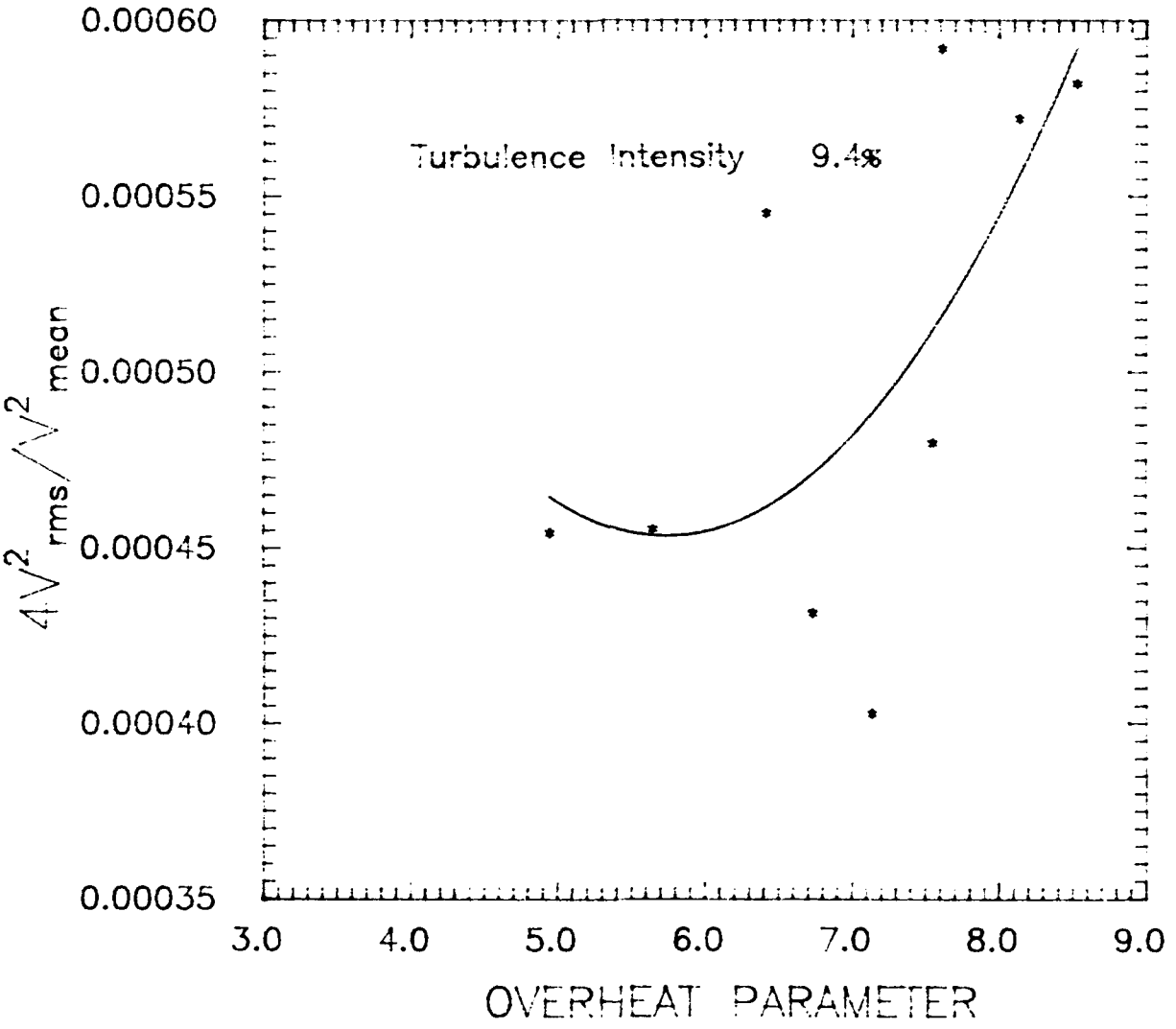

Figure 21: Hot Film Power Output as a Function of Overheat Parameter (NO Turbulence Injection)

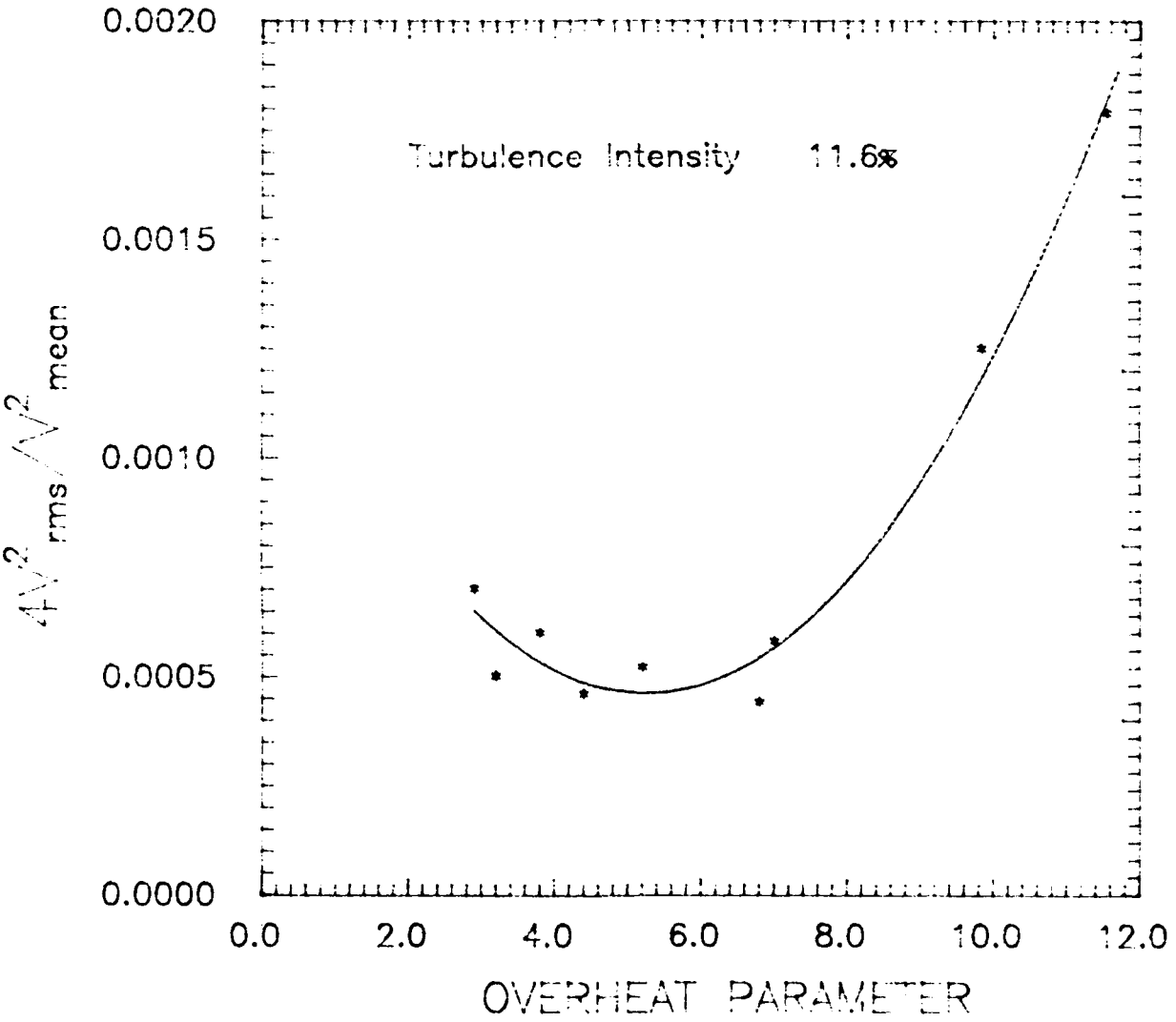

Figure 22: Hot Film Power Output as a Function of Overheat Parameter (With Turbulence Injection)

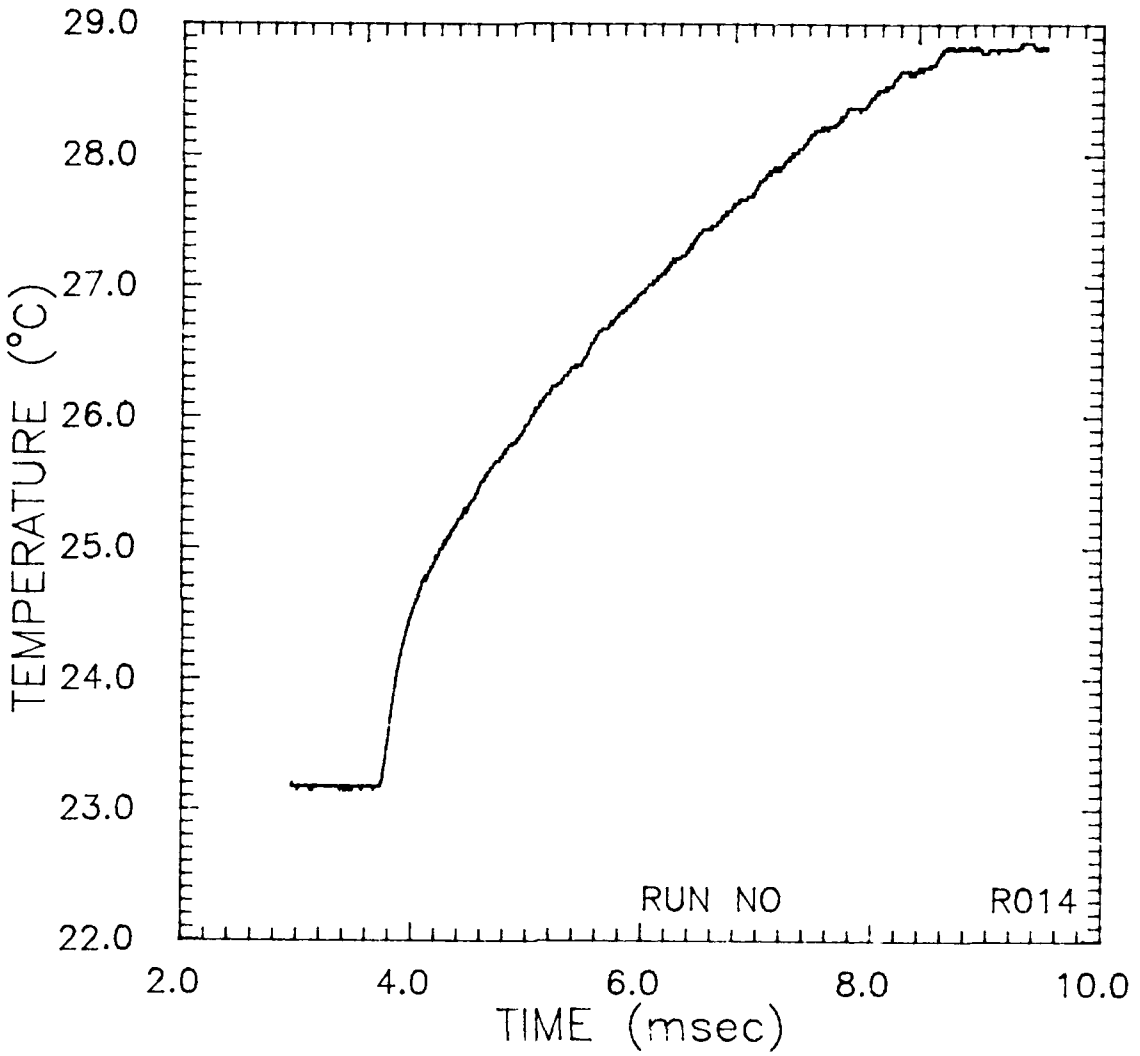

Figure 23: Temperature change as a function of time
Gage No 2

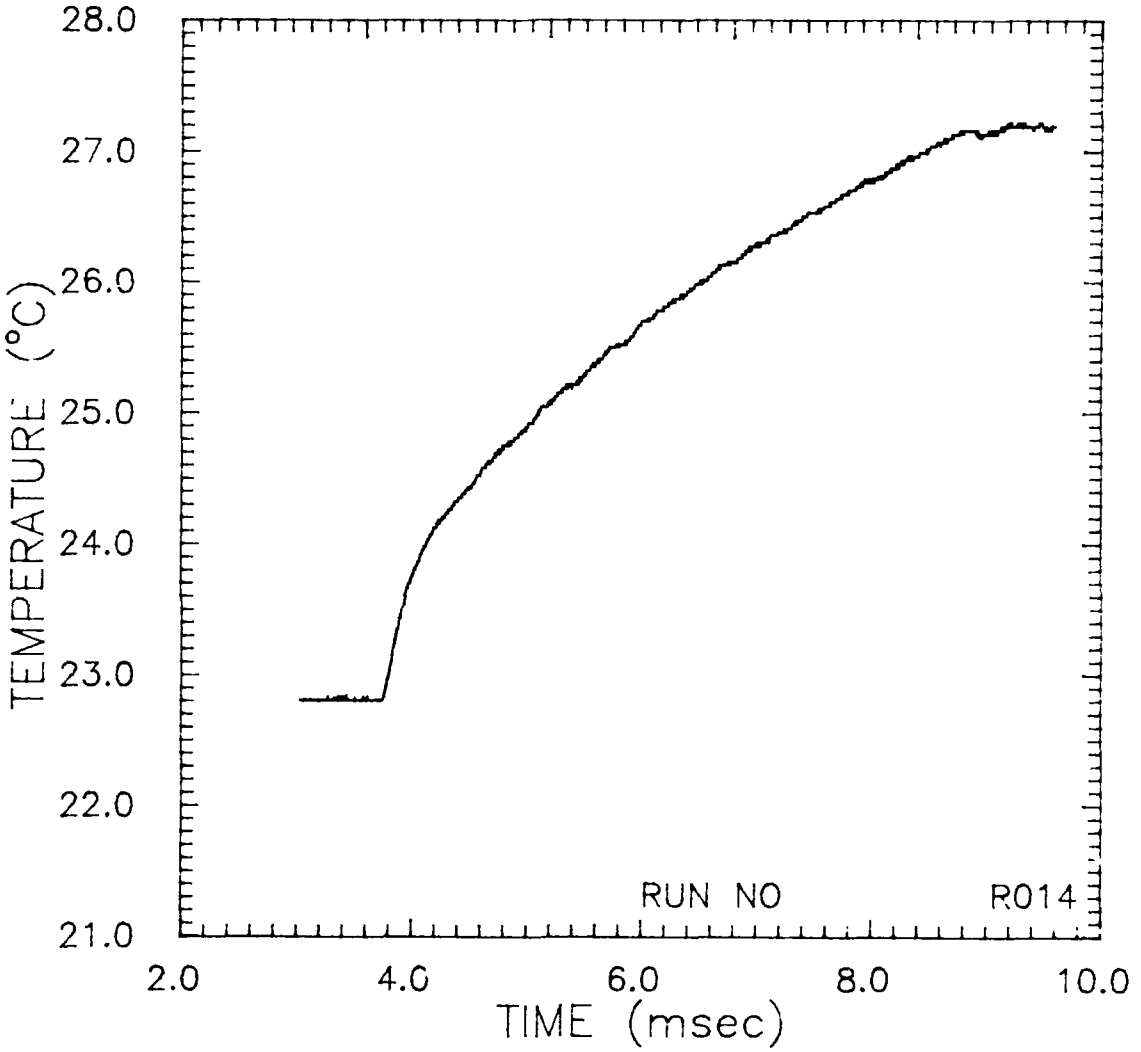

Figure 24: Temperature change as a function of time
Gage No 4

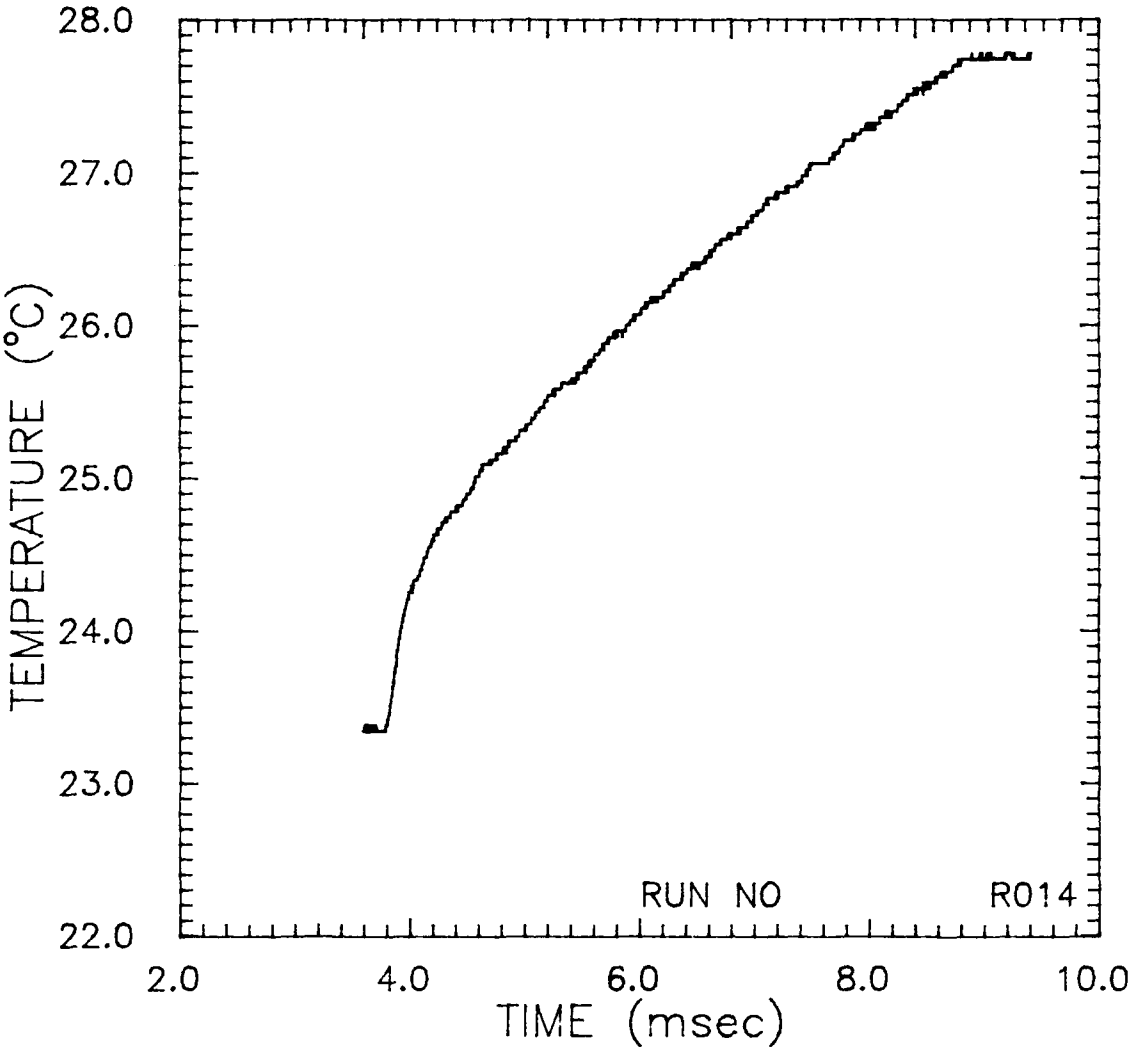

Figure 25: Temperature change as a function of time Gage No 6

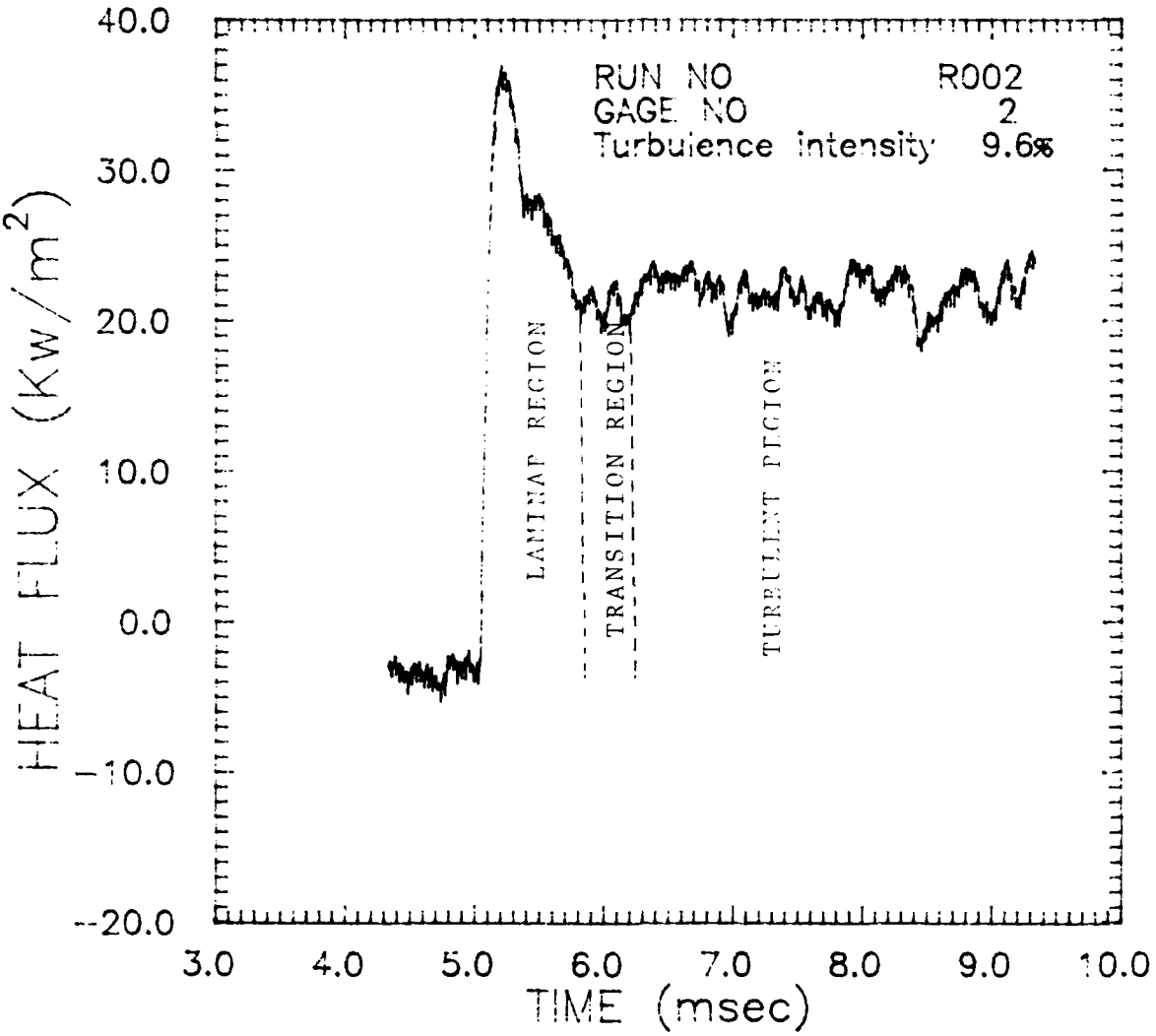

Figure 26: Heat Flux as a Function of Time
Run No R002

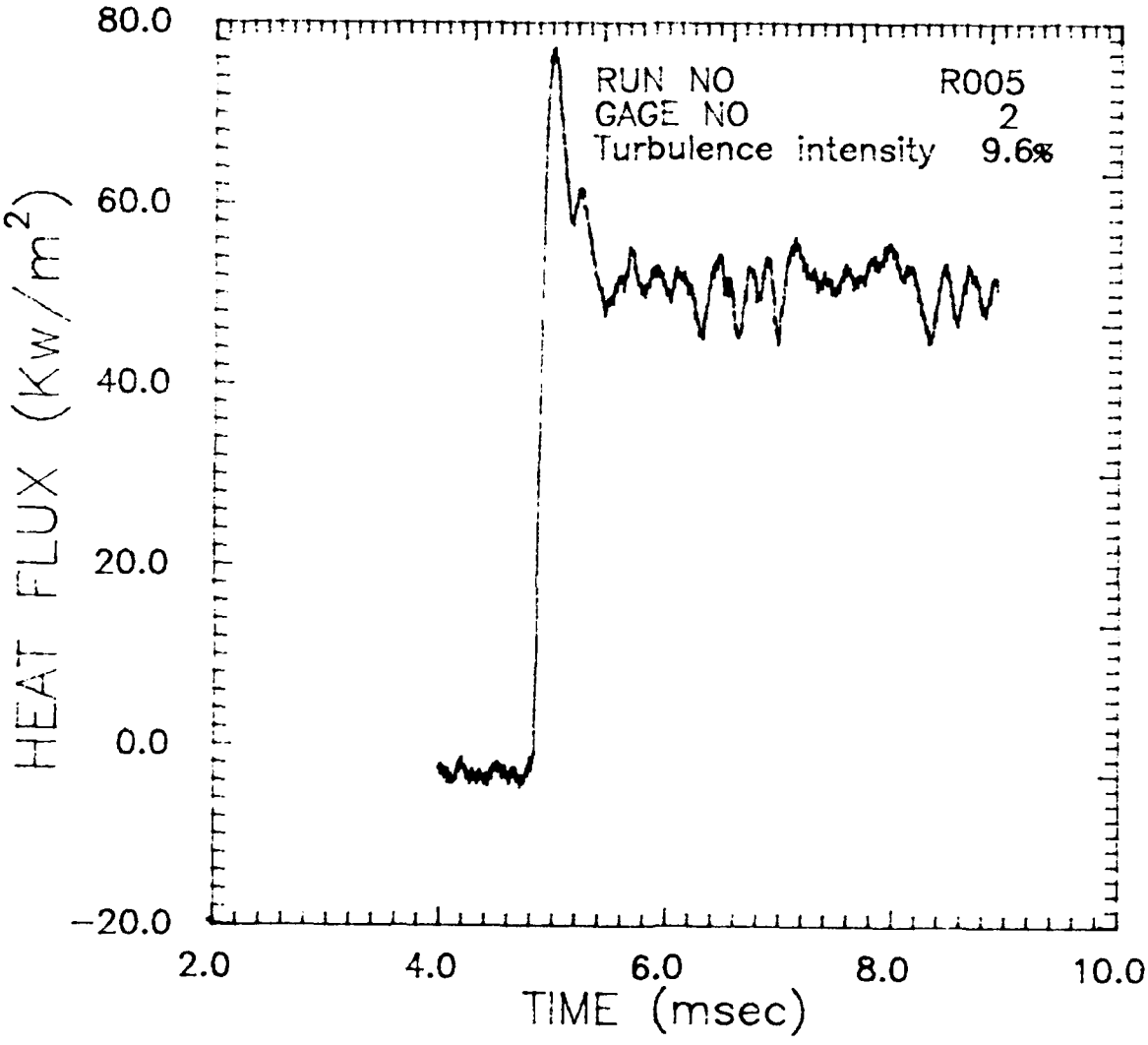

Figure 27: Heat Flux as a Function of Time
Run No R005

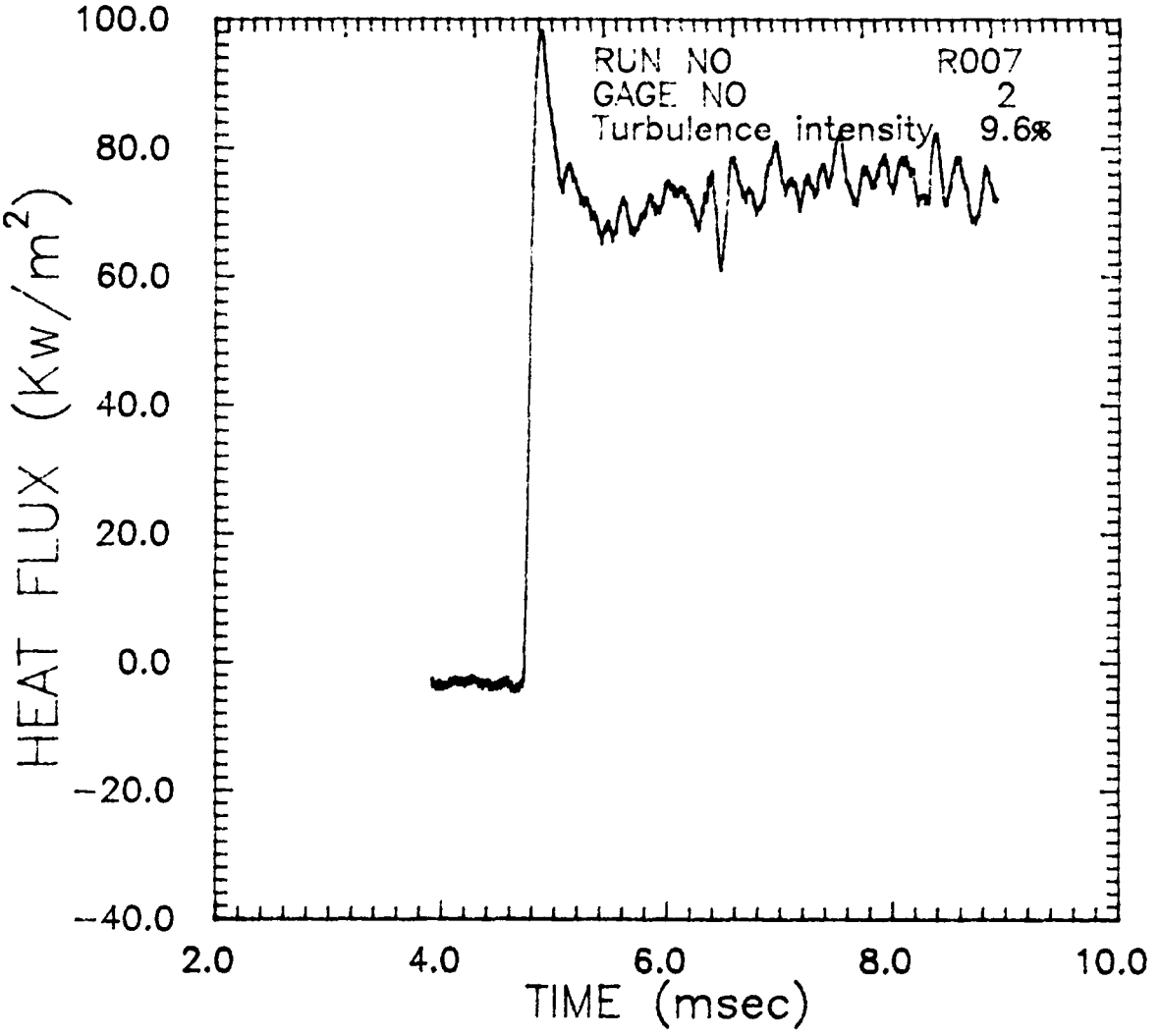

Figure 28: Heat Flux as a Function of Time
Run No R007

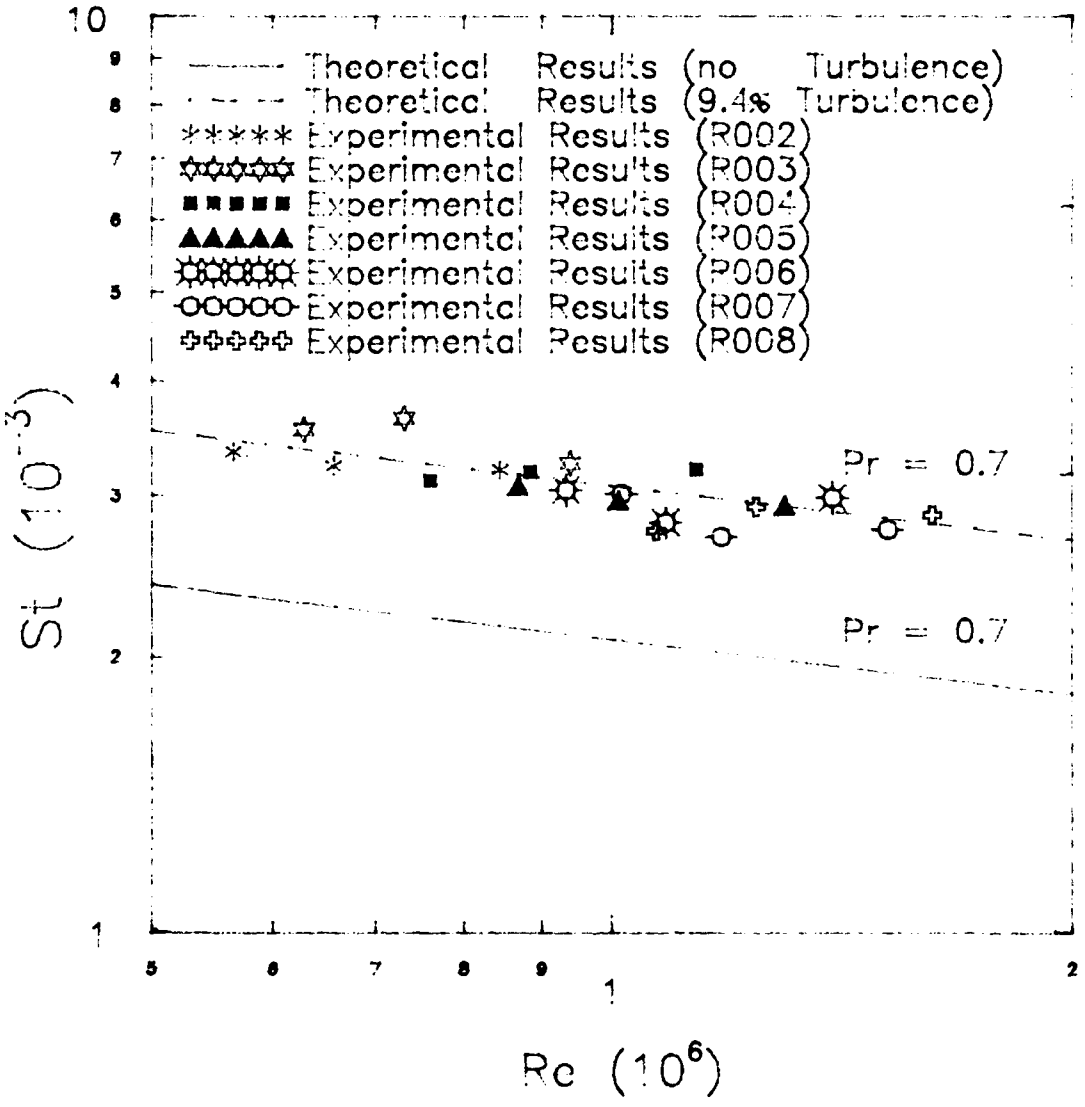

Figure 29: Stanton Number as a Function of Reynolds Number
No Turbulence Generation

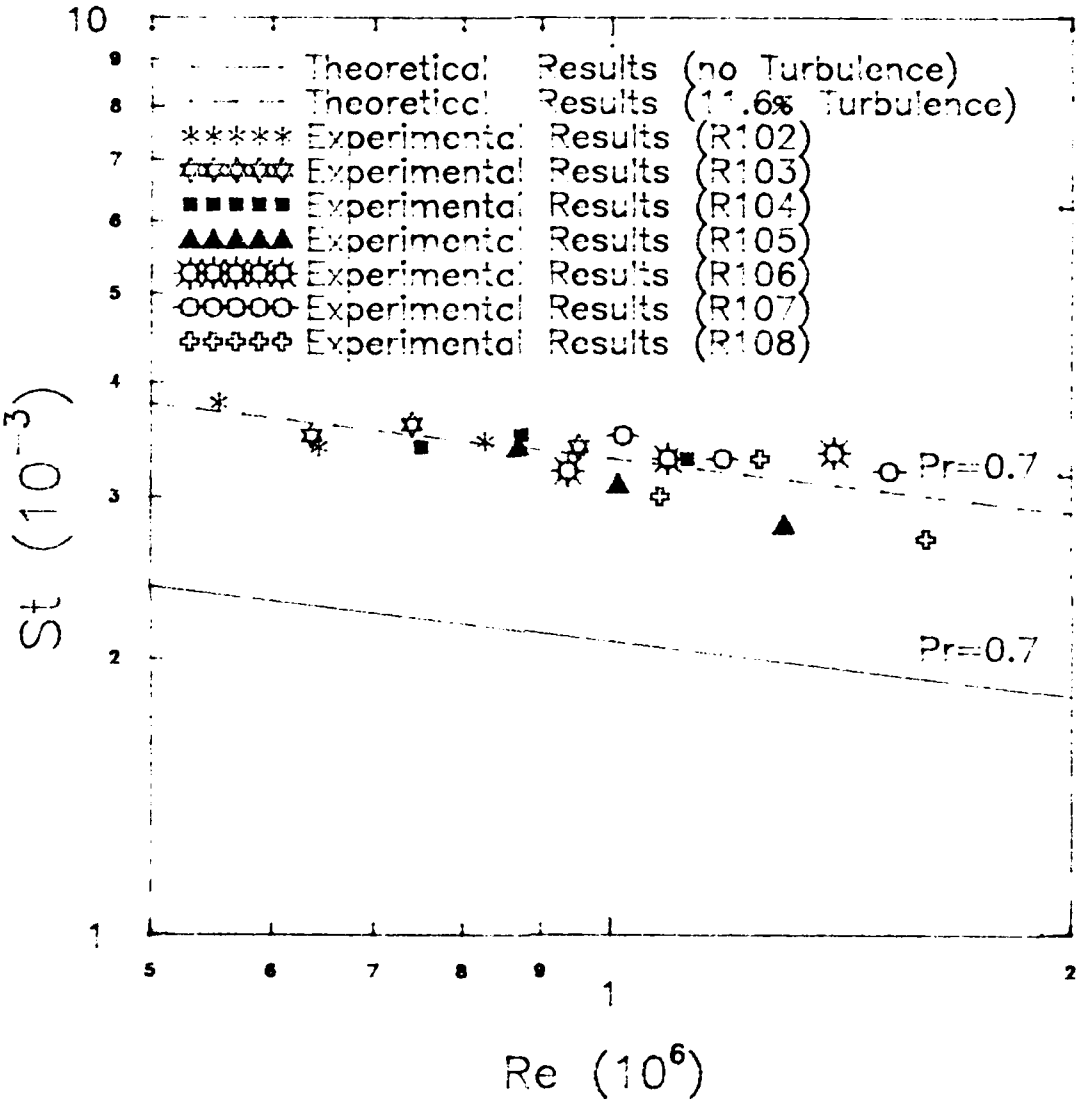

Figure 30: Stanton Number as a Function of Reynolds Numbe With Turbulence Generation

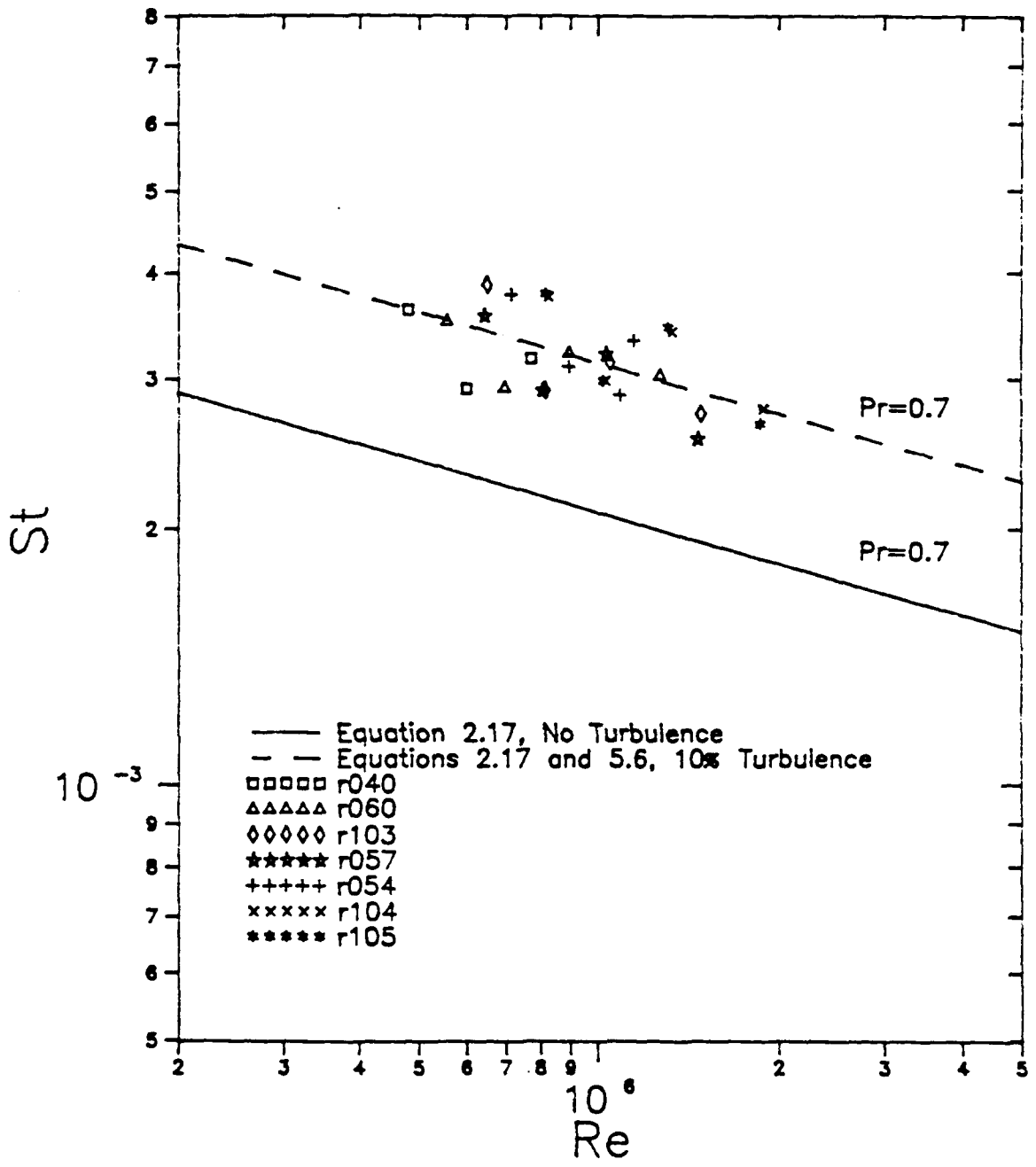

Figure 31: Stanton Number as a Function Reynolds Number, No Turbulence Generation (Rockwell, 1989)

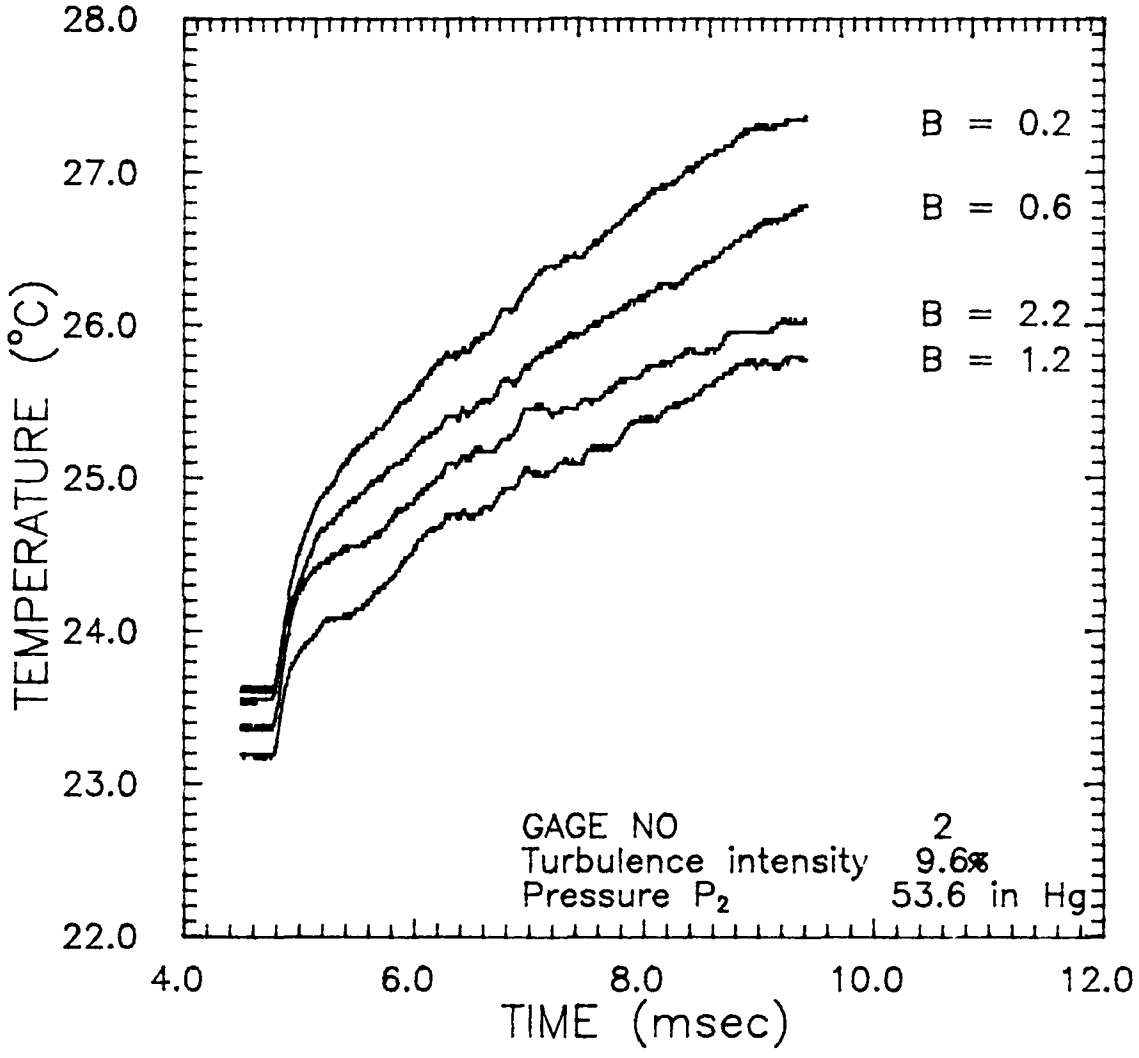

Figure 32: Temperature Change as a Function of Time with Film Cooling

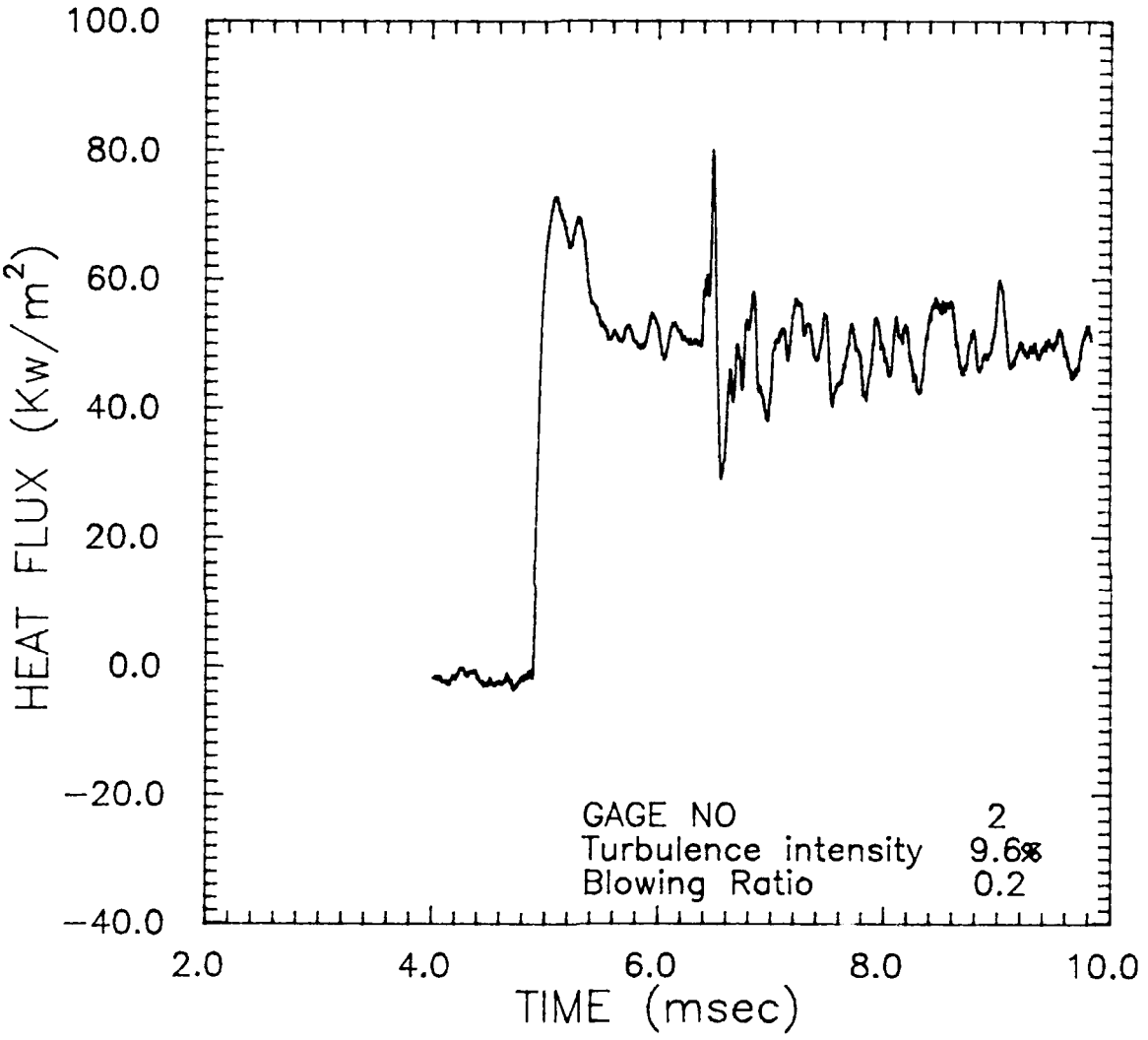

Figure 33: Heat Flux as a Function of Time: FC801

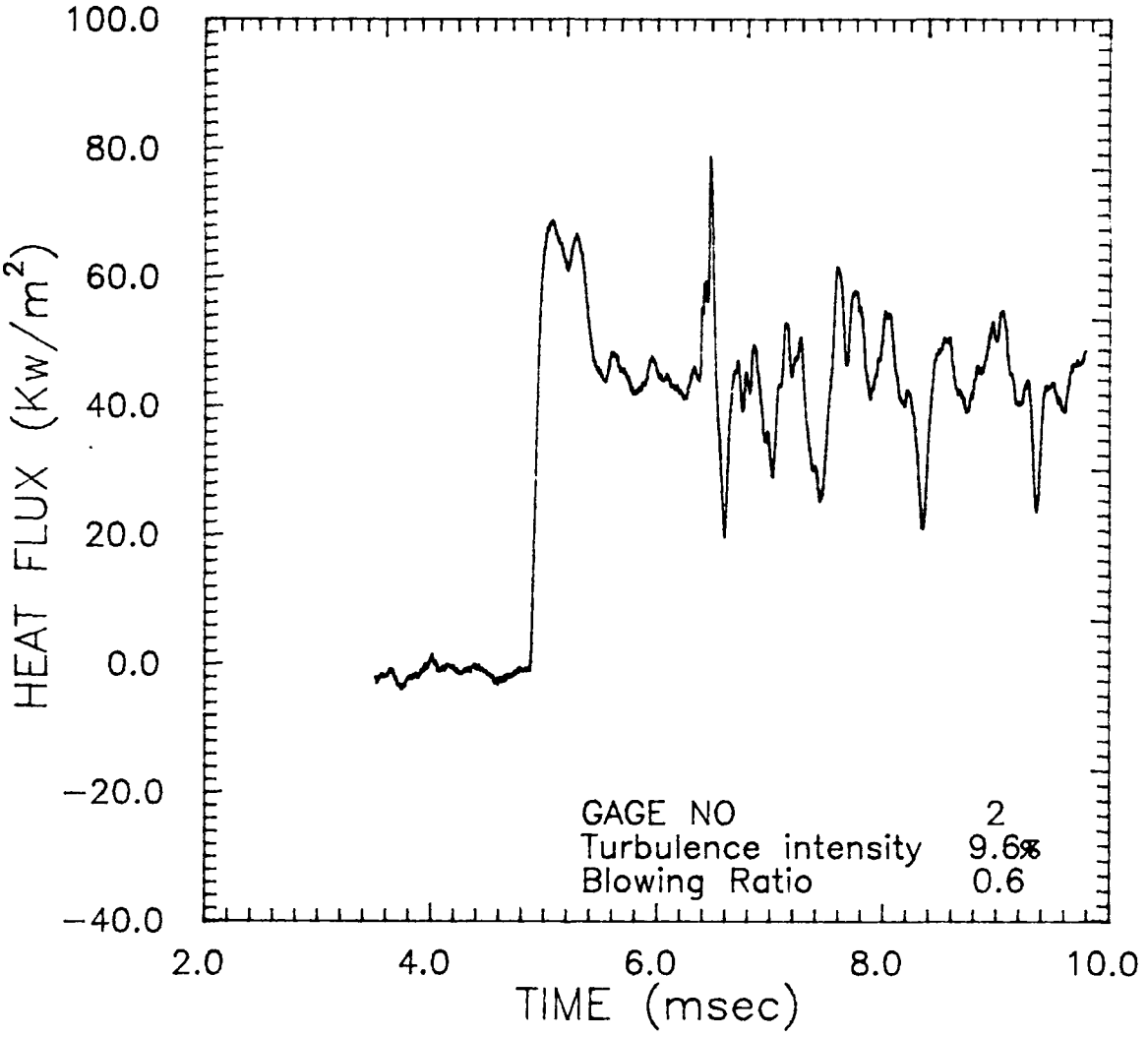

Figure 34: Heat Flux as a Function of Time: FC802

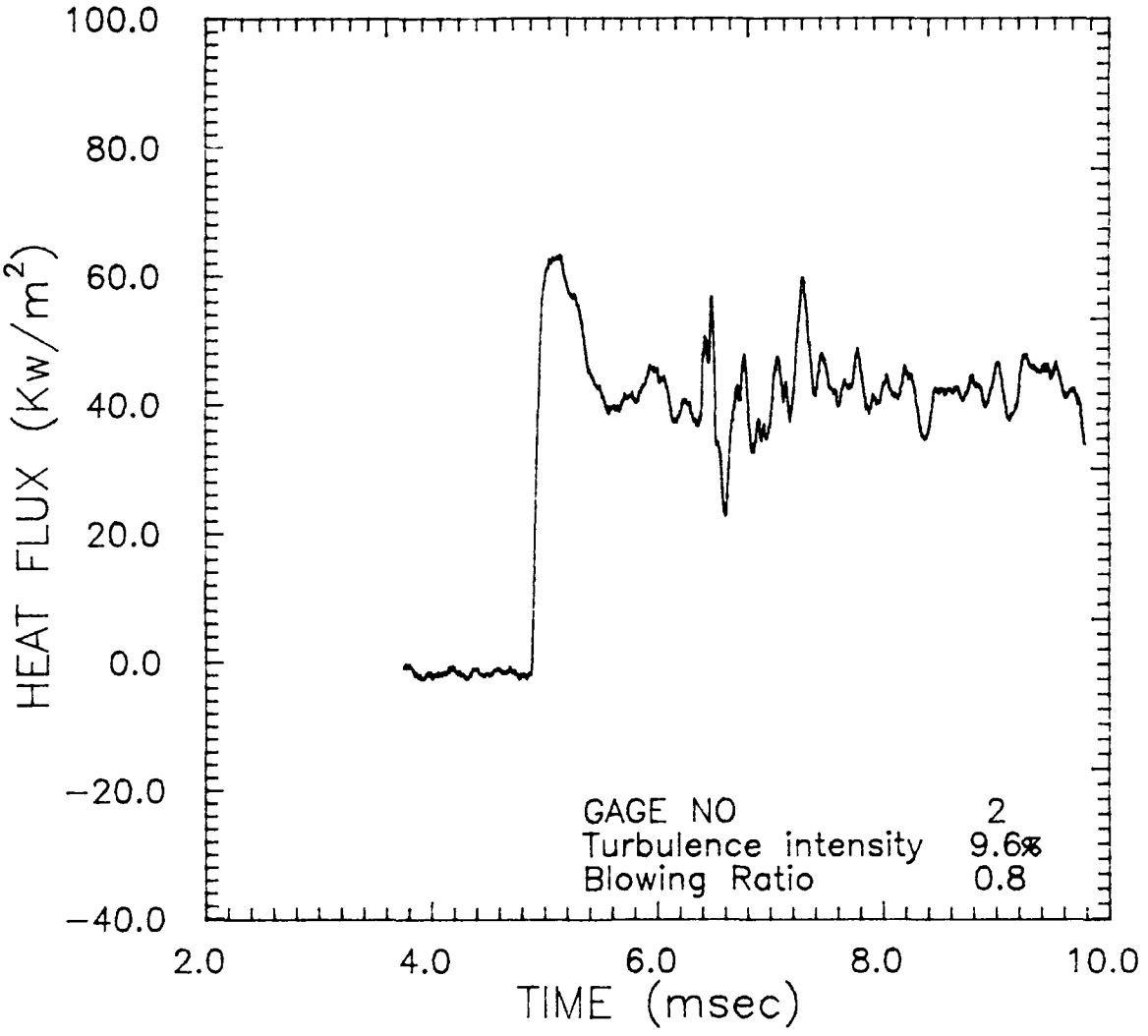

Figure 35: Heat Flux as a Function of Time: FC803

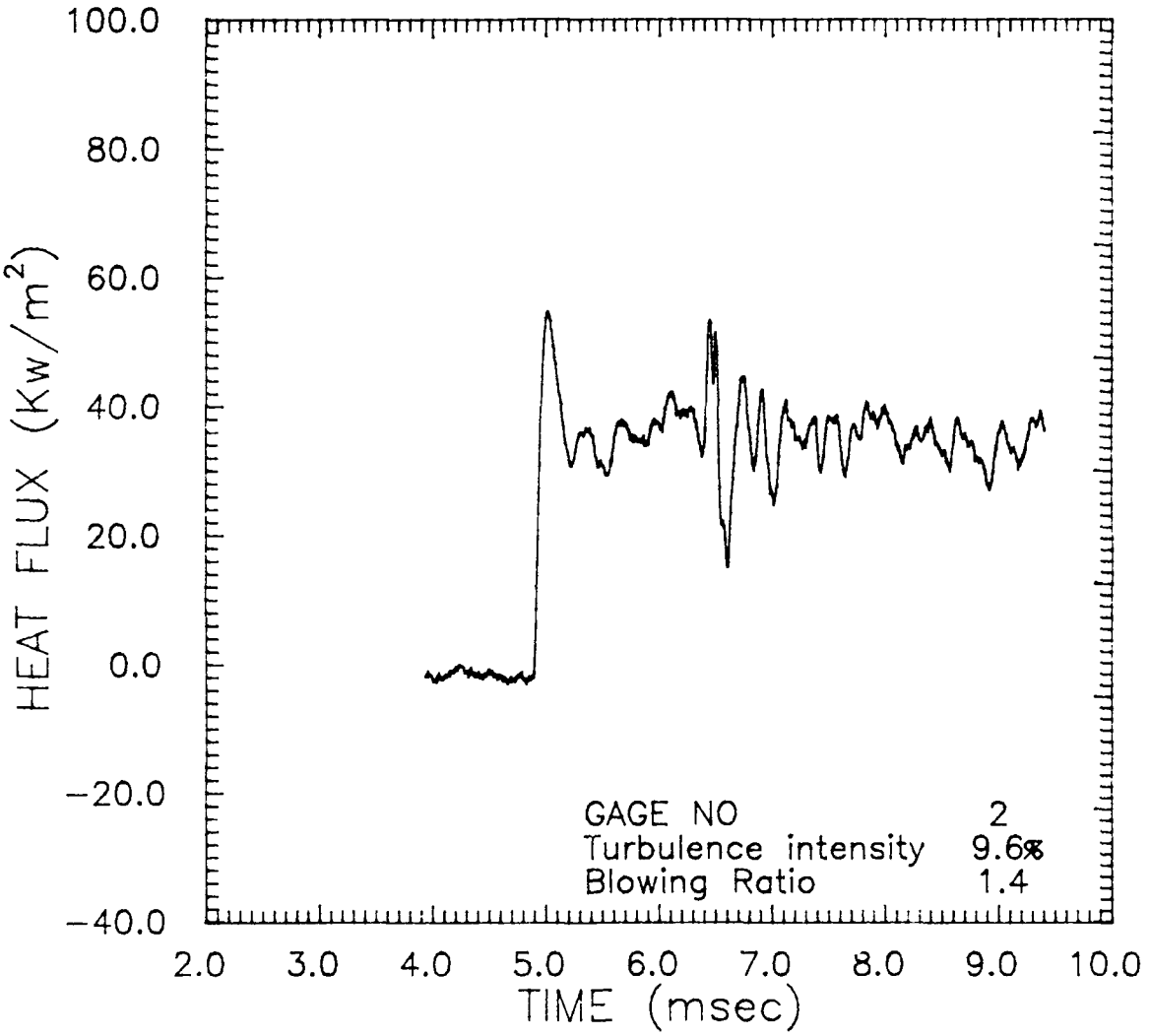

Figure 36: Heat Flux as a Function of Time: FC804

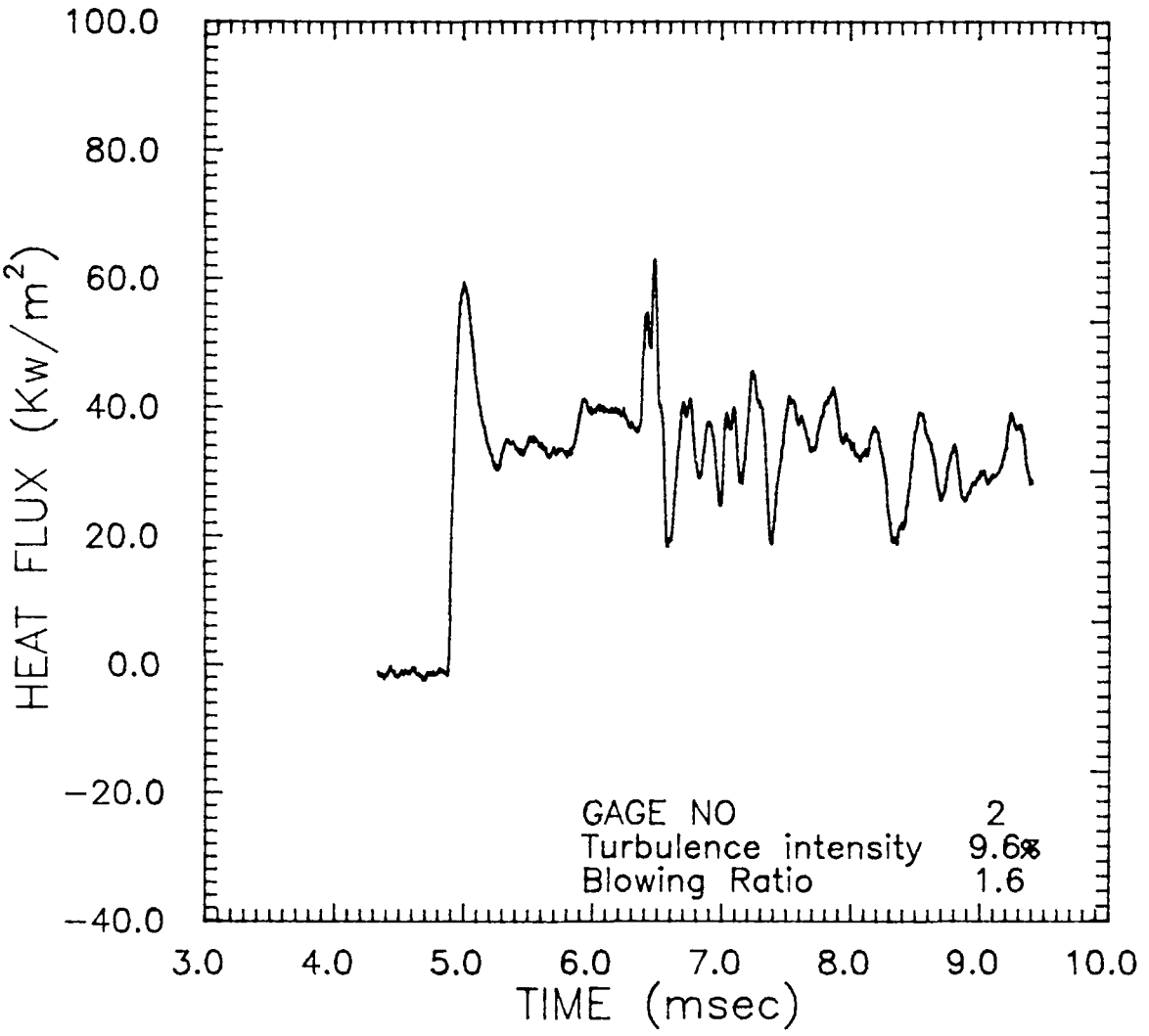

Figure 37: Heat Flux as a Function of Time: FC805

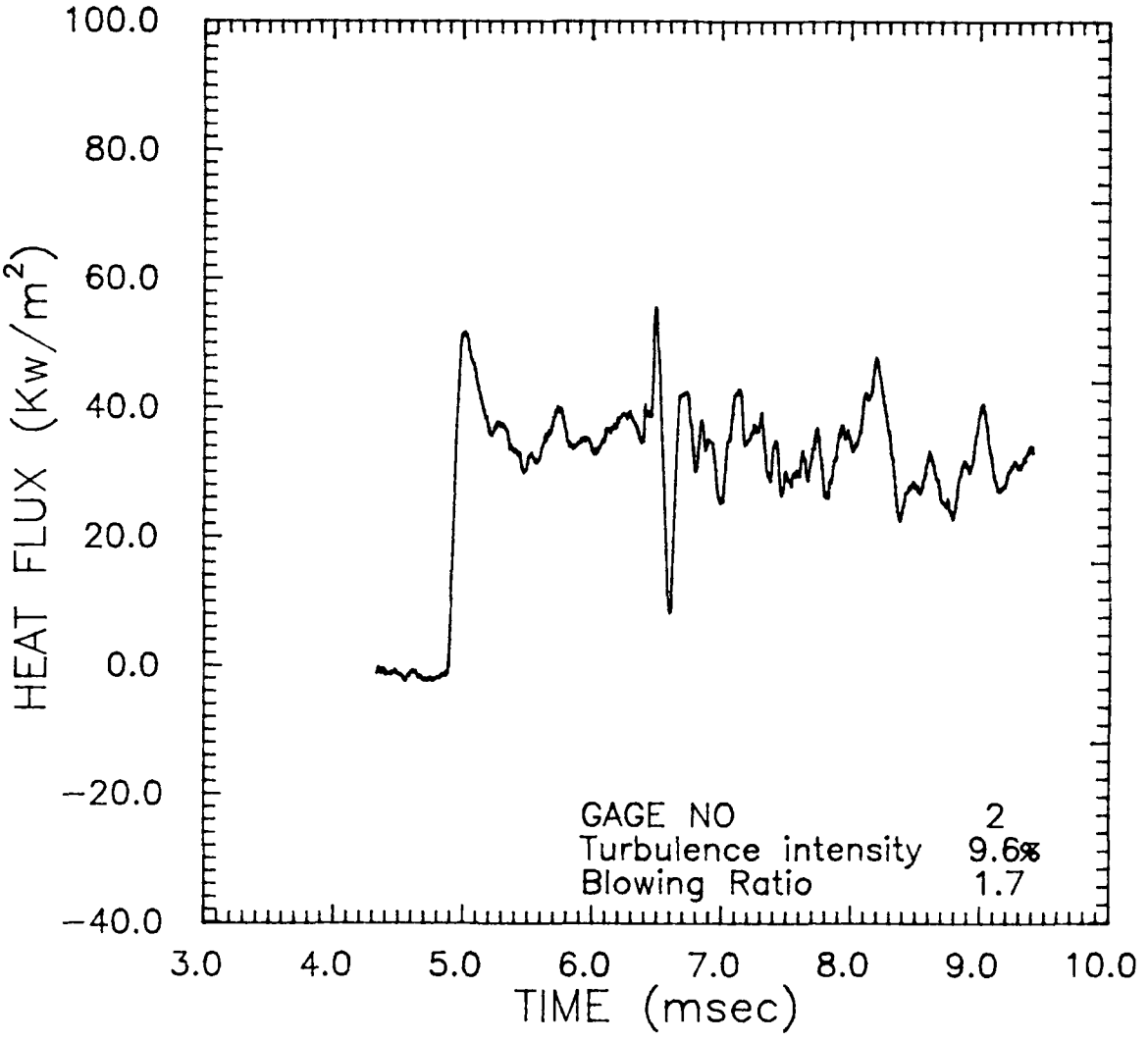

Figure 38: Heat Flux as a Function of Time: FC806

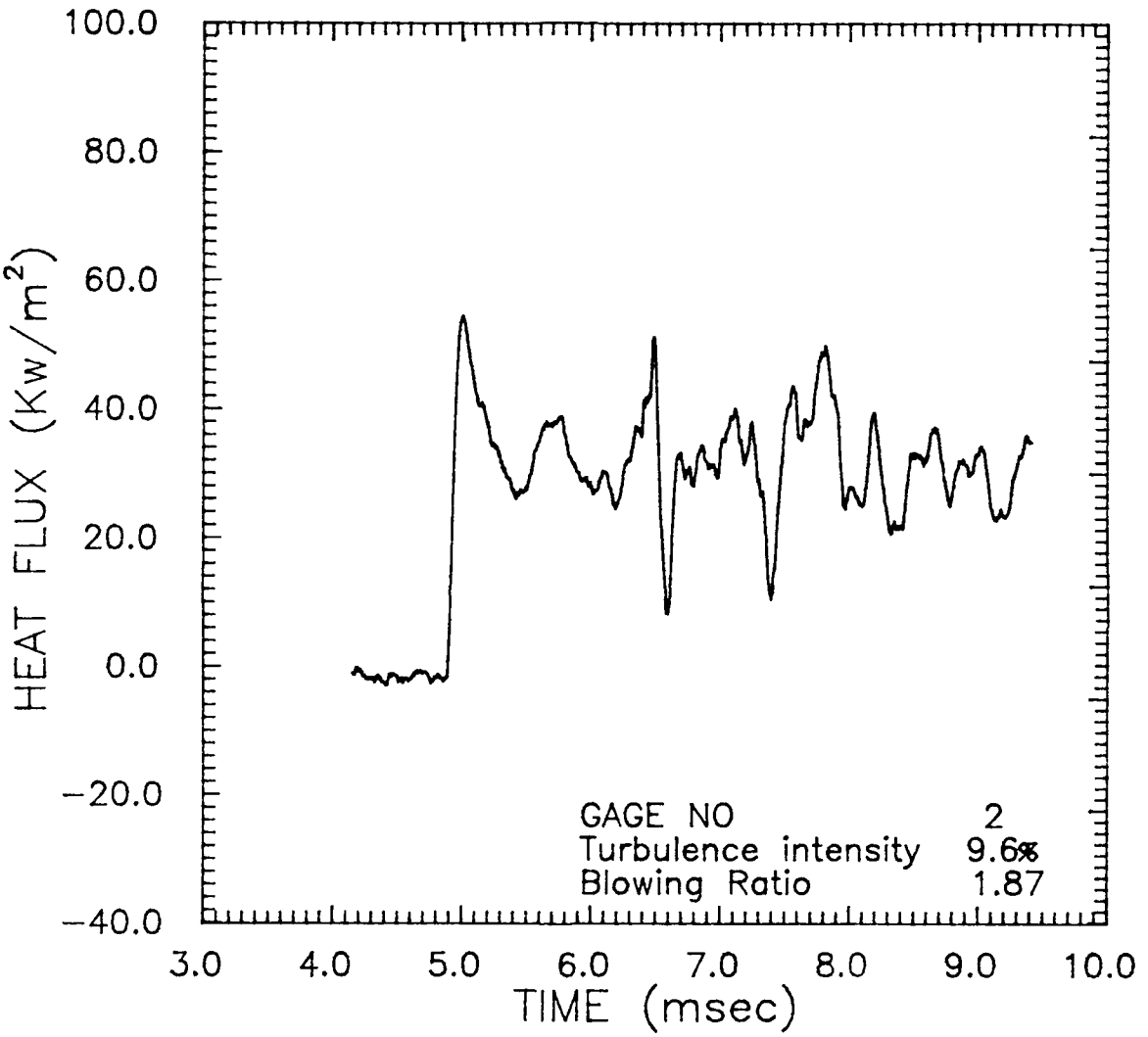

Figure 39: Heat Flux as a Function of Time: FC807

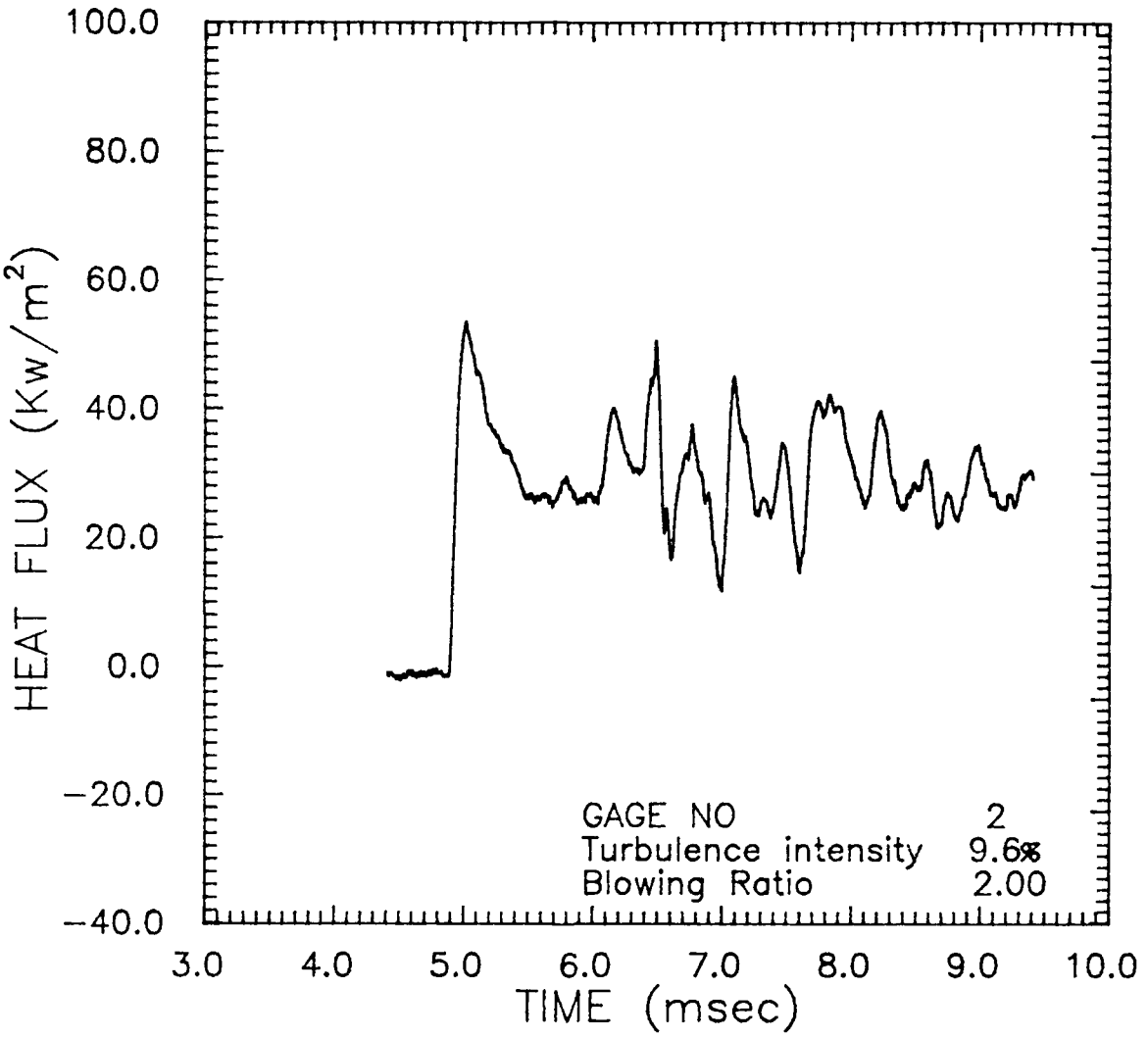

Figure 40: Heat Flux as a Function of Time: FC808

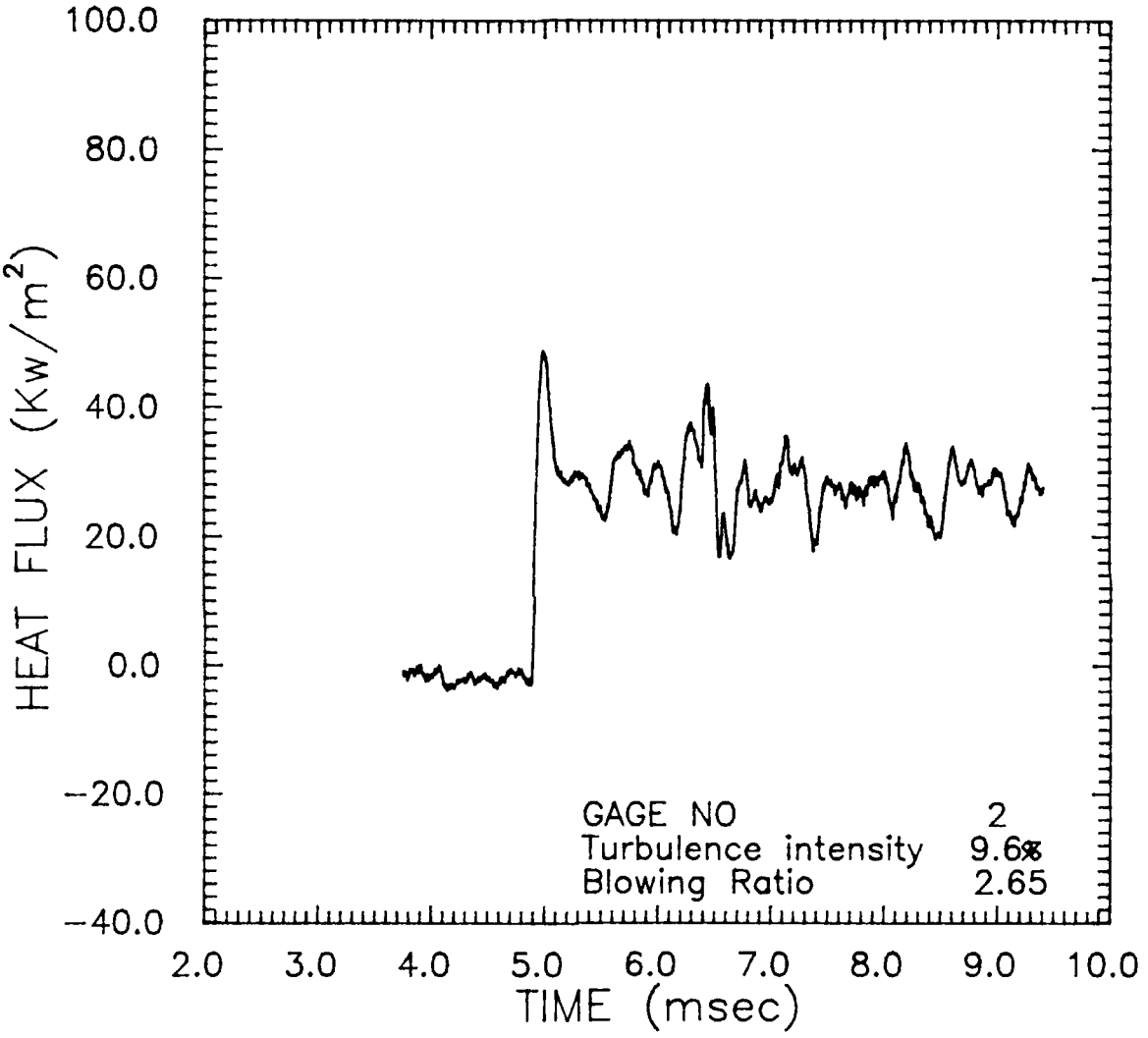

Figure 41: Heat Flux as a Function of Time: FC811

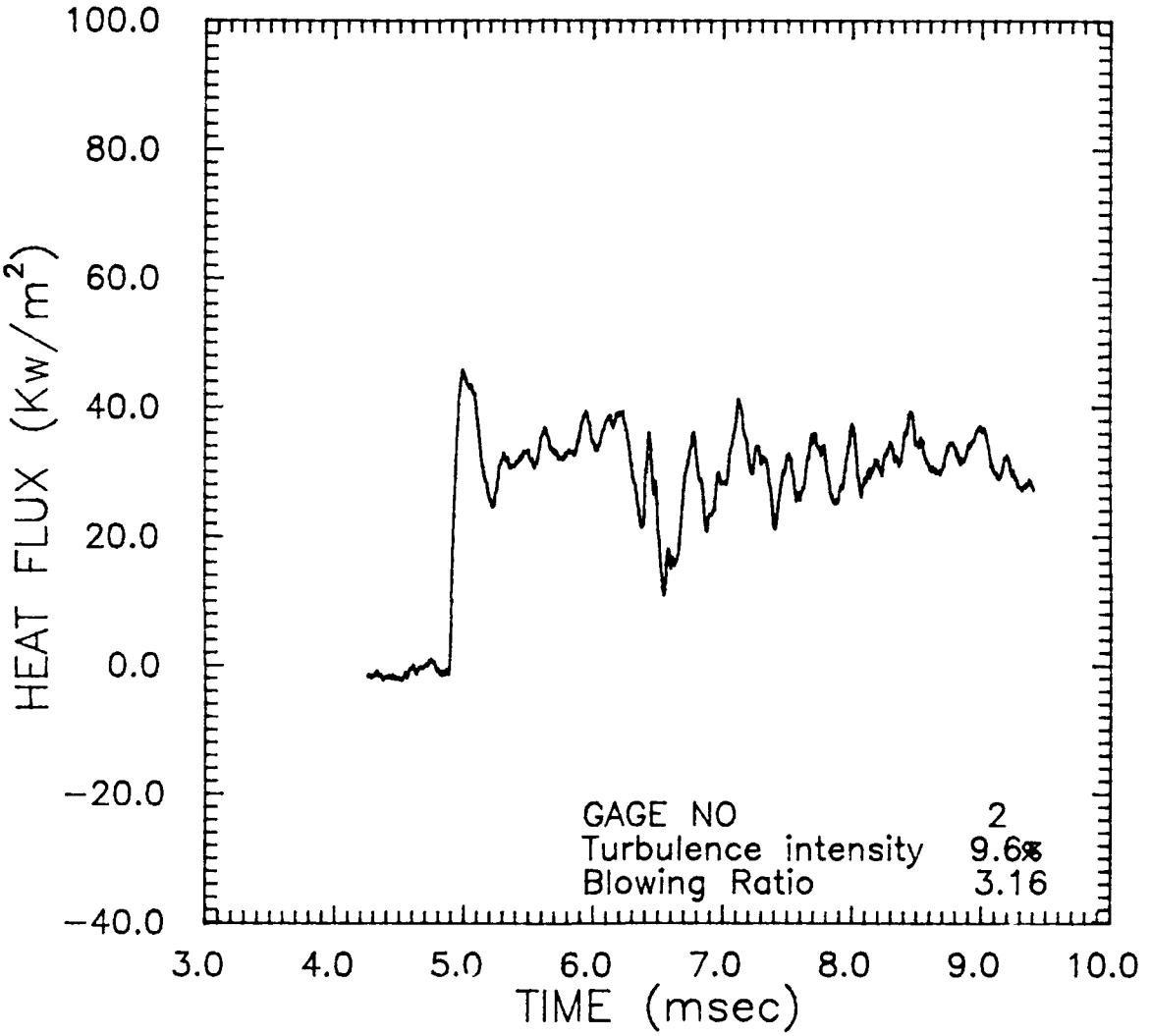

Figure 42: Heat Flux as a Function of Time: FC813

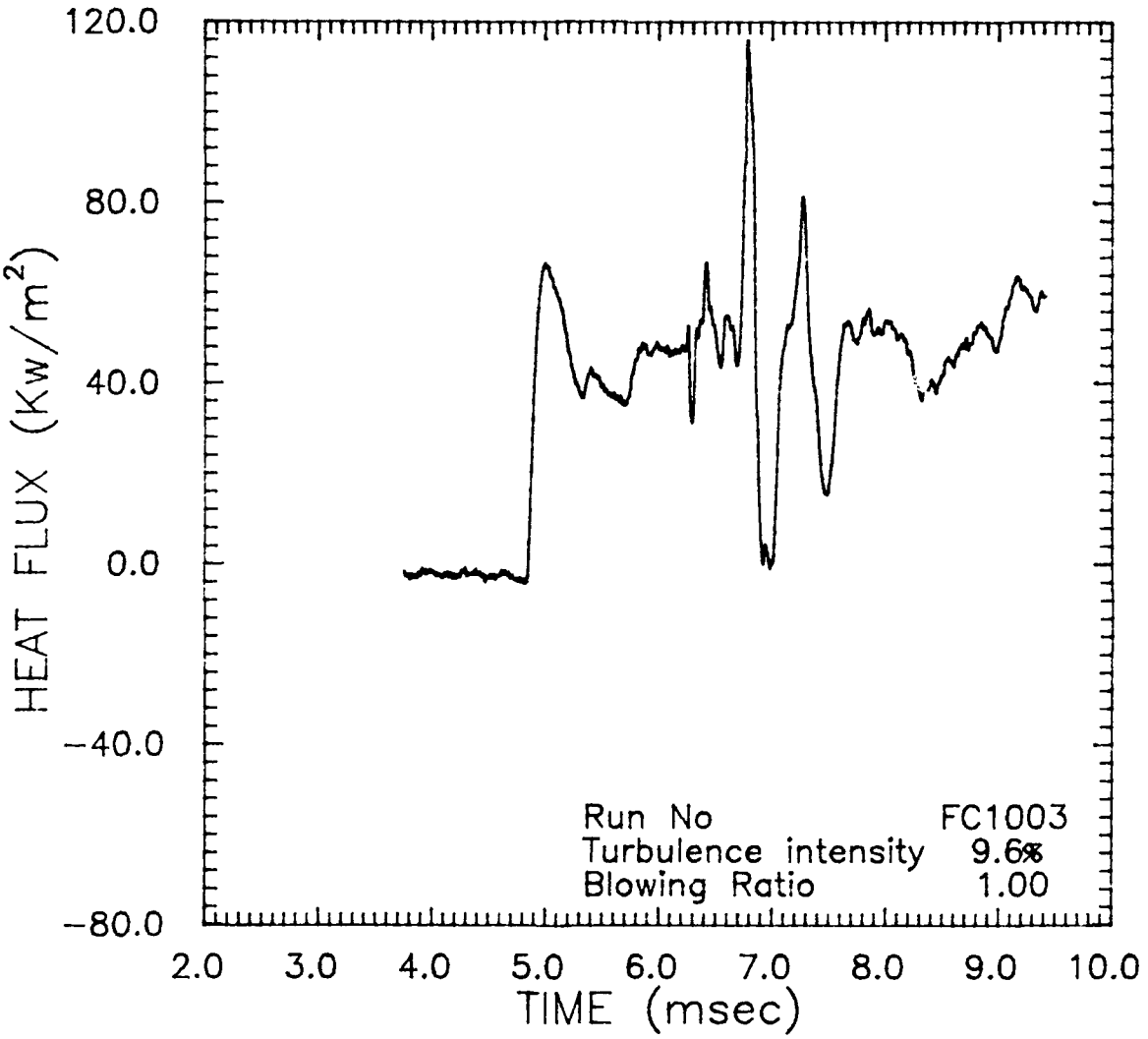

Figure 43: Heat Flux as a Function of Time: Gage No 2

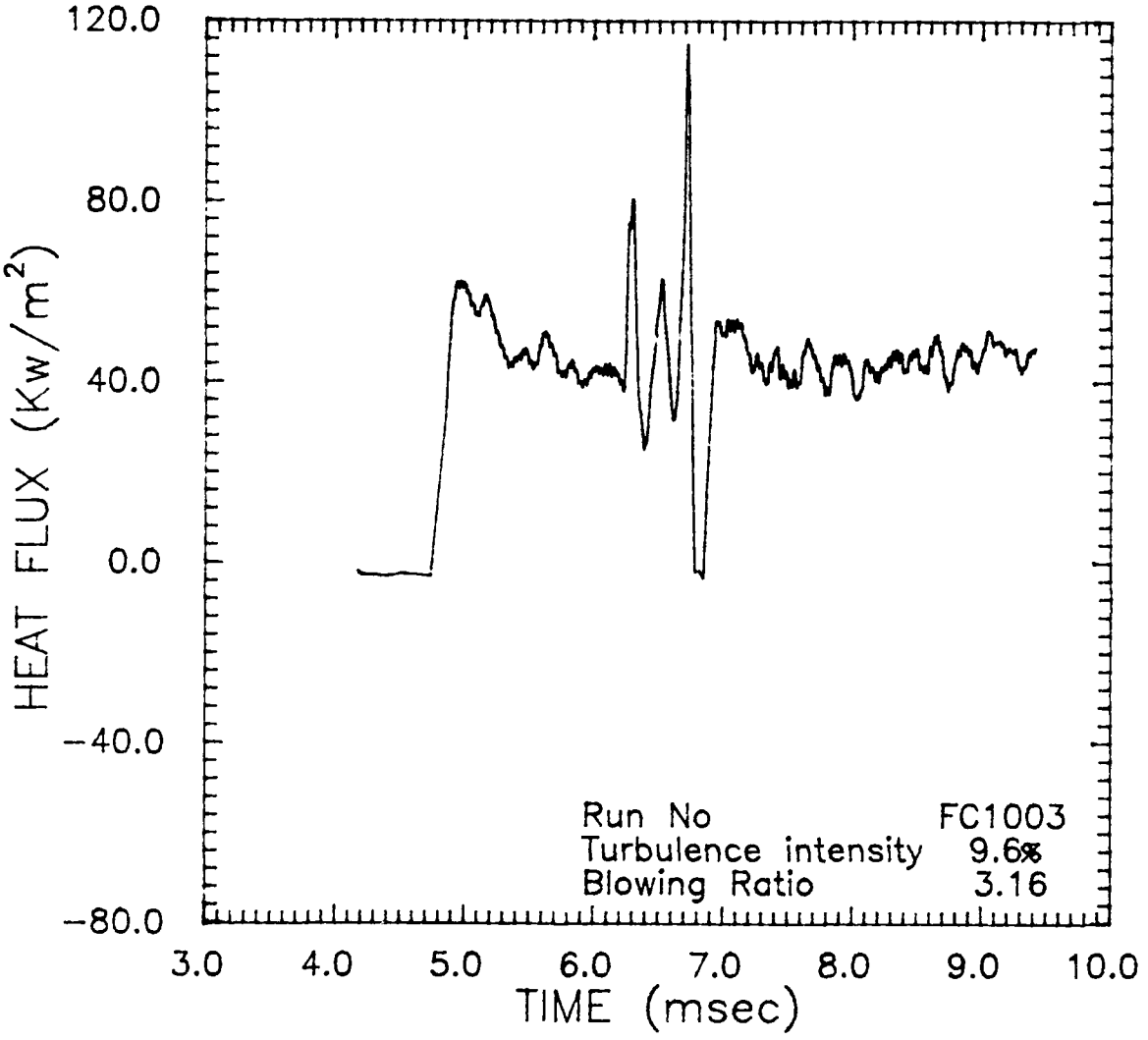

Figure 44: Heat Flux as a Function of Time: Gage No 4

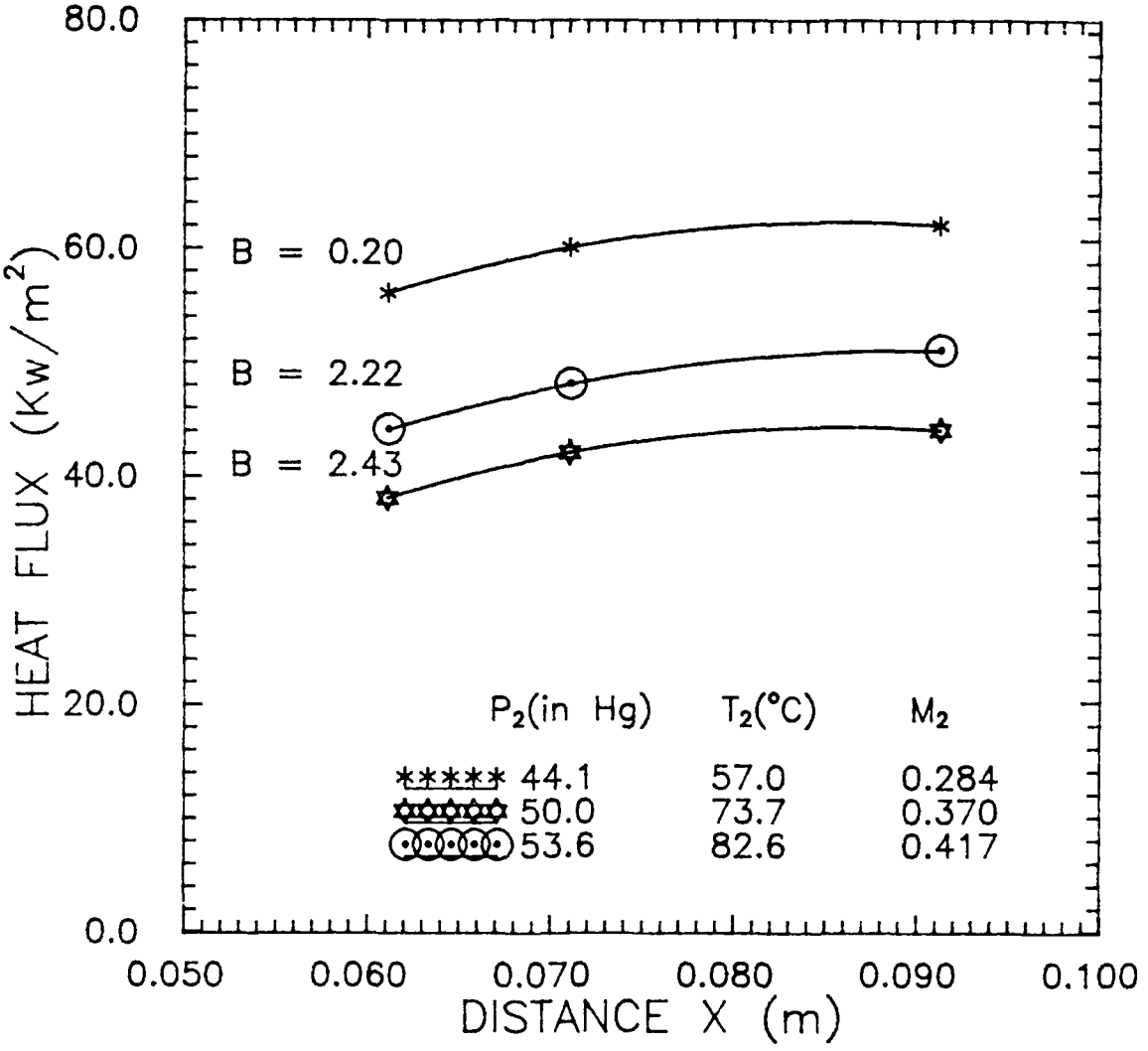

Figure 45: Heat Flux as a Function of Distance Along The Flat Plate

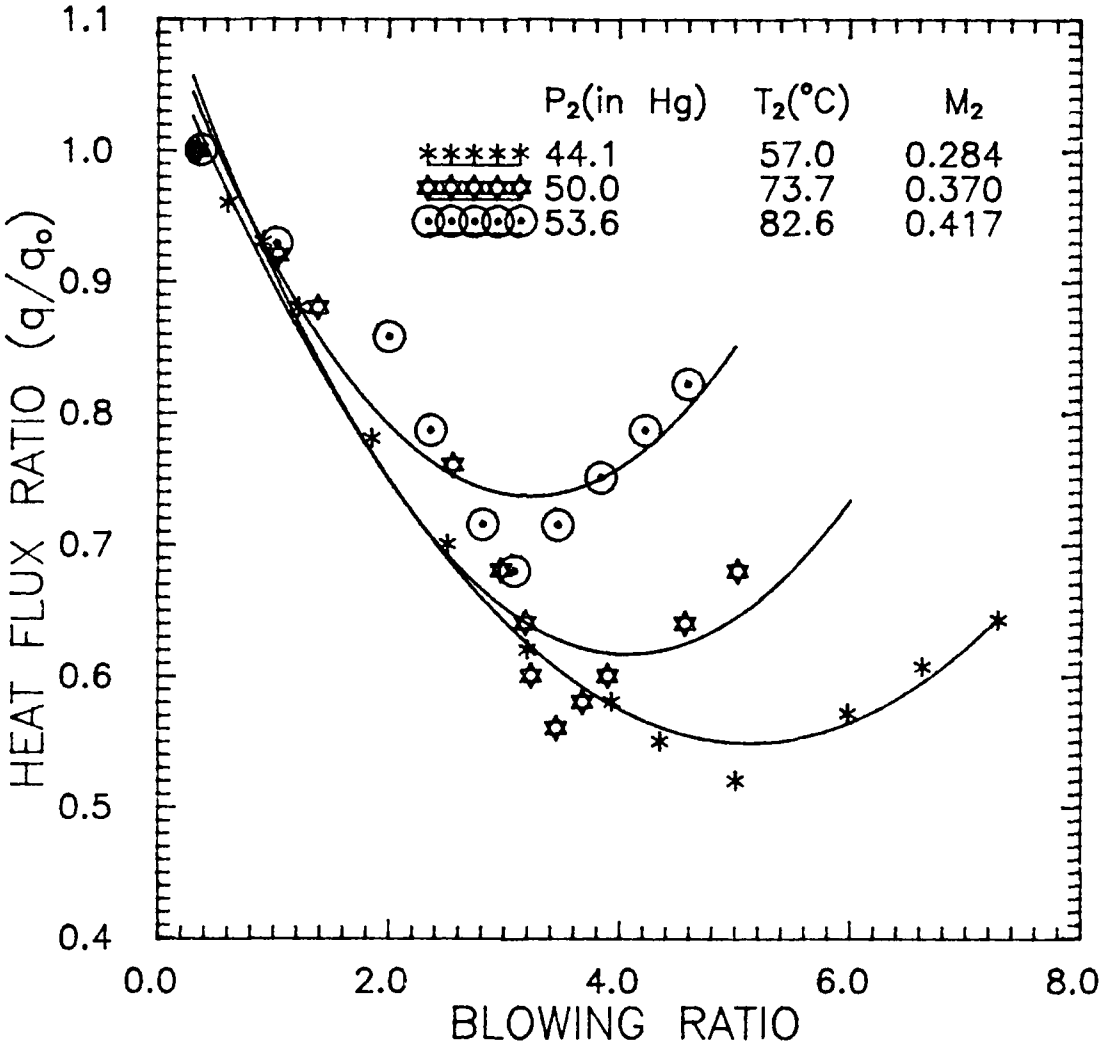

Figure 46: Heat Flux Ratio as a Function of Blowing Ratio

APPENDIX A

Derivation for $\sqrt{\rho C_p k}_{pyrex}$

One dimensional heat conduction equation is expressed as:

$$\frac{\partial T}{\partial t} = \frac{k}{\rho C_p} \frac{\partial^2 T}{\partial x^2} \tag{A.1}$$

where T is the difference between instantaneous and initial temperature, i.e $T(x,\emptyset) = \emptyset$.

For the case of a step function in heat transfer rate the boundry conditions are:

$$\begin{aligned} T(x,\emptyset) &= q(x,\emptyset) = \emptyset \\ q(\emptyset,t) &= q_0 = \text{constant} \end{aligned} \tag{A.2}$$

The solution to equation A-1 can be found in many references as:

$$T(0,t) = \frac{2q}{\sqrt{\pi(\rho C_p k)}} \sqrt{t} \tag{A.3}$$

Let R_0 be the initial resistance of the platinum foil in the heat flux gage. By passing a current of known amplitude, the resistance of the platinum foil changes to R_f.

R_f and R_0 are related to each other by the relationship:

$$R_f = R_0 (1 + \alpha T) \tag{A.4}$$

which would imply that:

$$T = \frac{\Delta R}{\alpha R_o} \tag{A.5}$$

ΔR can be related to the voltage signal across the heat flux gage $\Delta V(t)$, and the constant current through the film i, by:

$$\Delta R = \Delta V(t)/i \tag{A.6}$$

Substituting Equations A.4 and A.5 into Equation A.2 one obtains after some manipulation the following equation:

$$\Delta R = \frac{2q\alpha R_o\sqrt{t}}{\sqrt{\pi\rho C_p k}} \tag{A.7}$$

As explained in the calibration procedure for $\sqrt{\rho C_p k}$, the heat flux gage is first calibrated in air and the factor $\Delta R_1/\sqrt{t}$ is obtained from the resultant curve. If the gage is then calibrated with a small droplet of glycerine on top of the heat flux gage, the heat produced due to the passage of current would flow both into the glycerine and the gage substrate. If a fraction "m" of the heat generated diffuses into glycerine and $\Delta R_2/\sqrt{t}$ is the slope of the resultant curve then:

$$\frac{\sqrt{\rho C_p k_{gly}}}{R_o\alpha} = \frac{2mI^2R_o}{\sqrt{\pi}\dfrac{\Delta R_2}{\sqrt{t}}} \tag{A.8}$$

$$\frac{\sqrt{\rho C_p k_{subs}}}{R_o\alpha} = \frac{2(1-m)I^2R_o}{\sqrt{\pi}\dfrac{\Delta R_2}{\sqrt{t}}} \tag{A.9}$$

But also:

$$\frac{\sqrt{\rho C_p k_{subs}}}{R_o\alpha} = \frac{2I^2R_o}{\sqrt{\pi}\dfrac{\Delta R_1}{\sqrt{t}}} \tag{A.10}$$

From equations A-8, A-9, and A-1Ø, by manipulation we can

obtain the correct relationship for the bulk thermal diffusivity of the substrate as:

$$\sqrt{\rho C_p k_{subs}} = \frac{\sqrt{\rho C_p k_{gly}}}{\frac{\Delta R_1/\sqrt{t}}{\Delta R_2/\sqrt{t}} - 1} \qquad \text{(A.11)}$$

APPENDIX B

CALIBRATION OF HEAT FLUX GAGES FOR $\sqrt{\rho C_p K}$

The calibration procedure adopted to find the bulk thermal diffusivity of the heat flux gages is as follows:

A bridge circuitry shown in Figure 12 was constructed using precision resistors. The heat flux gage under calibration was used as one of the legs of the bridge circuitry whereas a variable resistor was used parallel to the leg adjacent to the heat transfer gage so as to ensure proper balancing of the bridge.

A 5ØØΩ resistor was used in series with the bridge to keep the current at a nominal value of less than 2.5 mamp to avoid any excessive passage of current through the circuit resulting in burning out the heat flux gage.

A 5 volt DC power supply from a Tektronix work station was used to balance the bridge. But to pass a single pulse of known amplitude through the circuit a Wavetek model signal generator was used.

The output of the bridge circuitry was connected to a differential amplifier for filtering and amplification. Having filtered the output at 1Ø Khz and amplified with a gain of 25Ø, it was fed into a digital oscilloscope for display and DL-12ØØ for recording. A schematic of the instrument interfacing is shown in Figure 13.

The first part of the calibration was accomplished by passing a single square pulse of 5 volts with a period and width of 1Ø msec and 5 msec respectively through the bridge circuitry. This allowed to raise the temperature of the heat flux gage resulting in a

change in resistance of the platinum foil of the gage which in turn unbalanced the previously balanced bridge.

The amplified output of the bridge was displayed and recorded simultaneously on the digital oscilloscope and the DL-12ØØ respectively. Figure B.1 shows the output voltage of the heat flux gage w.r.t time.

The second step of the calibration involved a repetition of the same procedure except that the heat flux gage was covered with a droplet of glycerine whose bulk thermal diffusivity was known.

Passage of the current, this time, not only allowed the generated heat to flow into the substrate of the gage but also into glycerine. The output of the heat flux gage was once again recorded and displayed on the DL-12ØØ and the digital oscilloscope respectively. Figure B.2 shows the output voltage of the heat flux gage, covered with glycerine, w.r.t time.

Figures B.1 and B.2 show that the output of the heat flux gage in both the experiments is parabolic with time. This would imply that a plot of the output voltage w.r.t $\sqrt{t}$ would be a linear curve. Figure B.3 illustrate an example of such a plot.

The slope of the curves illustrated in figure B.3, i.e $\Delta V_1/\sqrt{t}$ for the experiment with heat flux gage in air environment and $\Delta V_2/\sqrt{t}$ for the gage in glycerine environment, are used in Equation 36 to find out the correct value of the bulk thermal diffusivity of the heat flux gages. The calibration curves for each gage are shown in Figures B.3 to B.5.

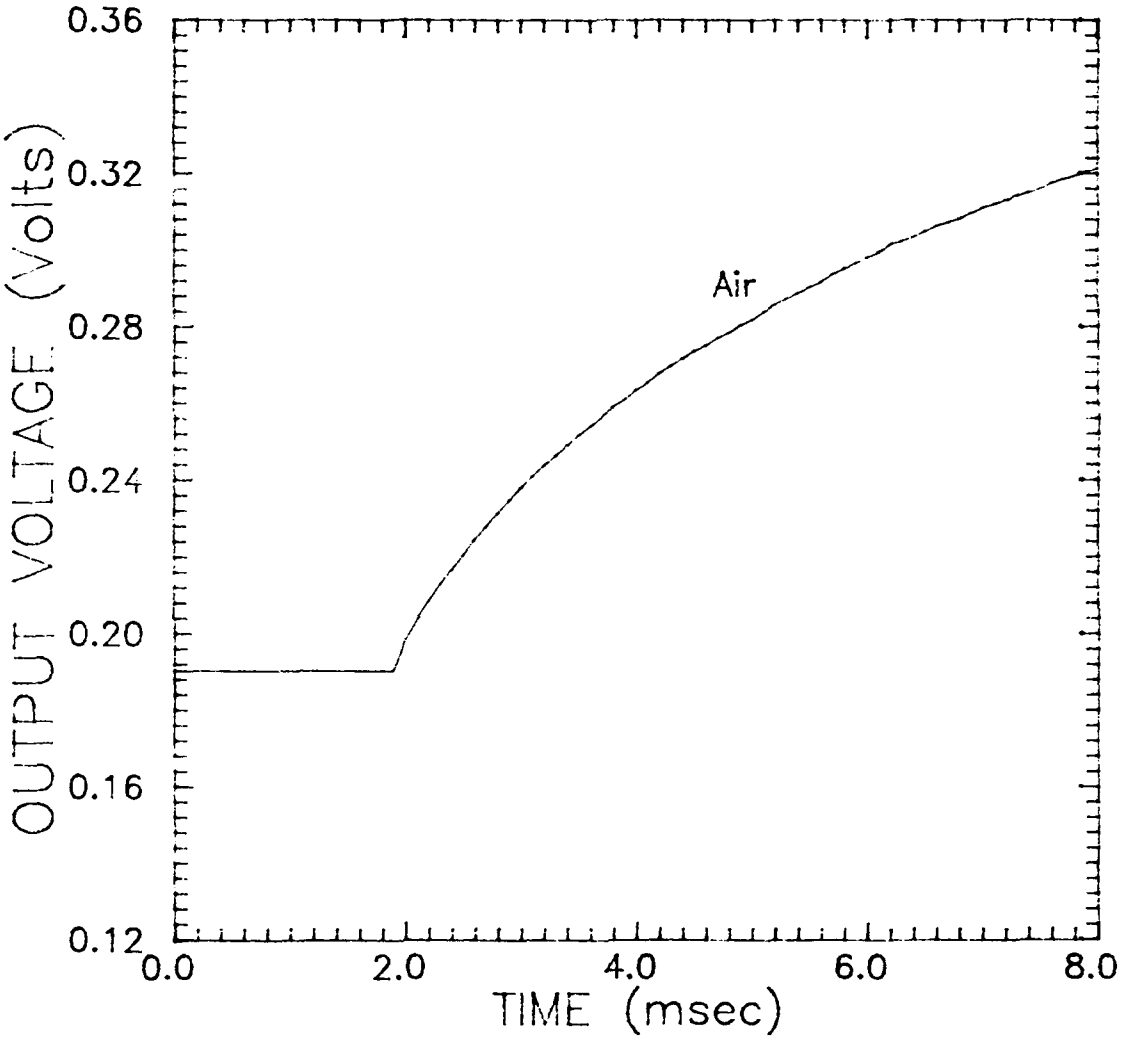

Figure B.1 : Parabolic Output of Heat Flux Gage No 4

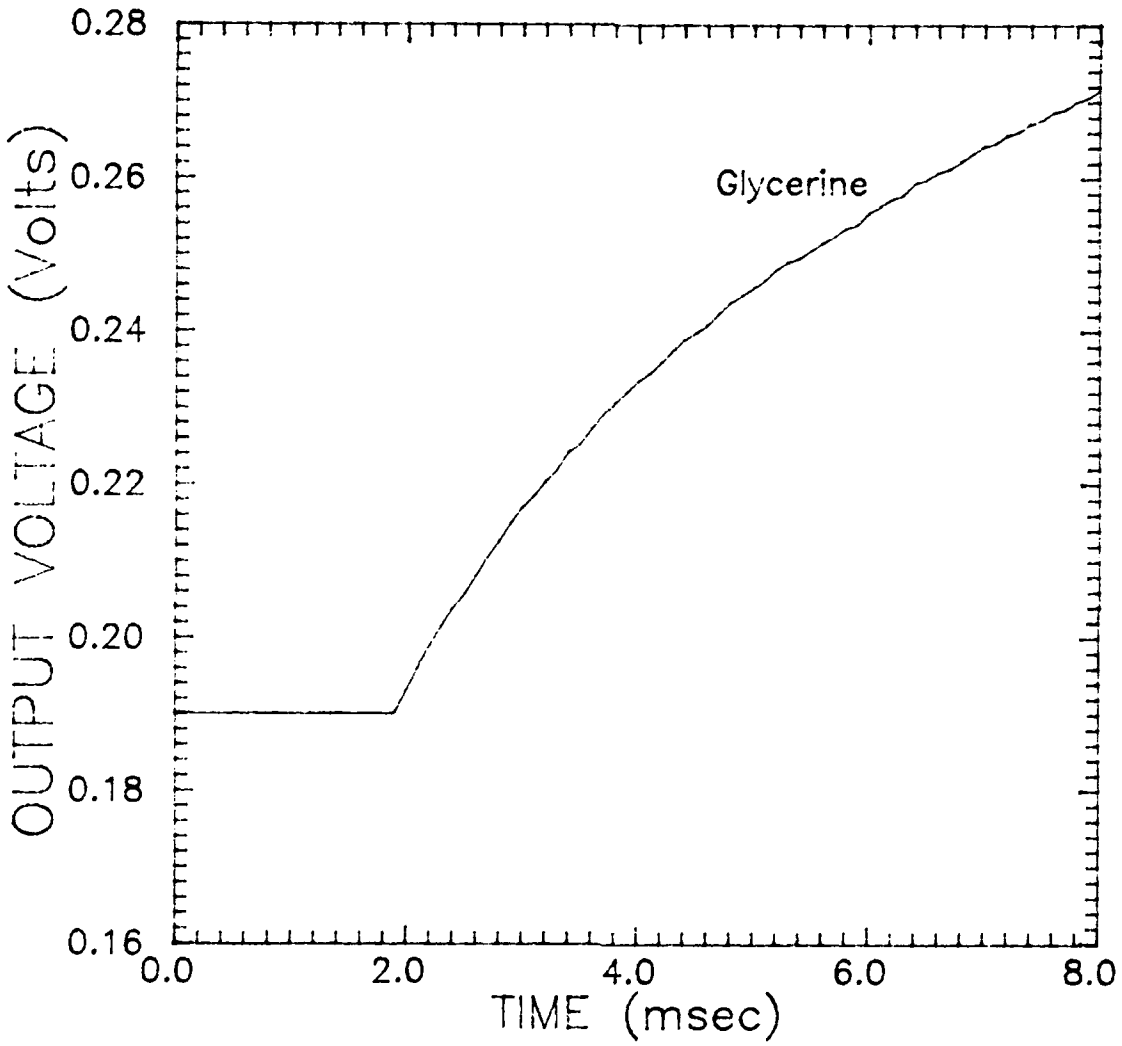

Figure B.2: Parabolic Output of Heat Flux Gage No 4

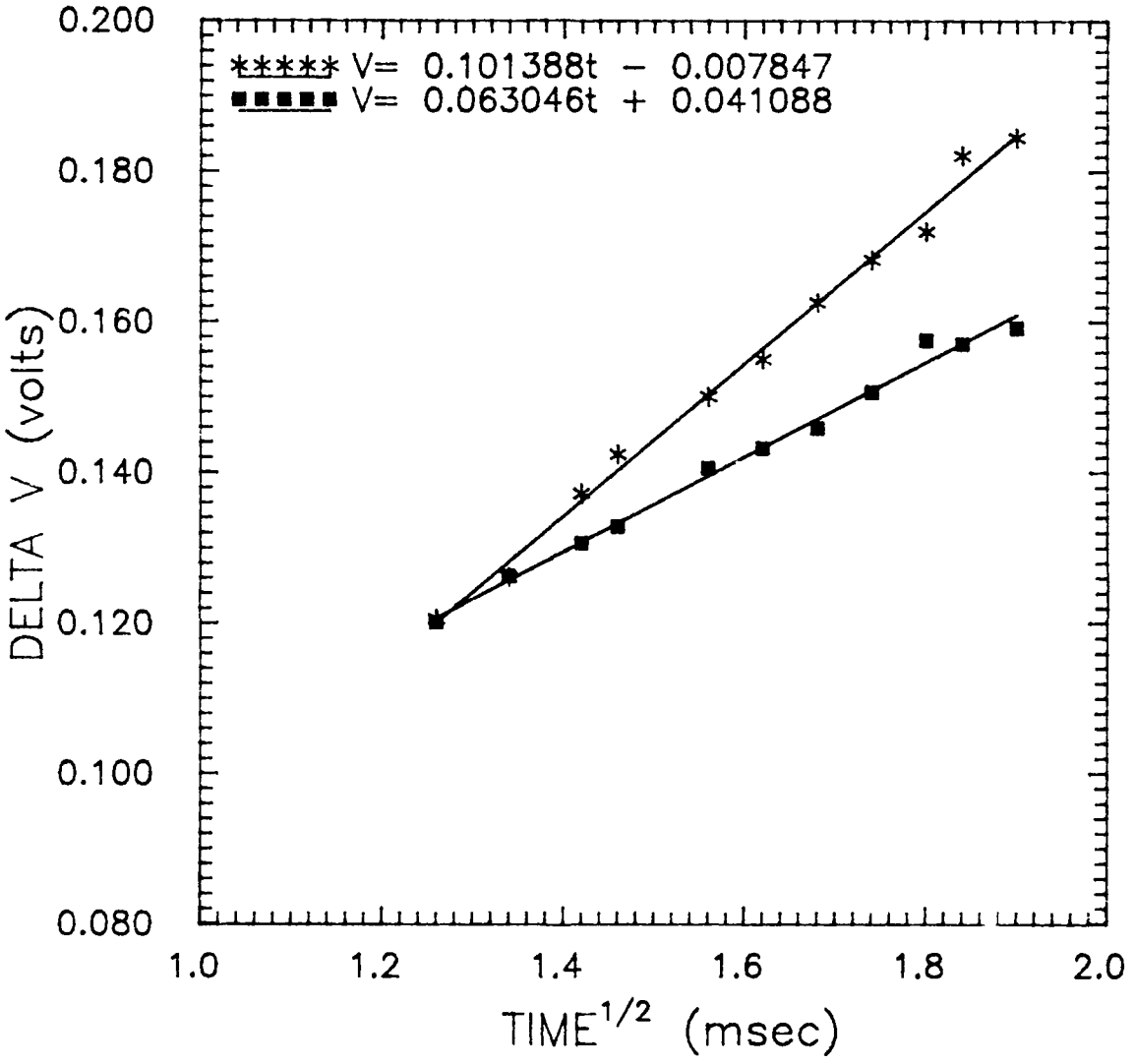

Figure B.3: Calibration Curves for Gage No 2

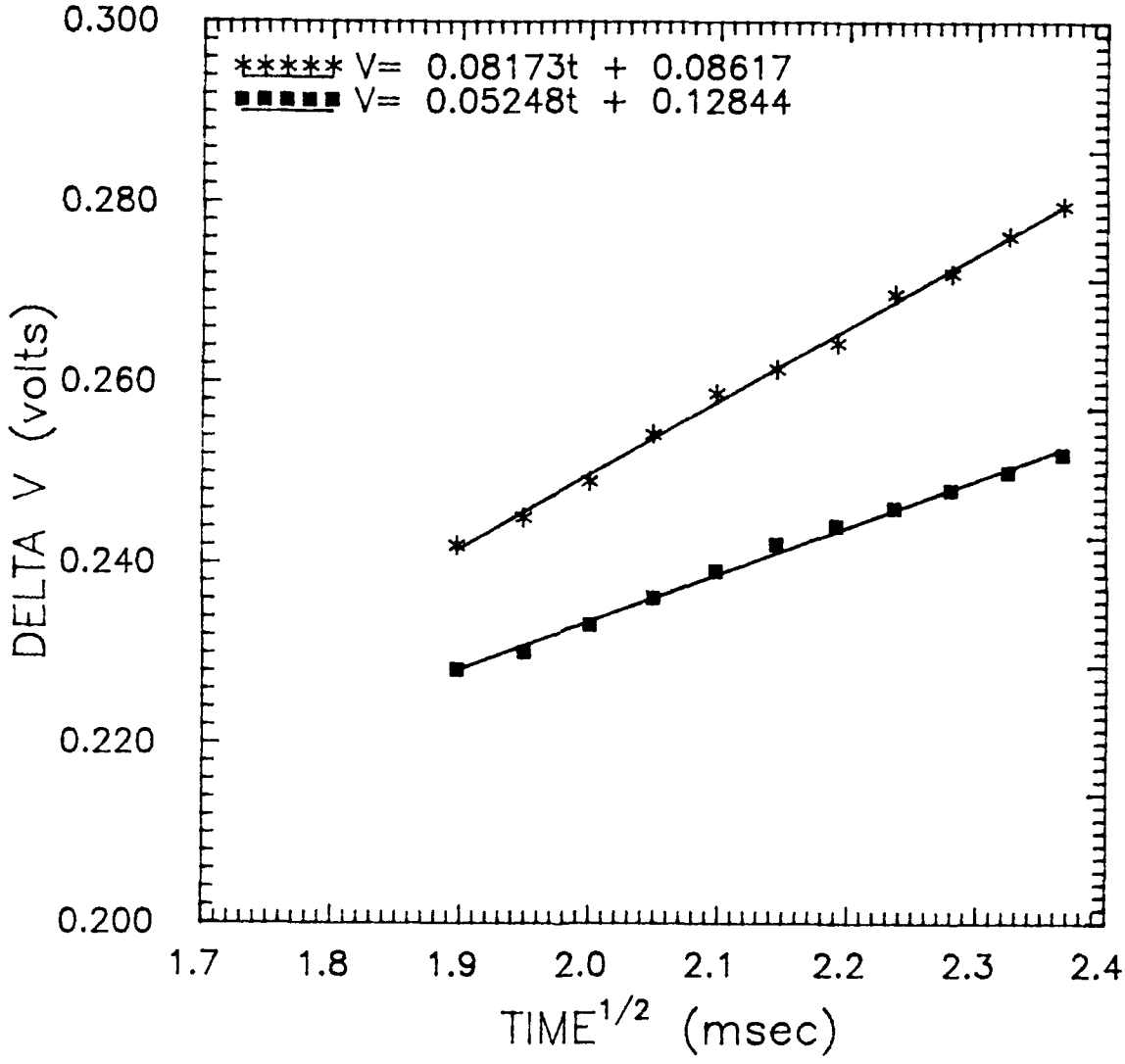

Figure B.4: Calibration Curves for Gage No 4

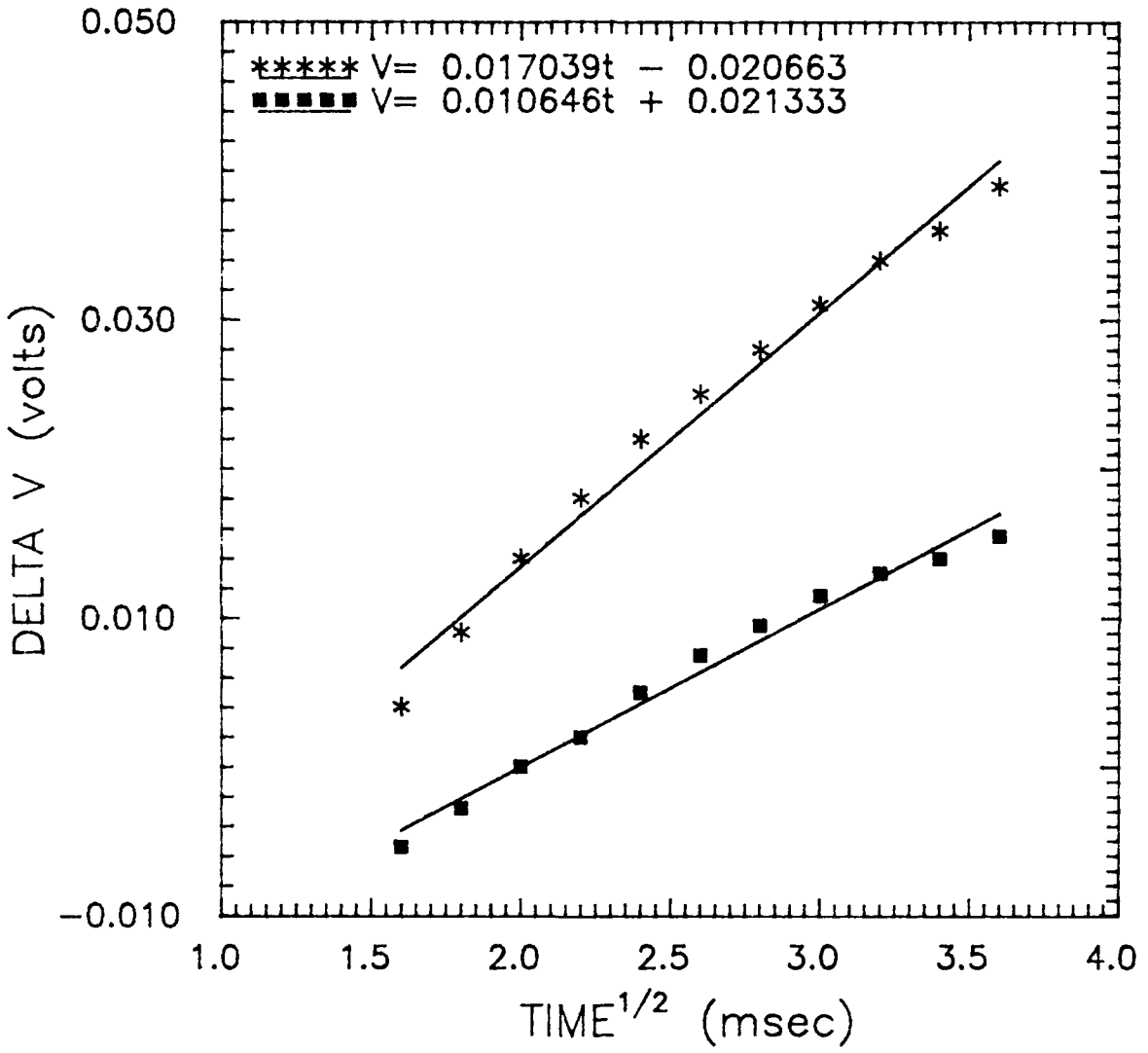

Figure B.5: Calibration Curves for Gage No 6

APPENDIX C

CALIBRATION OF HEAT FLUX GAGES FOR TEMPERATURE COEFFICIENT

The heat flux gages were calibrated for their temperature coefficient following the procedure mentioned in section IV.

The output voltage of the bridge circuitry was plotted against temperature. The calibration curves are shown as Figures C.1 to C.3.

The linear relationships obtained as a result of fitting a curve through the data are:

HEAT FLUX GAGE NO 2

V = Ø.Ø2418Ø6*T - 1.5Ø1

HEAT FLUX GAGE NO 4

V = Ø.Ø236467*T - 1.66Ø1

HEAT FLUX GAGE NO 6

V = Ø.Ø1788V*T - 1.42726

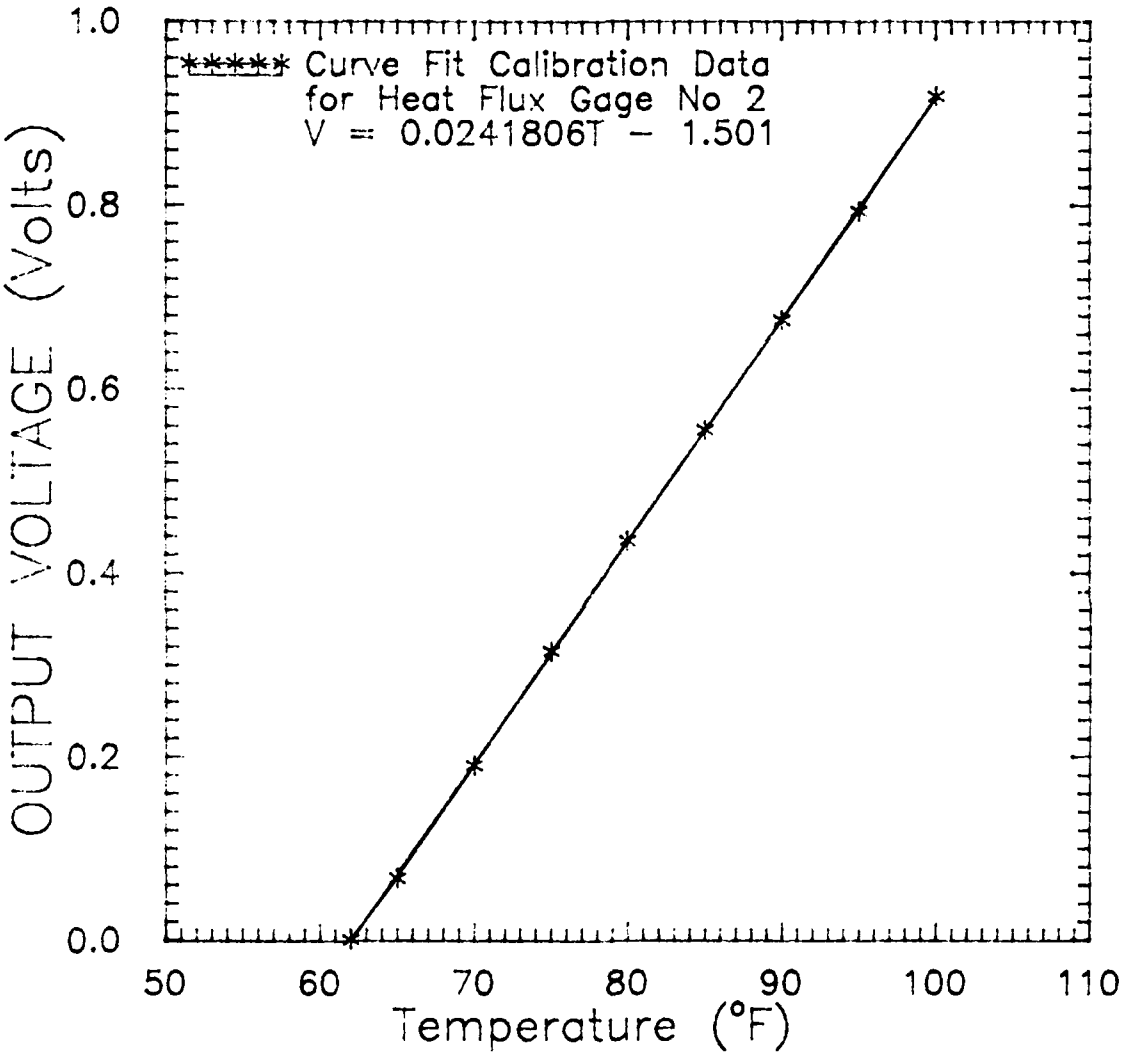

Figure C.1: Calibration Curve For Gage No 2

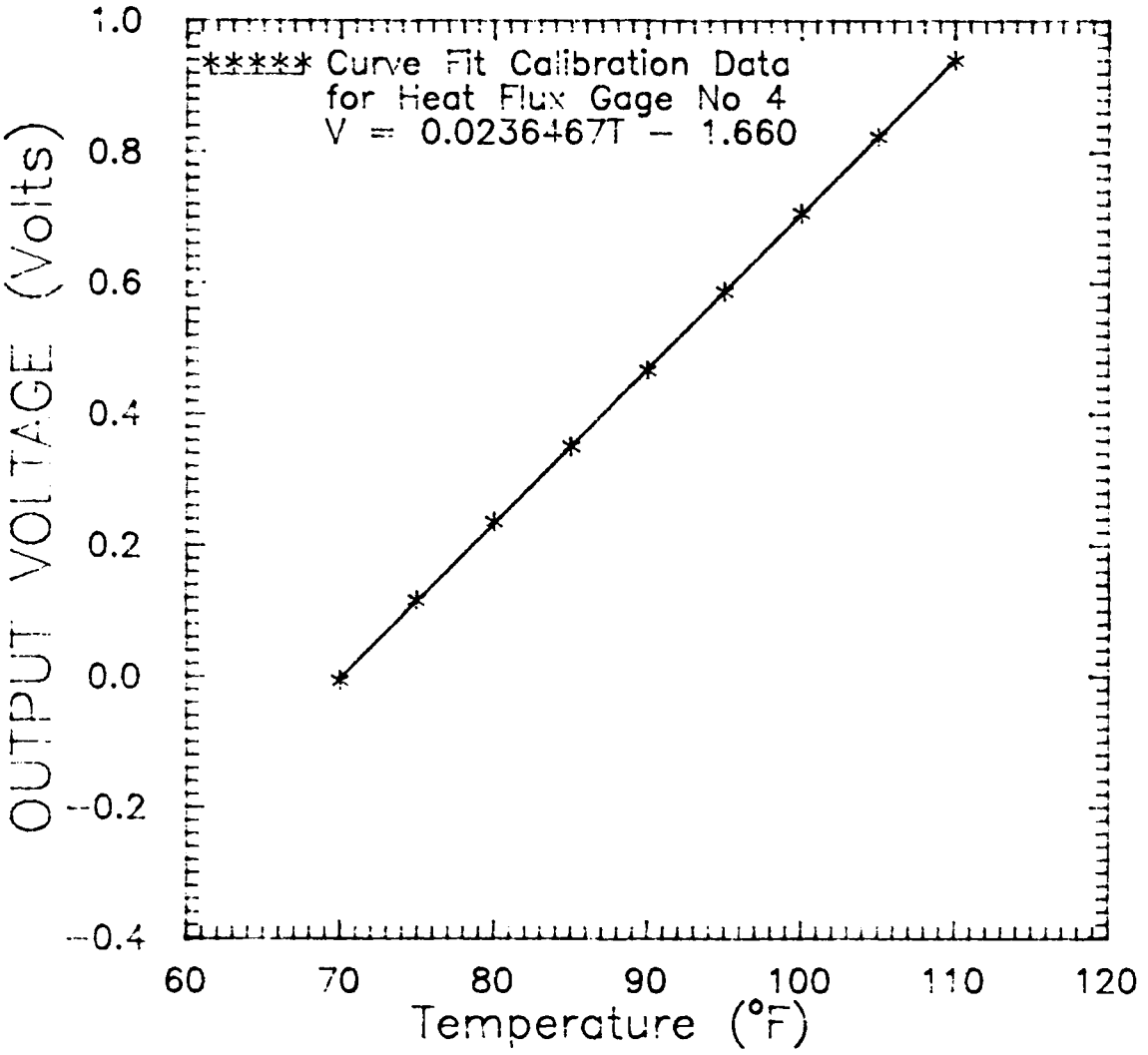

Figure C.2: Calibration Curve For Gage No 4

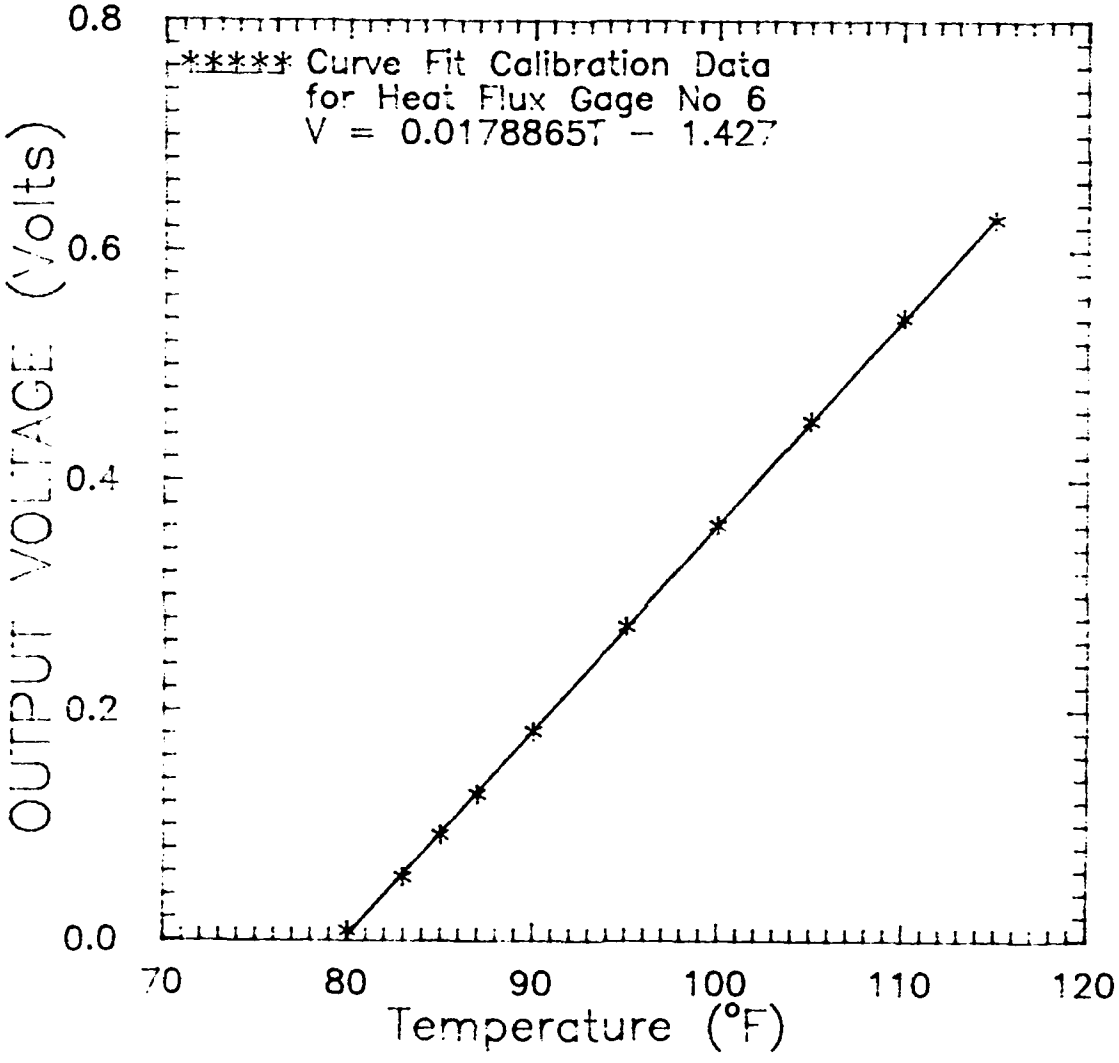

Figure C.3: Calibration Curve For Gage No 6

APPENDIX D

CALIBRATION OF PRESSURE TRANSDUCERS

The pressure transducers used during this study were calibrated using an AMETEK Model HK-5ØØ Pneumatic Dead Weight Tester. The output voltage of the pressure transducers was plotted as a function of pressure (psig).

The calibration curves are plotted un Figures D.1 to D.3. The least square fit of the calibration curves resulted in the following equations:

Forward Pressure Transducer

$$P = 19.887V - Ø.25537$$

Rear Pressure Transducer

$$P = 29.5Ø4V + Ø.2Ø712$$

Film Cooling Flow Pressure Transducer

$$P = 32.465V - Ø.Ø5925$$

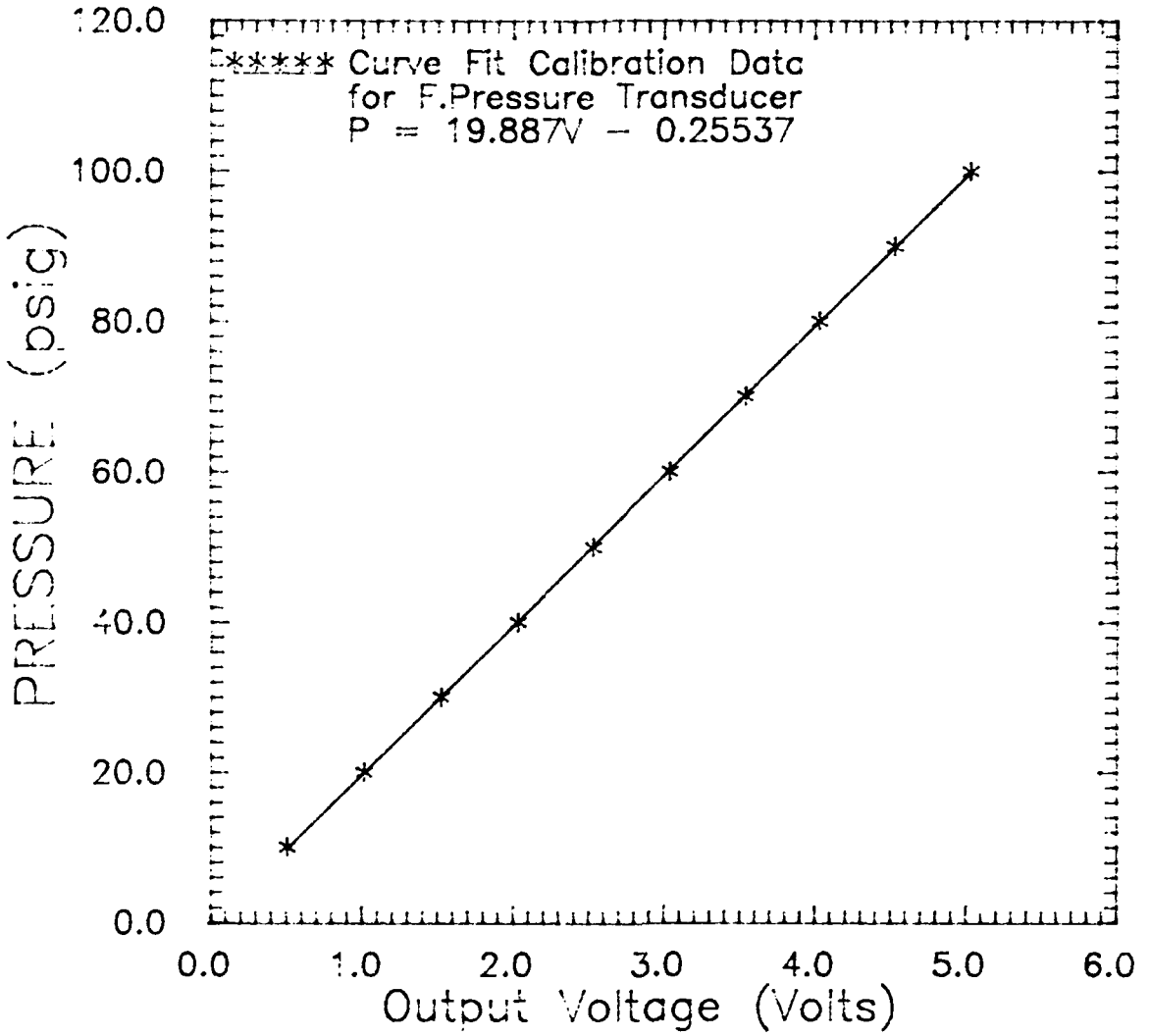

Figure D.1: Calibration Curve For Forward Pressure Transducer

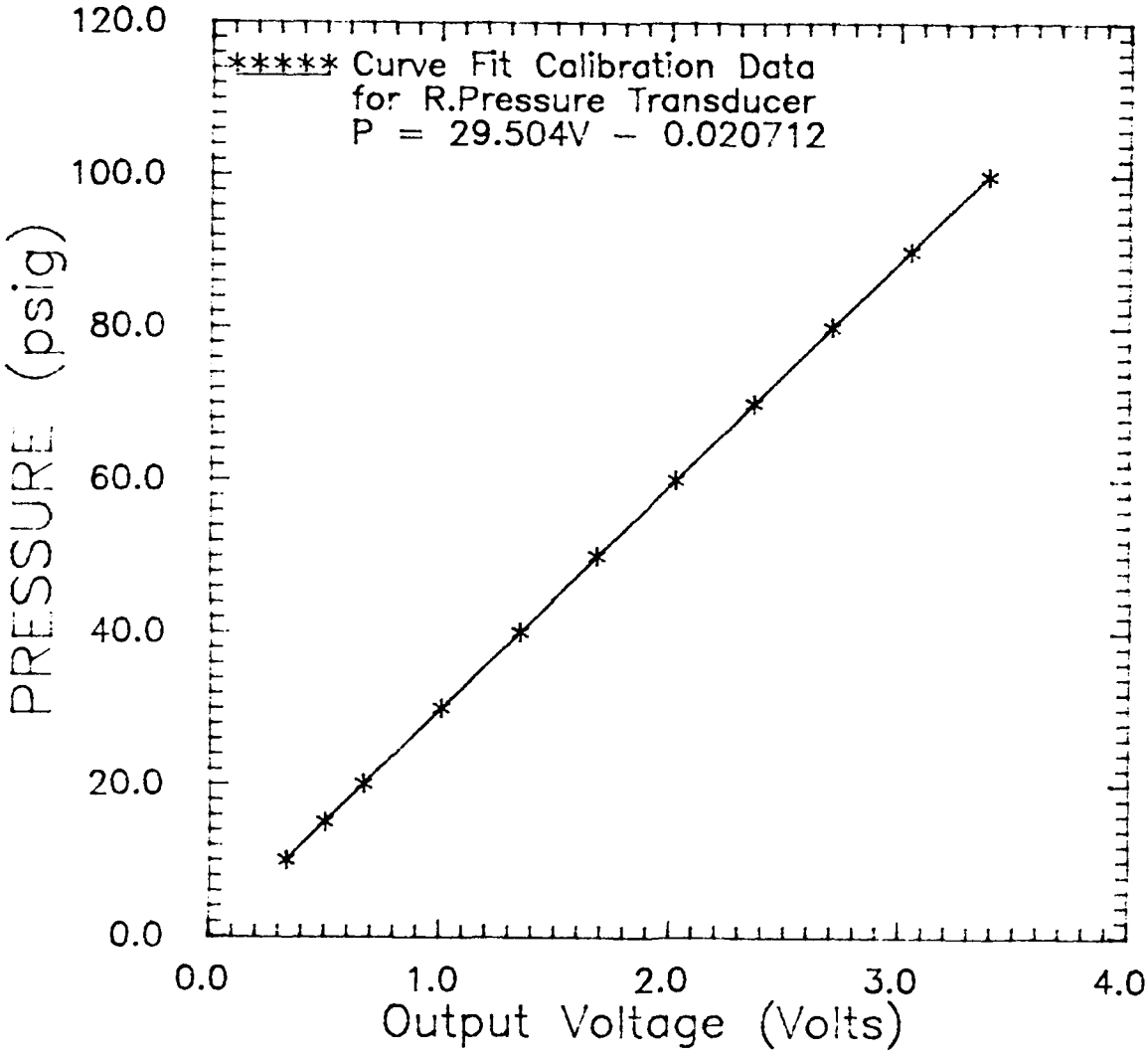

Figure D.2: Calibration Curve For Rear Pressure Transducer

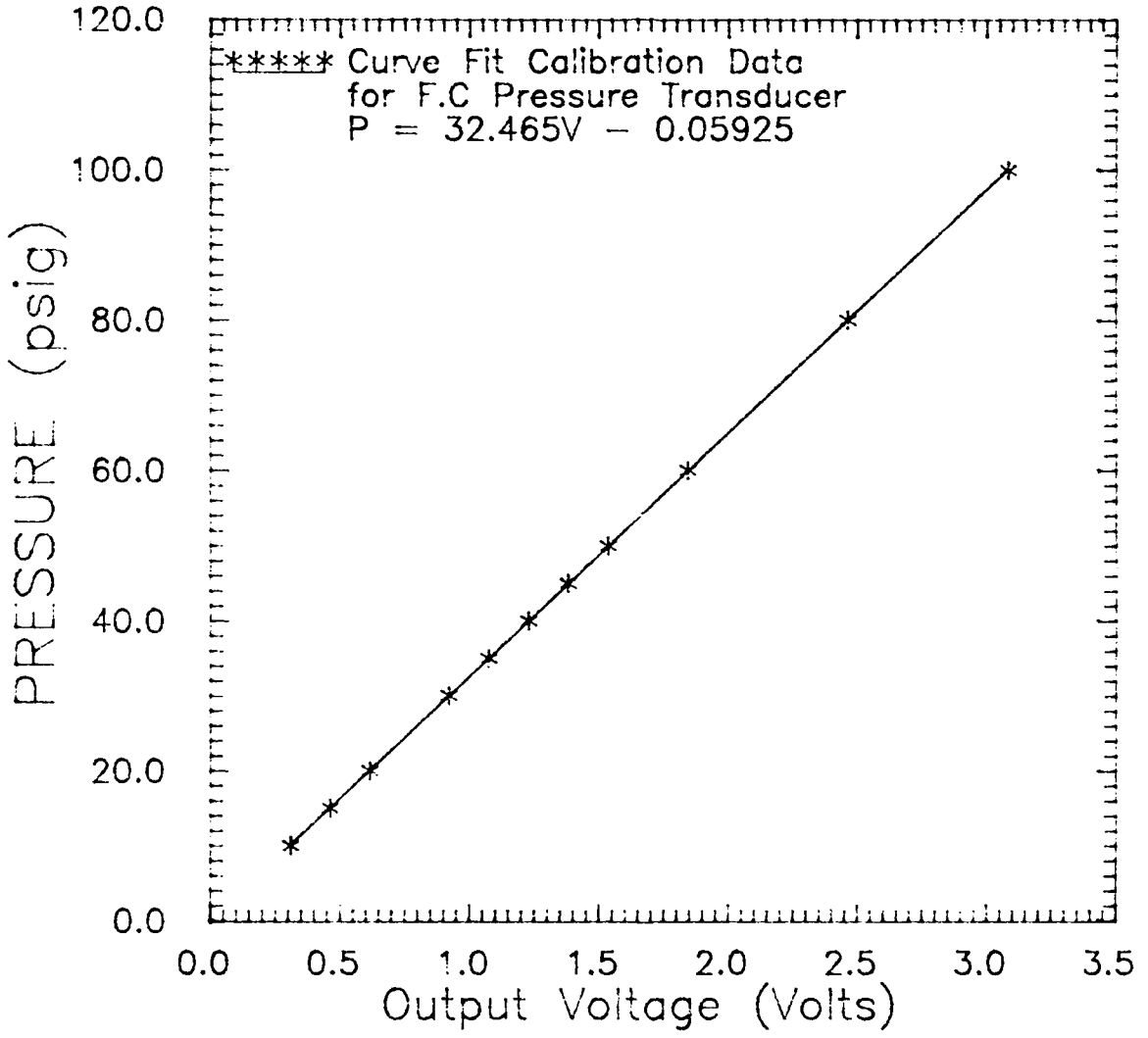

Figure D.3: Calibration Curve For F.C Pressure Transducer

APPENDIX E

NUMERICAL SUMMARY OF HEAT TRANSFER RUNS

Using the applicable equations stated in the text, a summary of some of the Heat Transfer tests is given in the next few pages.

RUN NO RØØ2

Driver Pressure	= P_4 = 6Ø.ØØ	inches of Hg (Gauge)
Driven Pressure	= P_1 = 29.Ø7	inches of Hg
Pressure Behind the Shock	= P_2 = 44.69	inches of Hg
Driver/Driven Temperature	= T_1 = 23.ØØ	degrees C
Temperature behind shock	= T_2 = 62.48	degrees C
Sonic speed	= a_1 = 344.87	meters/sec
Measured shock speed	= U_1 = 416.8Ø	meters/sec
Measured shock Mach No	= M_1 = 1.2Ø9	
Theoretical shock Mach No	= M_t = 1.286	
Flow velocity behind shock	= U_2 = 1Ø9.54	meters/sec
Flow Mach No behind shock	= M_2 = Ø.298	
Adiabatic wall Temperature	= T_{aw} = 67.74	degrees C
Reference Temperature	= T_r = 44.43	degrees C
Density	= ρ = 1.634	Kg/m^3
Dynamic Viscosity	= μ = 19.34E-6	Pa.s
Specific Heat	= C_p = 1ØØ5.5	$J/Kg\ ^0K$
Thermal conductivity	= K = 27.45E-3	$W/m^2\ ^0K$
Recovery Factor	= r = Ø.8824	
Prandtl Number	= Pr = Ø.7Ø87	

RESULTS BASED ON THEORETICAL HEAT FLUX AND MEASURED MACH NUMBER

x(m)	Re($1Ø^6$)	St	Nu	h	q(Kw/m^2)
Ø.Ø6112	Ø.5656	Ø.ØØ233	933.68	419.35	18.76
Ø.Ø71Ø4	Ø.6575	Ø.ØØ226	1Ø53.11	4Ø6.92	18.21
Ø.Ø9128	Ø.8448	Ø.ØØ215	1287.ØØ	387.Ø2	17.32

RESULTS BASED ON EXPERIMENTAL HEAT FLUX AND MEASURED MACH NUMBER

x(m)	Re($1Ø^6$)	St	Nu	h	q(Kw/m^2)
Ø.Ø6112	Ø.5654	Ø.ØØ335	1343.7Ø	6Ø3.49	27.ØØ
Ø.Ø71Ø4	Ø.6572	Ø.ØØ323	15Ø4.ØØ	581.14	26.ØØ
Ø.Ø9128	Ø.84442	Ø.ØØ32Ø	1915.ØØ	575.9Ø	25.77

RUN NO R003

Driver Pressure	= P_4 = 70.00	inches of Hg (Gauge)
Driven Pressure	= P_1 = 29.07	inches of Hg
Pressure Behind the Shock	= P_2 = 46.31	inches of Hg
Driver/Driven Temperature	= T_1 = 23.00	degrees C
Temperature behind shock	= T_2 = 66.12	degrees C
Sonic speed	= a_1 = 344.87	meters/sec
Measured shock speed	= U_1 = 423.56	meters/sec
Measured shock Mach No	= M_1 = 1.228	
Theoretical shock Mach No	= M = 1.297	
Flow velocity behind shock	= U_2 = 118.97	meters/sec
Flow Mach No behind shock	= M_2 = 0.322	
Adiabatic wall Temperature	= T_{aw} = 72.33	degrees C
Reference Temperature	= T_r = 45.80	degrees C
Density	= ρ = 1.675	Kg/m^3
Dynamic Viscosity	= μ = 19.38E-6	Pa.s
Specific Heat	= C_p = 1005.6	$J/Kg\ ^0K$
Thermal conductivity	= k = 27.5E-3	$W/m^2\ ^0K$
Recovery Factor	= r = 0.8827	
Prandtl Number	= Pr = 0.7084	

RESULTS BASED ON THEORETICAL HEAT FLUX AND MEASURED MACH NUMBER

x(m)	Re(10^6)	St	Nu	h	q(Kw/m^2)
0.06112	0.6285	0.00228	1015.47	457.03	22.55
0.07104	0.7305	0.00221	1145.36	443.37	21.87
0.09128	0.9386	0.00211	1399.70	421.69	20.80

RESULTS BASED ON EXPERIMENTAL HEAT FLUX AND MEASURED MACH NUMBER

x(m)	Re(10^6)	St	Nu	h	q(Kw/m^2)
0.06112	0.6287	0.00354	1576.00	709.51	35.00
0.07104	0.7308	0.00364	1937.60	729.78	36.00
0.09128	0.9390	0.00325	2161.77	651.28	32.13

RUN NO RØØ4

Driver Pressure	= P_4 = 8Ø	inches of Hg (Gauge)
Driven Pressure	= P_1 = 29.Ø9	inches of Hg
Pressure Behind the Shock	= P_2 = 49.78	inches of Hg
Driver/Driven Temperature	= T_1 = 23.ØØ	degrees C
Temperature behind shock	= T_2 = 73.73	degrees C
Sonic speed	= a_1 = 344.87	meters/sec
Measured shock speed	= U_1 = 437.66	meters/sec
Measured shock Mach No	= M_1 = 1.269	
Theoretical shock Mach No	= M_t = 1.323	
Flow velocity behind shock	= U_2 = 138.26	meters/sec
Flow Mach No behind shock	= M_2 = Ø.37Ø	
Adiabatic wall Temperature	= T_{aw} = 82.11	degrees C
Reference Temperature	= T_r = 5Ø.Ø4	degrees C
Density	= ρ = 1.7Ø1	Kg/m^3
Dynamic Viscosity	= μ = 19.57E-6	Pa.s
Specific Heat	= C_p = 1ØØ6.ØØ	$J/Kg\ ^0K$
Thermal conductivity	= k = 27.8E-3	$W/m^2\ ^0K$
Recovery Factor	= r = Ø.8829	
Prandtl Number	= Pr = Ø.7Ø81	

RESULTS BASED ON THEORETICAL HEAT FLUX AND MEASURED MACH NUMBER

x(m)	Re($1Ø^6$)	St	Nu	h	q(Kw/m^2)
Ø.Ø6112	Ø.76Ø4	Ø.ØØ22Ø	1182.ØØ	537.83	31.8Ø
Ø.Ø71Ø4	Ø.8839	Ø.ØØ213	1333.65	521.88	3Ø.85
Ø.Ø9128	1.1356	Ø.ØØ2Ø3	1629.8	496.37	29.34

RESULTS BASED ON EXPERIMENTAL HEAT FLUX AND MEASURED MACH NUMBER

x(m)	Re($1Ø^6$)	St	Nu	h	q(Kw/m^2)
Ø.Ø6112	Ø.76Ø5	Ø.ØØ311	1673.ØØ	761.29	45.ØØ
Ø.Ø71Ø4	Ø.8841	Ø.ØØ318	1988.7Ø	778.21	46.ØØ
Ø.Ø9128	1.1358	Ø.ØØ32Ø	2574.ØØ	783.8Ø	46.33

RUN NO RØØ5

Driver Pressure	= P_4 = 9Ø.ØØ	inches of Hg (Gauge)
Driven Pressure	= P_1 = 29.Ø7	inches of Hg
Pressure Behind the Shock	= P_2 = 52.6Ø	inches of Hg
Driver/Driven Temperature	= T_1 = 23.ØØ	degrees C
Temperature behind shock	= T_2 = 79.78	degrees C
Sonic speed	= a_1 = 344.87	meters/sec
Measured shock speed	= U_1 = 448.82	meters/sec
Measured shock Mach No	= M_1 = 1.3Ø2	
Theoretical shock Mach No	= M_t = 1.347	
Flow velocity behind shock	= U_2 = 153.19	meters/sec
Flow Mach No behind shock	= M_2 = Ø.4Ø7	
Adiabatic wall Temperature	= T_{aw} = 9Ø.1Ø	degrees C
Reference Temperature	= T_r = 53.45	degrees C
Density	= ρ = 1.829	Kg/m^3
Dynamic Viscosity	= μ = 19.73E-6	Pa.s
Specific Heat	= C_p = 1ØØ6.34	$J/Kg\ ^0K$
Thermal conductivity	= k = 28.Ø2E-3	$W/m^2\ ^0K$
Recovery Factor	= r = Ø.8831	
Prandtl Number	= Pr = Ø.7Ø77	

RESULTS BASED ON THEORETICAL HEAT FLUX AND MEASURED MACH NUMBER

x(m)	Re($1Ø^6$)	St	Nu	h	q(Kw/m^2)
Ø.Ø6112	Ø.8679	Ø.ØØ214	1314.ØØ	6Ø2.83	4Ø.45
Ø.Ø71Ø4	1.ØØ89	Ø.ØØ2Ø8	1482.ØØ	584.96	39.25
Ø.Ø9128	1.2928	Ø.ØØ197	1811.ØØ	556.36	37.33

RESULTS BASED ON EXPERIMENTAL HEAT FLUX AND MEASURED MACH NUMBER

x(m)	Re($1Ø^6$)	St	Nu	h	q(Kw/m^2)
Ø.Ø6112	Ø.8684	Ø.ØØ3Ø7	1884.11	864.38	58.ØØ
Ø.Ø71Ø4	1.ØØ94	Ø.ØØ296	2114.45	834.58	56.ØØ
Ø.Ø9128	1.297Ø	Ø.ØØ292	268Ø.22	823.33	55.25

RUN NO RØØ6

Driver Pressure	= P_4 = 1ØØ.ØØ	inches of Hg (Gauge)
Driven Pressure	= P_1 = 29.Ø7	inches of Hg
Pressure Behind the Shock	= P_2 = 53.61	inches of Hg
Driver/Driven Temperature	= T_1 = 23.ØØ	degrees C
Temperature behind shock	= T_2 = 81.91	degrees C
Sonic speed	= a_1 = 344.87	meters/sec
Measured shock speed	= U_1 = 455.53	meters/sec
Measured shock Mach No	= M_1 = 1.32	
Theoretical shock Mach No	= M_t = 1.37	
Flow velocity behind shock	= U_2 = 161.63	meters/sec
Flow Mach No behind shock	= M_2 = Ø.428	
Adiabatic wall Temperature	= T_{aw} = 93.39	degrees C
Reference Temperature	= T_r = 54.75	degrees C
Density	= ρ = 1.868	Kg/m^3
Dynamic Viscosity	= μ = 19.8ØE-6	Pa.s
Specific Heat	= C_p = 1ØØ6.5	$J/Kg\ ^0K$
Thermal conductivity	= k = 28.13E-3	$W/m^2\ ^0K$
Recovery Factor	= r = Ø.8831	
Prandtl Number	= Pr = Ø.7Ø74	

RESULTS BASED ON THEORETICAL HEAT FLUX AND MEASURED MACH NUMBER

x(m)	Re($1Ø^6$)	St	Nu	h	q(Kw/m^2)
Ø.Ø6112	Ø.932Ø	Ø.ØØ211	139Ø.6Ø	64Ø.Ø4	45.Ø5
Ø.Ø71Ø4	1.Ø833	Ø.ØØ2Ø5	1568.47	621.Ø6	43,72
Ø.Ø9128	1.3919	Ø.ØØ195	1916.76	59Ø.69	41.58

RESULTS BASED ON EXPERIMENTAL HEAT FLUX AND MEASURED MACH NUMBER

x(m)	Re($1Ø^6$)	St	Nu	h	q(Kw/m^2)
Ø.Ø6112	Ø.9333	Ø.ØØ3Ø4	1913.7Ø	923.43	65.ØØ
Ø.Ø71Ø4	1.Ø841	Ø.ØØ28Ø	2147.32	85Ø.27	59.ØØ
Ø.Ø9128	1.3939	Ø.ØØ298	2938.56	9Ø5.58	62.8Ø

RUN NO RØØ7

Driver Pressure	= P_4 =	11Ø..ØØ	inches ofHg(Gauge)
Driven Pressure	= P_1 =	29.Ø7	inches of Hg
Pressure Behind the Shock	= P_2 =	52.43	inches of Hg
Driver/Driven Temperature	= T_1 =	23.ØØ	degrees C
Temperature behind shock	= T_2 =	87.78	degrees C
Sonic speed	= a_1 =	344.87	meters/sec
Measured shock speed	= U_1 =	463.53	meters/sec
Measured shock Mach No	= M_1 =	1.344	
Theoretical shock Mach No	= M_t =	1.39Ø	
Flow velocity behind shock	= U_2 =	172.46	meters/sec
Flow Mach No behind shock	= M_2 =	Ø.453	
Adiabatic wall Temperature	= T_{aw} =	1ØØ.85	degrees C
Reference Temperature	= T_r =	58.ØØ	degrees C
Density	= ρ =	1.918	Kg/m^3
Dynamic Viscosity	= μ =	19.93E-6	Pa.s
Specific Heat	= C_p =	1ØØ6.8	$J/Kg\ ^0K$
Thermal conductivity	= k =	28.37E-3	$W/m^2\ ^0K$
Recovery Factor	= r =	Ø.8833	
Prandtl Number	= Pr =	Ø.7Ø72	

RESULTS BASED ON THEORETICAL HEAT FLUX AND MEASURED MACH NUMBER

x(m)	Re($1Ø^6$)	St	Nu	h	q(Kw/m^2)
Ø.Ø6112	1.Ø144	Ø.ØØ2Ø7	1487.85	69Ø.65	53.767
Ø.Ø71Ø4	1.1791	Ø.ØØ2Ø1	1678.17	67Ø.175	52.17
Ø.Ø9128	1.515Ø	Ø.ØØ191	2Ø5Ø.82	637.4Ø5	49.62

RESULTS BASED ON EXPERIMENTAL HEAT FLUX AND MEASURED MACH NUMBER

x(m)	Re($1Ø^6$)	St	Nu	h	q(Kw/m^2)
Ø.Ø6112	1.Ø145	Ø.ØØ3Ø1	16Ø5.ØØ	1ØØ1.93	78.ØØ
Ø.Ø71Ø4	1.1792	Ø.ØØ27Ø	2251.6Ø	899.17	7Ø.ØØ
Ø.Ø9128	1.5151	Ø.ØØ275	2946.6Ø	915.82	71.3Ø

RUN NO RØØ8

Driver Pressure	= P_4 = 12Ø.ØØ	inches of Hg(Gauge)
Driven Pressure	= P_1 = 29.Ø7	inches of Hg
Pressure Behind the Shock	= P_2 = 57.86	inches of Hg
Driver/Driven Temperature	= T_1 = 23.ØØ	degrees C
Temperature behind shock	= T_2 = 9Ø.74	degrees C
Sonic speed	= a_1 = 344.87	meters/sec
Measured shock speed	= U_1 = 468.94	meters/sec
Measured shock Mach No	= M_1 = 1.36Ø	
Theoretical shock Mach No	= M_t = 1.41Ø	
Flow velocity behind shock	= U_2 = 179.43	meters/sec
Flow Mach No behind shock	= M_2 = Ø.469	
Adiabatic wall Temperature	= T_{aw} = 1Ø4.88	degrees C
Reference Temperature	= T_r = 59.7Ø	degrees C
Density	= ρ = 1.951	Kg/m^3
Dynamic Viscosity	= μ = 2Ø.Ø2E-6	Pa.s
Specific Heat	= C_p = 1ØØ7.ØØ	$J/Kg\ ^0K$
Thermal conductivity	= k = 28.51E-3	$W/m^2\ ^0K$
Recovery Factor	= r = Ø.8834	
Prandtl Number	= Pr = Ø.7Ø7Ø	

RESULTS BASED ON THEORETICAL HEAT FLUX AND MEASURED MACH NUMBER

x(m)	Re($1Ø^6$)	St	Nu	h	q(Kw/m^2)
Ø.Ø6112	1.Ø721	Ø.ØØ2Ø5	1555.ØØ	725.35	59.39
Ø.Ø71Ø4	1.2462	Ø.ØØ199	1754.ØØ	7Ø3.85	57.63
Ø.Ø9128	1.6Ø12	Ø.ØØ189	2143.ØØ	669.43	54.81

RESULTS BASED ON EXPERIMENTAL HEAT FLUX AND MEASURED MACH NUMBER

x(m)	Re($1Ø^6$)	St	Nu	h	q(Kw/m^2)
Ø.Ø6112	1.Ø689	Ø.ØØ274	2Ø68.3Ø	964.83	79.ØØ
Ø.Ø71Ø4	1.2425	Ø.ØØ291	2556.3Ø	1Ø25.89	84.ØØ
Ø.Ø9128	1.5964	Ø.ØØ285	3216.7Ø	1ØØ4.7Ø	82.3Ø

RUN NO R1Ø2

Driver Pressure	= P_4 = 6Ø.ØØ	inches of Hg (Gauge)
Driven Pressure	= P_1 = 29.21	inches of Hg
Pressure Behind the Shock	= P_2 = 44.48	inches of Hg
Driver/Driven Temperature	= T_1 = 24.ØØ	degrees C
Temperature behind shock	= T_2 = 63.12	degrees C
Sonic speed	= a_1 = 345.47	meters/sec
Measured shock speed	= U_1 = 416.34	meters/sec
Measured shock Mach No	= M_1 = 1.2Ø5	
Theoretical shock Mach No	= M_t = 1.27Ø	
Flow velocity behind shock	= U_2 = 1Ø8.1Ø	meters/sec
Flow Mach No behind shock	= M_2 = Ø.294	
Adiabatic wall Temperature	= T_{aw} = 68.1Ø	degrees C
Reference Temperature	= T_r = 45.6Ø	degrees C
Density	= ρ = 1.623	Kg/m^3
Dynamic Viscosity	= μ = 19.34E-6	Pa.s
Specific Heat	= C_p = 1ØØ5.5	$J/Kg\ ^0K$
Thermal conductivity	= k = 27.46E-3	$W/m^2\ ^0K$
Recovery Factor	= r = Ø.883	
Prandtl Number	= Pr = Ø.7Ø9	

RESULTS BASED ON THEORETICAL HEAT FLUX AND MEASURED MACH NUMBER

x(m)	Re($1Ø^6$)	St	Nu	h	q(Kw/m^2)
Ø.Ø6112	Ø.5545	Ø.ØØ234	919.2Ø	413.ØØ	18.21
Ø.Ø71Ø4	Ø.6446	Ø.ØØ227	1Ø37.ØØ	4ØØ.84	17.68
Ø.Ø9128	Ø.8282	Ø.ØØ216	1267.ØØ	381.16	16.81

RESULTS BASED ON EXPERIMENTAL HEAT FLUX AND MEASURED MACH NUMBER

x(m)	Re($1Ø^6$)	St	Nu	h	q(Kw/m^2)
Ø.Ø6112	Ø.5538	Ø.ØØ38Ø	1492	67Ø.5	29.6
Ø.Ø71Ø4	Ø.6439	Ø.ØØ342	1552	6ØØ.Ø	26.5
Ø.Ø9128	Ø.8273	Ø.ØØ345	2Ø23	6Ø8.73	26.9

RUN NO R1Ø3

Driver Pressure	= P_4 = 7Ø.ØØ	inches of Hg (Gauge)
Driven Pressure	= P_1 = 29.21	inches of Hg
Pressure Behind the Shock	= P_2 = 46.6Ø	inches of Hg
Driver/Driven Temperature	= T_1 = 24.ØØ	degrees C
Temperature behind shock	= T_2 = 66.51	degrees C
Sonic speed	= a_1 = 345.47	meters/sec
Measured shock speed	= U_1 = 424.9Ø	meters/sec
Measured shock Mach No	= M_1 = 1.232	
Theoretical shock Mach No	= M_t = 1.3Ø5	
Flow velocity behind shock	= U_2 = 119.45	meters/sec
Flow Mach No behind shock	= M_2 = Ø.324	
Adiabatic wall Temperature	= T_{aw} = 73.6Ø	degrees C
Reference Temperature	= T_r = 46.8Ø	degrees C
Density	= ρ = 1.69	Kg/m^3
Dynamic Viscosity	= μ = 19.39E-6	Pa.s
Specific Heat	= C_p = 1ØØ5.6	$J/Kg\ ^0K$
Thermal conductivity	= k = 27.5E-3	$W/m^2\ ^0K$
Recovery Factor	= r = Ø.883	
Prandtl Number	= Pr = Ø.7Ø8	

RESULTS BASED ON THEORETICAL HEAT FLUX AND MEASURED MACH NUMBER

x(m)	Re($1Ø^6$)	St	Nu	h	q(Kw/m^2)
Ø.Ø6112	Ø.6363	Ø.ØØ23	1Ø25.3Ø	461.33	22.9
Ø.Ø71Ø4	Ø.7396	Ø.ØØ22	1156.4Ø	447.64	22.2
Ø.Ø9128	Ø.95Ø3	Ø.ØØ21	1413.18	425.75	21.2

RESULTS BASED ON EXPERIMENTAL HEAT FLUX AND MEASURED MACH NUMBER

x(m)	Re($1Ø^6$)	St	Nu	h	q(Kw/m^2)
Ø.Ø6112	Ø.6372	Ø.ØØ35	1578.9	71Ø.43	35.2
Ø.Ø71Ø4	Ø.74Ø7	Ø.ØØ36	1887.9	73Ø.8Ø	36.3
Ø.Ø9128	Ø.9517	Ø.ØØ34	2291.Ø	69Ø.2Ø	34.2

RUN NO R1Ø4

Driver Pressure	= P_4 =	8Ø.ØØ	inches of Hg (Gauge)
Driven Pressure	= P_1 =	29.21	inches of Hg
Pressure Behind the Shock	= P_2 =	5Ø.22	inches of Hg
Driver/Driven Temperature	= T_1 =	24.ØØ	degrees C
Temperature behind shock	= T_2 =	74.38	degrees C
Sonic speed	= a_1 =	345.47	meters/sec
Measured shock speed	= U_1 =	438.2Ø	meters/sec
Measured shock Mach No	= M_1 =	1.272	
Theoretical shock Mach No	= M_t =	1.33Ø	
Flow velocity behind shock	= U_2 =	139.22	meters/sec
Flow Mach No behind shock	= M_2 =	Ø.373	
Adiabatic wall Temperature	= T_{aw} =	83.48	degrees C
Reference Temperature	= T_r =	5Ø.95	degrees C
Density	= ρ =	1.72	Kg/m^3
Dynamic Viscosity	= μ =	19.57E-6	Pa.s
Specific Heat	= C_p =	1ØØ6.ØØ	$J/Kg\ ^0K$
Thermal conductivity	= k =	27.8ØE-3	$W/m^2\ ^0K$
Recovery Factor	= r =	Ø.883	
Prandtl Number	= Pr =	Ø.7Ø8	

RESULTS BASED ON THEORETICAL HEAT FLUX AND MEASURED MACH NUMBER

x(m)	Re($1Ø^6$)	St	Nu	h	q(Kw/m^2)
Ø.Ø6112	Ø.7511	Ø.ØØ22Ø	1171.Ø	517.18	3Ø.76
Ø.Ø71Ø4	Ø.873Ø	Ø.ØØ212	132Ø.5	516.71	3Ø.73
Ø.Ø9128	1.1217	Ø.ØØ2Ø3	1614.Ø	491.45	29.23

RESULTS BASED ON EXPERIMENTAL HEAT FLUX AND MEASURED MACH NUMBER

x(m)	Re($1Ø^6$)	St	Nu	h	q(Kw/m^2)
Ø.Ø6112	Ø.7512	Ø.ØØ34	18Ø8.4	822.57	48.9
Ø.Ø71Ø4	Ø.8732	Ø.ØØ35	2163.84	846.76	5Ø.4
Ø.Ø9128	1.122Ø	Ø.ØØ33	2621.44	798.38	47.5

RUN NO R1Ø5

Driver Pressure	= P_4 = 9Ø.Ø		inches of Hg (Gauge)
Driven Pressure	= P_1 = 29.3		inches of Hg
Pressure Behind the Shock	= P_2 = 53.61		inches of Hg
Driver/Driven Temperature	= T_1 = 23.ØØ		degrees C
Temperature behind shock	= T_2 = 8Ø.13		degrees C
Sonic speed	= a_1 = 344.87		meters/sec
Measured shock speed	= U_1 = 448.9Ø		meters/sec
Measured shock Mach No	= M_1 = 1.3Ø2		
Theoretical shock Mach No	= M_t = 1.345		
Flow velocity behind shock	= U_2 = 153.3Ø		meters/sec
Flow Mach No behind shock	= M_2 = Ø.411		
Adiabatic wall Temperature	= T_{aw} = 9Ø.15		degrees C
Reference Temperature	= T_r = 53.5Ø		degrees C
Density	= ρ = 1.83		Kg/m^3
Dynamic Viscosity	= μ = 19.73E-6		Pa.s
Specific Heat	= C_p = 1ØØ6.34		$J/Kg\ ^0K$
Thermal conductivity	= k = 28.Ø4E-3		$W/m^2\ ^0K$
Recovery Factor	= r = Ø.883		
Prandtl Number	= Pr = Ø.7Ø8		

RESULTS BASED ON THEORETICAL HEAT FLUX AND MEASURED MACH NUMBER

x(m)	Re($1Ø^6$)	St	Nu	h	q(Kw/m^2)
Ø.Ø6112	Ø.869Ø	Ø.ØØ214	1315.6	6Ø3.6	4Ø.5
Ø.Ø71Ø4	1.Ø1Ø1	Ø.ØØ2Ø7	1483.9	585.7	39.33
Ø.Ø9128	1.2979	Ø.ØØ197	1813.4	557.1	37.41

RESULTS BASED ON EXPERIMENTAL HEAT FLUX AND MEASURED MACH NUMBER

x(m)	Re($1Ø^6$)	St	Nu	h	q(Kw/m^2)
Ø.Ø6112	Ø.8692	Ø.ØØ33	2Ø43	937.3	62.94
Ø.Ø71Ø4	1.Ø1Ø3	Ø.ØØ31	2217	875.2	58.75
Ø.Ø9128	1.2982	Ø.ØØ3Ø	2757	847.Ø	56.87

RUN NO R1Ø6

Driver Pressure	= P_4 = 1ØØ	inches of Hg (Gauge)
Driven Pressure	= P_1 = 29.3	inches of Hg
Pressure Behind the Shock	= P_2 = 54.2	inches of Hg
Driver/Driven Temperature	= T_1 = 23	degrees C
Temperature behind shock	= T_2 = 82.3	degrees C
Sonic speed	= a_1 = 344.87	meters/sec
Measured shock speed	= U_1 = 455.5Ø	meters/sec
Measured shock Mach No	= M_1 = 1.325	
Theoretical shock Mach No	= M_t = 1.369	
Flow velocity behind shock	= U_2 = 162.2	meters/sec
Flow Mach No behind shock	= M_2 = Ø.43	
Adiabatic wall Temperature	= T_{aw} = 93.5	degrees C
Reference Temperature	= T_r = 55.2	degrees C
Density	= ρ = 1.868	Kg/m^3
Dynamic Viscosity	= μ = 19.8ØE-6	Pa.s
Specific Heat	= C_p = 1ØØ6.5	$J/Kg\ ^0K$
Thermal conductivity	= k = 28.13E-3	$W/m^2\ ^0K$
Recovery Factor	= r = Ø.883	
Prandtl Number	= Pr = Ø.7Ø7	

RESULTS BASED ON THEORETICAL HEAT FLUX AND MEASURED MACH NUMBER

x(m)	Re($1Ø^6$)	St	Nu	h	q(Kw/m^2)
Ø.Ø6112	Ø.9353	Ø.ØØ211	1394	641.6	45.23
Ø.Ø71Ø4	1.Ø871	Ø.ØØ2Ø5	1572	622.6	43.9Ø
Ø.Ø9128	1.3968	Ø.ØØ195	1922	592.2	41.75

RESULTS BASED ON EXPERIMENTAL HEAT FLUX AND MEASURED MACH NUMBER

x(m)	Re($1Ø^6$)	St	Nu	h	q(Kw/m^2)
Ø.Ø6112	Ø.93717	Ø.ØØ32	212Ø.3	975.87	68.8
Ø.Ø71Ø4	1.Ø8933	Ø.ØØ33	2541.5	1ØØ6.36	71.Ø
Ø.Ø9128	1.39967	Ø.ØØ34	3315.1	1Ø21.61	72.Ø

RUN NO R1Ø7

Driver Pressure	= P_4 = 11Ø	inches of Hg (Gauge)
Driven Pressure	= P_1 = 29.3	inches of Hg
Pressure Behind the Shock	= P_2 = 55.1	inches of Hg
Driver/Driven Temperature	= T_1 = 23	degrees C
Temperature behind shock	= T_2 = 88.Ø	degrees C
Sonic speed	= a_1 = 344.87	meters/sec
Measured shock speed	= U_1 = 4464	meters/sec
Measured shock Mach No	= M_1 = 1.344	
Theoretical shock Mach No	= M_t = 1.39Ø	
Flow velocity behind shock	= U_2 = 173.3	meters/sec
Flow Mach No behind shock	= M_2 = Ø.455	
Adiabatic wall Temperature	= T_{aw} = 1Ø1	degrees C
Reference Temperature	= T_r = 58.5	degrees C
Density	= ρ = 1.918	Kg/m^3
Dynamic Viscosity	= μ = 19.93E-6	Pa.s
Specific Heat	= C_p = 1ØØ6.8	$J/Kg\ ^0K$
Thermal conductivity	= k = 28.37E-3	$W/m^2\ ^0K$
Recovery Factor	= r = Ø.883	
Prandtl Number	= Pr = Ø.7Ø7	

RESULTS BASED ON THEORETICAL HEAT FLUX AND MEASURED MACH NUMBER

x(m)	Re($1Ø^6$)	St	Nu	h	q(Kw/m^2)
Ø.Ø6112	1.Ø1754	Ø.ØØ2Ø7	1491	692.3	54.ØØ
Ø.Ø71Ø4	1.18276	Ø.ØØ2Ø1	1682	671.7	52.4Ø
Ø.Ø9128	1.51972	Ø.ØØ191	2Ø56	638.9	49.83

RESULTS BASED ON EXPERIMENTAL HEAT FLUX AND MEASURED MACH NUMBER

x(m)	Re($1Ø^6$)	St	Nu	h	q(Kw/m^2)
Ø.Ø6112	1.Ø1795	Ø.ØØ35	2519	1169.3	91.2
Ø.Ø71Ø4	1.18323	Ø.ØØ33	2761	11Ø2.43	86.Ø
Ø.Ø9128	1.52Ø283	Ø.ØØ32	344Ø	1Ø69.Ø3	83.4

RUN NO R1Ø8

Driver Pressure	= P_4 = 12Ø	inches of Hg(Gauge)
Driven Pressure	= P_1 = 29.3	inches of Hg
Pressure Behind the Shock	= P_2 = 58.4	inches of Hg
Driver/Driven Temperature	= T_1 = 23	degrees C
Temperature behind shock	= T_2 = 91	degrees C
Sonic speed	= a_1 = 344.87	meters/sec
Measured shock speed	= U_1 = 47Ø	meters/sec
Measured shock Mach No	= M_1 = 1.37	
Theoretical shock Mach No	= M_t = 1.41	
Flow velocity behind shock	= U_2 = 18Ø.7	meters/sec
Flow Mach No behind shock	= M_2 = Ø.472	
Adiabatic wall Temperature	= T_{aw} = 1Ø5.2	degrees C
Reference Temperature	= T_r = 6Ø.6	degrees C
Density	= ρ = 1.951	Kg/m^3
Dynamic Viscosity	= μ = 2Ø.Ø2E-6	Pa.s
Specific Heat	= C_p = 1ØØ7	$J/Kg\ ^0K$
Thermal conductivity	= k = 28.51E-3	$W/m^2\ ^0K$
Recovery Factor	= r = Ø.883	
Prandtl Number	= Pr = Ø.7Ø7	

RESULTS BASED ON THEORETICAL HEAT FLUX AND MEASURED MACH NUMBER

x(m)	Re($1Ø^6$)	St	Nu	h	q(Kw/m^2)
Ø.Ø6112	1.Ø763	Ø.ØØ2Ø5	1559.7	727.61	59.81
Ø.Ø71Ø4	1.251Ø	Ø.ØØ199	1759.3	7Ø6.Ø4	58.Ø4
Ø.Ø9128	1.6Ø74	Ø.ØØ189	215Ø.Ø	671.52	55.2Ø

RESULTS BASED ON EXPERIMENTAL HEAT FLUX AND MEASURED MACH NUMBER

x(m)	Re($1Ø^6$)	St	Nu	h	q(Kw/m^2)
Ø.Ø6112	1.Ø765	Ø.ØØ311	2366.9Ø	11Ø4	91
Ø.Ø71Ø4	1.2512	Ø.ØØ323	2857.35	1147	94
Ø.Ø9128	1.6Ø77	Ø.ØØ285	3239.4Ø	1Ø12	83

APPENDIX F

A summary of the Film cooling Runs is given in the following pages.

FILM COOLING RUNS FOR P_4 = 6Ø" Hg

Driver Pressure	= P_4 =	6Ø.ØØ	inches of Hg (Gauge)
Driven Pressure	= P_1 =	29.Ø7	inches of Hg
Pressure Behind the Shock	= P_2 =	44.69	inches of Hg
Driver/Driven Temperature	= T_1 =	23.ØØ	degrees C
Temperature behind shock	= T_2 =	62.48	degrees C
Sonic speed	= a_1 =	344.87	meters/sec
Measured shock speed	= U_1 =	416.8Ø	meters/sec
Measured shock Mach No	= M_1 =	1.2Ø9	
Theoretical shock Mach No	= M_t =	1.286	
Flow velocity behind shock	= U_2 =	1Ø9.54	meters/sec
Flow Mach No behind shock	= M_2 =	Ø.298	
Prandtl Number	= Pr =	Ø.7Ø87	

Run No	P_c (psia)	ρ_c	ρ_2	U_2	U_c	B	q (Kw/m_2) Gage No 2
FC6Ø1	21.76	1.78	1.58	1Ø3.4	27.4	Ø.3Ø	28.1
FC6Ø2	22.Ø6	1.79	1.58	1Ø3.4	55.1	Ø.6Ø	27.3
FC6Ø3	22.56	1.8Ø	1.58	1Ø3.4	82.5	Ø.91	24.6
FC6Ø4	23.27	1.81	1.58	1Ø3.4	1Ø9.3	1.22	24.2
FC6Ø5	25.41	1.89	1.58	1Ø3.4	162.Ø	1.85	23.Ø
FC6Ø6	28.63	1.92	1.58	1Ø3.4	212.5	2.51	22.5
FC6Ø7	33.2Ø	2.ØØ	1.58	1Ø3.4	26Ø.2	3.2Ø	21.2
FC6Ø8	39.43	2.1Ø	1.58	1Ø3.4	3Ø4.6	3.93	18.Ø
FC6Ø9	43.6Ø	2.27	1.58	1Ø3.4	312.9	4.35	17.2
FC61Ø	5Ø.16	2.61	1.58	1Ø3.4	313.2	5.Ø1	15.Ø
FC611	59.9Ø	3.11	1.58	1Ø3.4	313.2	5.98	16.Ø
FC612	66.39	3.45	1.58	1Ø3.4	313.2	6.63	17.3
FC613	72.89	3.79	1.58	1Ø3.4	313.2	7.28	18.3
FC614	79.38	4.13	1.58	1Ø3.4	313.2	7.93	19.Ø
FC615	85.87	4.46	1.58	1Ø3.4	313.2	8.57	2Ø.Ø
FC616	92.37	4.8Ø	1.58	1Ø3.4	313.2	9.22	21.2
FC617	98.86	5.14	1.58	1Ø3.4	313.2	9.87	22.1

FILM COOLING RUNS FOR P_4 = 8Ø" Hg

Driver Pressure	= P_4 =	8Ø.ØØ	inches of Hg (Gauge)
Driven Pressure	= P_1 =	29.21	inches of Hg
Pressure Behind the Shock	= P_2 =	5Ø.22	inches of Hg
Driver/Driven Temperature	= T_1 =	24.ØØ	degrees C
Temperature behind shock	= T_2 =	74.38	degrees C
Sonic speed	= a_1 =	345.47	meters/sec
Measured shock speed	= U_1 =	438.2Ø	meters/sec
Measured shock Mach No	= M_1 =	1.272	
Theoretical shock Mach No	= M_t =	1.33Ø	
Flow velocity behind shock	= U_2 =	139.22	meters/sec
Flow Mach No behind shock	= M_2 =	Ø.373	
Prandtl Number	= Pr =	Ø.7Ø8	

Run No	P_c (psia)	ρ_2	ρ_c	U_2	U_c	B	q (Kw/m_2) Gage No 2
FC8Ø1	24.78	1.7Ø	1.2Ø	138.2	4Ø.2	Ø.34	5Ø
FC8Ø2	26.73	1.7Ø	2.Ø4	138.2	119.6	1.Ø4	46
FC8Ø3	28.53	1.7Ø	2.Ø8	138.2	156.7	1.39	44
FC8Ø4	38.16	1.7Ø	2.26	138.2	265.1	2.55	4Ø
FC8Ø5	43.23	1.7Ø	2.34	138.2	297.9	2.97	34
FC8Ø6	46.21	1.7Ø	2.39	138.2	313.6	3.18	32
FC8Ø7	46.86	1.7Ø	2.41	138.2	314.9	3.23	3Ø
FC8Ø8	5Ø.11	1.7Ø	2.58	138.2	314.9	3.45	27
FC8Ø9	53.36	1.7Ø	2.75	138.2	314.9	3.68	28
FC81Ø	56.6Ø	1.7Ø	2.91	138.2	314.9	3.9Ø	29
FC811	66.34	1.7Ø	3.41	138.2	314.9	4.56	3Ø
FC812	72.84	1.7Ø	3.75	138.2	314.9	5.Ø2	32
FC813	79.33	1.7Ø	4.Ø8	138.2	314.9	5.46	34

FILM COOLING RUNS FOR P_4 = 1ØØ" Hg

Driver Pressure	= P_4 = 1ØØ	inches of Hg (Gauge)
Driven Pressure	= P_1 = 29.3	inches of Hg
Pressure Behind the Shock	= P_2 = 54.2	inches of Hg
Driver/Driven Temperature	= T_1 = 23	degrees C
Temperature behind shock	= T_2 = 82.3	degrees C
Sonic speed	= a_1 = 344.87	meters/sec
Measured shock speed	= U_1 = 455.5Ø	meters/sec
Measured shock Mach No	= M_1 = 1.325	
Theoretical shock Mach No	= M_t = 1.369	
Flow velocity behind shock	= U_2 = 162.2	meters/sec
Flow Mach No behind shock	= M_2 = Ø.43	
Prandtl Number	= Pr = Ø.7Ø7	

Run No	P_c (psia)	ρ_2	ρ_c	U_2	U_c	B	q (Kw/m_2) Gage No 4
FC1ØØ1	26.68	1.78	2.14	157.5	48.11	Ø.37	6Ø
FC1ØØ2	29.13	1.78	2.19	157.5	13Ø.12	1.Ø2	53
FC1ØØ3	36.48	1.78	2.35	157.5	236.68	1.99	45
FC1ØØ4	41.72	1.78	2.43	157.5	27Ø.64	2.35	4Ø
FC1ØØ5	48.6Ø	1.78	2.54	157.5	3Ø8.77	2.81	39
FC1ØØ6	53.36	1.78	2.74	157.5	314.63	3.Ø8	42
FC1ØØ7	59.85	1.78	3.Ø7	157.5	314.63	3.45	44
FC1ØØ8	66.34	1.78	3.4Ø	157.5	314.63	3.83	46
FC1ØØ9	72.84	1.78	3.74	157.5	314.63	4.21	48
FC1Ø1Ø	79.33	1.78	4.Ø7	157.5	314.63	4.58	51

Vita

Rakhman Gul was born on the 1Øth of October 1962 in Badin Khel, N.W.F.P, Pakistan. He recieved his primary and high school education at Burn Hall School, Abbottabad and obtained his Senior Cambridge Certificate in 1979. In September of 1979 he joined the Pakistan Air Force. After having completed his F.Sc from P.A.F College Sargodha he joined the P.A.F College of Aeronautical Engineering in September 1981. He graduated from the P.A.F College of Aeronautical Engineering in 1985 with a Bachelors Degree in Aerospace and subsequently got commisioned in the Engineering Branch of Pakistan Air Force. He was selected for a Master of Science Degree at Air Force Institute of Technology, U.S.A in 1989.